Aus dem Institut für Pflanzenbau und Pflanzenzüchtung
der Christian-Albrechts-Universität zu Kiel
- Acker- und Pflanzenbau -

Remote sensing and simulation modelling as tools for improving nitrogen efficiency for winter oilseed rape (*Brassica napus* L.)

Dissertation
zur Erlangung des Doktorgrades
der Agrar- und Ernährungswissenschaftlichen Fakultät
der Christian-Albrechts-Universität zu Kiel

vorgelegt von

Dipl. Biol. Karla Müller

aus Bielefeld

Kiel, 2008

Dekan: Prof. Dr. U. Latacz-Lohmann
1. Berichterstatter: Prof. Dr. H. Kage
2. Berichterstatter: Prof. Dr. F. Taube
Tag der mündlichen Prüfung: 09.02.2009

Table of contents

Figures

Chapter 1

Chapter 2

Chapter 3

Chapter 4

Chapter 5

Tables

Chapter 2

Chapter 3

Chapter 1

General introduction

1. Background

Winter oilseed rape (OSR) became more and more important during the last decades. Reasons for the rising importance of OSR are its profitability, the potential to grow OSR as a renewable resource for biofuel production and its beneficial value as preceding crop. The acreage of OSR sums up to 13 % of the total arable land, regarding northern Germany, OSR occupies even 20 % (Statistisches Bundesamt, 2007). However, OSR is one of the most inefficient crops concerning N (Lickfett et al., 1993; Lickfett and Przemeck, 1995; Sieling, 1997). Reasons are early leaf fall during the growth period, early harvest allowing a long time for mineralization of residues, low N-harvest indices compared to cereal crops ranging between 0.6 and 0.7 (Malagoli et al., 2005). Additionally, wheat as the typical following crop takes up low amounts of nitrogen before winter. As a consequence, these factors can increase the risk of N losses after harvest by leaching into the groundwater (Chalmers and Darby, 1992). The implementation of the EU Nitrate Directive, which sets a maximum of nitrate in the groundwater of 50 mg l^{-1}, into German legislation ("Düngeverordnung") led to the restriction of N balance surpluses to 60 kg ha^{-1} averaged for a three year crop rotation. Thus, there is need of action to minimize the surplus of nitrogen after harvest of OSR. In order to reduce these problems several approaches in plant production are discussed like an adjusted nitrogen fertilizer application (Sieling et al., 1997; Lickfett and Przemeck, 1995), a changed crop rotation (Lickfett et al., 1994) or a reduced tillage (Henke, 2008). Plant breeders work on genotypes with a higher N efficiency (Lickfett et al., 2001; Behrens, 2002; Nyikako, 2003). Especially for cereal crops an improvement of nitrogen efficiency was found, caused by a site specific nitrogen application (Blackmer and White, 1998, Raun et al., 2002; Ebertseder et al., 2003, Delin, 2005). The reason is that yield varies within fields because of different soil properties and therefore different water availability. The uniform amount of fertilizer is determined on sites with highest nitrogen demand, thus high yielding sites (McBratney and Whelan, 1999). Low yielding sites cannot use these amounts of nitrogen, so that surpluses of nitrogen and therefore nitrogen losses are high.

For OSR there are hardly any experiences on site specific fertilization. Yield maps of OSR indicate that yields show even higher variability for OSR than for cereal crops (Joernsgaard and Halmoe, 2002), so that high site specific differences concerning nitrogen uptake can be assumed. Figure 1 exemplifies the large seed yield variation within a field, which has been fertilized according to usual practice, varying between 33 to 63 dt ha^{-1} with a coefficient of variation of 7.5 %. There are two different main concepts concerning site specific nitrogen fertilization.

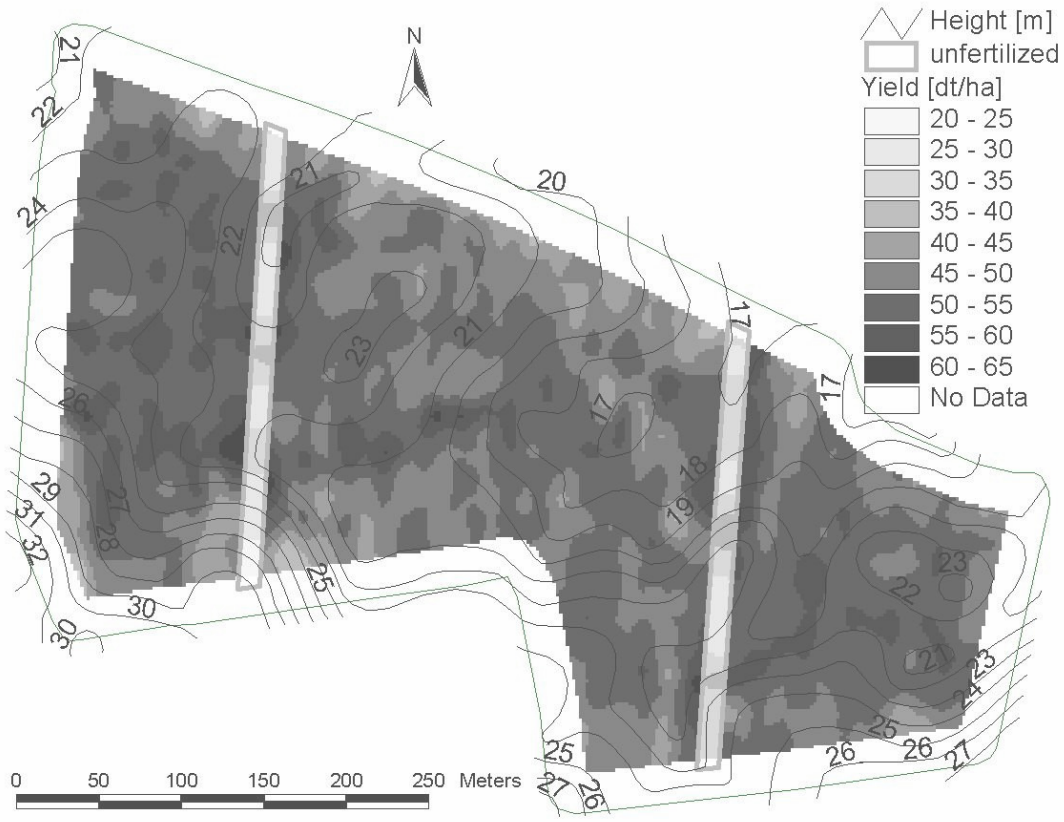

Figure 1: Yield map of winter oilseed rape in 2004, Hohenschulen, derived by a yield mapping system

The first concept is based on the in-field characterization of yield and management zones for the determination of the nitrogen fertilizer amount (Khosla et al., 2002; Koch et al., 2004). Historical, constant high and low yielding sites, which are mainly caused by water deficit, are determined. Locations, which are mainly affected by maritime weather conditions, show variation concerning growth due to other factors than water availability, so that constant sites can hardly be characterized. Therefore, the applicability of the management zone concept is limited.

The second, a remote sensing based concept, uses different current crop characteristics concerning canopy reflection for the derivation of fertilizer amount. For the calculation of the amount of fertilizer, site specific information about produced dry matter and N uptake are taken into account. The relation of canopy reflection to crop parameters can depend on developmental stages and climatic conditions (Sembiring et al., 2001; Sticksel et al., 2003). This concept neither considers the time course of development and growth nor historical information on yield or soil characteristics for the derivation of site specific fertilization. Since

yield limiting factors like water availability cannot be taken into account, this concept can lead to over fertilization (Geesing et al., 2001).

The application of a dynamic plant growth model, which can consider different information, e.g. current and historical weather data, current crop data and historical yield data, has potential to negotiate limitations of both concepts (Figure 2). Historical yield data and soil properties can as well be considered for yield prediction as sensor based information that can be used to initiate, parameterize and update the model concerning current plant growth. The information on the current crop status should be highly resoluted concerning time and site specificity. Since destructive measurements are too labour intensive and limited concerning the scale factor, indirect methods should be developed and established to gain information on plant area, produced biomass and current nitrogen supply of the crops. Models can also provide information on onset and duration of different growth phases, which can be used by growth stage depending management treatments like fertilization (Barlog, 2004; Ghersa and Holt, 1995).

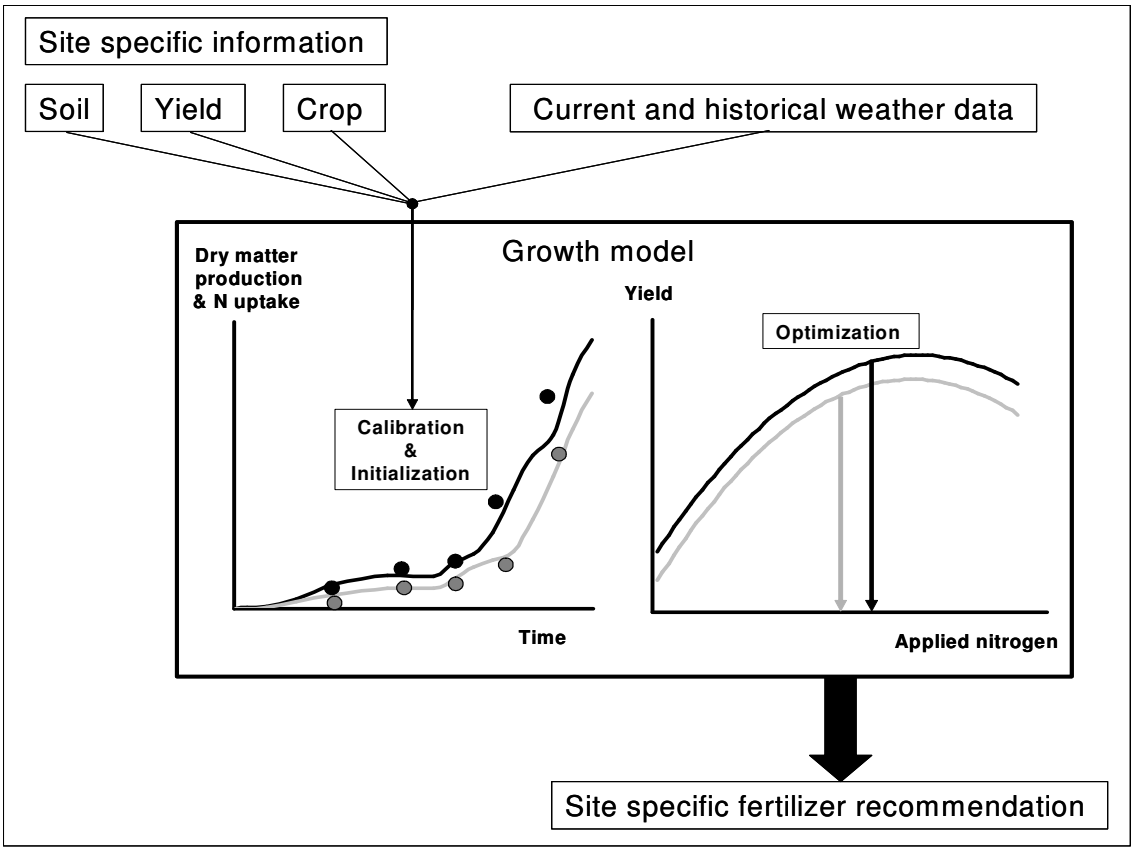

Figure 2: Outline for the implementation and translation of site specific information into a growth modeland the derivation of site specific fertilizer recommendations

2. Objectives

The objectives of this thesis are on the one hand to establish a sensory, non-destructive method to achieve information on site specific variability. This should be obtained by measuring canopy reflectance that saves intensive destructive measurements in the fields. On the other hand, a phenological model should be developed and parameterized on German conditions to predict developmental stages with a high resolution. Afterwards, a crop growth model for OSR should be developed, to predict plant parameters like biomass and nitrogen supply of the crops in the time course, so that the need for fertilizer and yield can be derived. Closing, the two models should be connected, so that different growth traits during the vegetation period inside the growth model can be controlled by development. In combination with appropriate fertilizer algorithms, these investigations can contribute to a site specific fertilization recommendation.

Chapter 2 deals with the testing of a non-destructive method for the estimation of different crop canopy parameters of OSR. From hyperspectral reflectance measurements vegetation indices (VI) were derived that were tested on their prediction power for three plant parameters: green area index (GAI), shoot dry matter (DM_{shoot}) and total nitrogen amount in the shoot (N_{shoot}). The derivation of VI was conducted according to a new approach by systematically testing all waveband ratios, out of 61 available wavebands, in two different forms: a simple ratio (SR) form λ_1/λ_2 and a normalized difference index (NDI) form $(\lambda_1-\lambda_2)/(\lambda_1+\lambda_2)$. To obtain variability among the investigated crops, reflectance measurements were conducted on four differently fertilized winter oilseed rape crops.

For the prediction of developmental stages, a phenological model for OSR was developed that is described in chapter 3. The model is based on BRASNAP-PH (Habekotté, 1997), which allows for the prediction of four developmental stages (DVS): emergence, the onset and end of flowering and maturity. To obtain a more detailed description of development according to the BBCH scale (Lancashire et al., 1991), BRASNAP-PH was modified in different ways. Some parameters were deleted or displaced, an additional developmental rate was implemented, enabling the calculation of leaf development and stem elongation rates separately. Also, equations for the derivation of BBCH stages out of DVS were implemented. During leaf development, BBCH stages were derived from the number of visible leaves, which were estimated using the newly estimated phyllochron. These structural changes of the model enabled an easier parameterization from field observations, because BBCH stage is defined by visible events of plant morphology. The model was calibrated and validated on a large data set obtained throughout Germany.

Chapter 4 presents an empirical crop growth model for OSR that calculates plant dry matter production (DM_{plant}), its partitioning into leaf and stem dry matter (DM_{leaf} and DM_{stem}), the derivation of leaf and stem area (LAI and SAI), the nitrogen concentration of leaf and stem

(Nc_{leaf} and Nc_{stem}) as well as the amount of nitrogen in leaf and stem and in the aboveground dry matter of the shoot (N_{leaf}, N_{stem}, N_{shoot}). Dry matter production relies on the concept of light use efficiency, LUE (Jones and Kiniry, 1986; Williams et al., 1989). Parameters, which could not be optimized inside the model because of structure and availability of data, were taken form literature or derived from external data; others were optimized inside the model. Prediction power for plant parameters were tested on three independent data sets.

Concluding, chapter 5 discusses the common context of the described studies regarding their relevance for site specific fertilization for OSR.

References

Barlóg, P. G. (2004). "Effect on timing and nitrogen fertilizer application on winter oilseed rape (*Brassica napus* L.) I. Growth Dynamics and seed yield." Journal of Agronomy and Crop Science 190: 305-131.

Behrens, T. (2002). "Stickstoffeffizienz von Winterraps (*Brassica napus* L.) in Abhängigkeit von der Sorte, sowie der Menge, Zeit und Form variierter Stickstoffdüngung." Universität Göttingen.

Blackmer, A. M., White, S. E. (1998). "Using precision farming technologies to improve management of soil and fertilizer nitrogen." Australian Journal of Agricultural Research 49: 555-564.

Chalmer, A. G., Darby, R. J. (1992)."Nitrogen application to oilseed rape and implications for potential leaching loss." Aspects of Applied Biology 30: 425-430.

Delin, S. (2005). "Site-specific nitrogen fertilization demand in relation to plant available soil nitrogen and water." PhD Thesis, Dept. of Soil Sciences, Acta Universitatis agriculturae Sueciae Vol.6.

Ebertseder, T., Gutser, R., Hege U., Brandhuber, R., Schmidhalter, U. (2003). "Strategies for site-specific nitrogen fertilization with respect to long-term environmental demands." Paper presented at the 4th ECPA, Berlin.

Geesing, D., Gutser, R., Schmidhalter, U. (2001). "Importance of spatial and temporal soil water variability for nitrogen management decisions." Third European Conference on Precision Agriculture, Montpellier: 569-664.

Ghersa, C. M., Holt, J. S. (1995). "Using phenology prediction in weed management: a review." Weed Research 35: 461-470.

Habekotté, B. (1997). "A model of the phenological development of winter oilseed rape (*Brassica napus* L.)." Field Crops Research 54: 127-136.

Henke, J. (2008). "Entwicklung und Bewertung von Strategien zur Verbesserung der Stickstoffeffizienz im Winterrapsanbau." Dissertation, Christian-Albrechts-Universität zu Kiel.

Joernsgaard, B., Halmoe, S. (2002). "Intra-field yield variation over crops and years." European Journal of Agronomy 19: 23-33.

Jones, C. A., Kiniry, J. R. (1986). "CEREZ-Maiz. A simulation study of maize growth and development." Texas A & M University Press, College Station: 1-194.

Khosla et al. (2002)."Use of site specific management zones to improve nitrogen management for precision agriculture." Journal of Soil and Water Conservation 57: 513-518.

Koch, B., Khosla, R., Frasier, M., Westfall, D. G., Inman, D. (2004). "Economic feasibility of variable rate nitrogen application utilizing site-specific management zones." Agron. J. 96: 1572–1580.

Lancashire, P.D., Bleiholder, H., Langelüddecke, P., Stauss, R., Boom, T.V.D., Weber, E., Witzenberger, A. (1991). "An uniformdecimal code for growth stages of crops and weeds." Annals of Applied Biology 119: 561-601.

Lickfett, T., Kreikenbohm, G., Goebel, C., Przemeck, E. (1993). "Über den Anstieg des Rest-Nmin nach Winterraps und Maßnahmen zur seiner Vermeidung." VDLUFA-Schriftenreihe 36: 91-94.

Lickfett, T., Przemeck, E. (1994). "Stickstoffsalden von Rapsfruchtfolgen bei verminderter Produktionsintensität." VDLUFA-Schriftenreihe 38: 769-772.

Lickfett, T., Przemeck, E. (1995). "Ausnutzungsgrad von Mineraldünger-Stickstoff in Rapsfruchtfolgen unterschiedlicher Produktionsintensität." VDLUFA-Schriftenreihe 40: 833-836.

Lickferr, T., Behrens, T., Ulas, A., Horst, W., Wiesler F. (2001). "Lösen N-effiziente Genotypen kurzfristig das Nitratproblem nach Raps?" VDLUFA-Schriftenreihe 57: 1-4.

Malagoli, P., Laine, P., Rossato, L., Ourry, A. (2005). "Dynamics of Nitrogen Uptake and Mobilization in field-grown Winter Oilseed Rape (*Brassica napus* L.) from Stem Extension to Harvest I. Global N Flows between Vegetative and Reproduction Tissues in relation to Leaf Fall and their Residual N." Annals of Botany 95: 863-861.

McBratney, A. B., Whelan, B. M. (1999). "The null hypothesis of precision agriculture." Paper presented at the 2nd ECPD, Odense.

Nyikako, J. A. (2003). "Genetic Variation for Nitrogen Efficiency in Oilseed Rape (*Brassica napus* L.)." Dissertation, Universität Göttingen.

Raun, W. R., Solie, J. B., Johnson, G. V., Stone, M. L., Mullen, R. W., Freemann, K. W., Thomason, W. E., Lukina, E. V. (2002). "Improving Nitrogen Use Efficiency in Cereal

Grain Production with Optical Sensing and Variable Rate Application." Agronomy Journal 94: 815-820.

Sembiring, H., Lees, H. L., et al. (2001)." Effect of Growth Stage and Variety on Spectral Radiance in Winter Wheat." Journal of Plant Nutrition 24: 885-898.

Sieling, K., Günther-Borstel, O., Hanus, H. (1997). "Effect of slurry application and mineral nitrogen fertilization on N leaching in different crop combinations." Journal of Agricultural Science 128: 79-86.

Sieling, K. (1997). "Effect of preceding crop combination and N fertilization on yield of six oil-seed rape cultivars (*Brassica napus* L.)." European Journal of Agronomy 7: 301-306.

Statistisches Bundesamt (2007). "Land- und Forstwirtschaft, Fischerei, Landwirtschaftliche Bodennutzung, Anbau auf dem Ackerland, Agrarstrukturerhebung 2007". Fachserie 3, Reihe 3.1.2.: Wiesbaden.

Sticksel, E., Schächtl, J., Huber, G., Liebler, J., Maidl, F. X. (2003). "Tagesgänge ausgewählter Vegetationsindizes in Winterweizen." Mitteilungen der Gesellschaft für Pflanzenbauwissenschaften 15: 75-78.

Williams, J. R., Jones, C. A., Kiniry, J. R., Spanel, D. A. (1989). "The EPIC crop growth model." Transactions of American Society of Agricultural Engineers 32: 497-511.

Chapter 2

Analysis of Vegetation Indices derived from Hyperspectral Reflection Measurements for estimating Crop Canopy Parameters of Oilseed Rape (*Brassica napus* L.)

Karla Müller, Ulf Böttcher, Franziska Meyer-Schatz, Henning Kage

Biosystems Engineering 101 (2008), 172-182

Abstract

Vegetation indices (VIs), which are derived from hyperspectral measurements, may be useful non-destructive measures to estimate crop canopy parameters. A systematic analysis of the reflectance spectrum of oilseed rape (OSR) for the derivation of VIs has not been conducted yet. We therefore derived in our study VIs from 61 available wavebands of the spectral range from 400 nm to 1000 nm systematically and compared the best ones to commonly used indices. Hyperspectral reflectance and destructive measurements of crop canopy parameters were therefore carried out in 2005 and 2006 in northern Germany for calibration and in 2006 for validation at the same location. For the derivation of VIs for OSR, three different approaches were tested. The approaches differed in the way of the waveband combinations by combining two wavebands in a simple ratio form (SR) λ1/ λ2, a normalized difference index form (NDI) (λ1-λ2)/(λ1+λ2) or by using a stepwise forward multiple regression (MR), which identifies the best linear combination of all available bands in a linear combination. The derived VIs were tested for their predictive power for crop canopy parameters like green area index (GAI), shoot dry matter (DM_{shoot}) and total nitrogen amount in the shoot (N_{shoot}) and were compared to commonly used indices.

Waveband combinations of two near-infrared bands resulted in the best prediction of the tested crop canopy parameters for calibration and validation data sets. Correlation coefficients (r^2) yielded values up to 0.82 between new indices and N_{shoot}. Especially, NDI 750,740 was best predicting GAI, whereas either NDI or SR forms of 740 nm and 780 nm showed best results predicting DM_{shoot} and N_{shoot} and outperformed commonly used indices. Predicting crop canopy parameters by MR showed good results for calibration, but highest variation for validation among all newly derived indices.

Nomenclature

CD	Coefficient of determination
DM_{shoot}	Shoot dry matter, g m^{-2}
EF	Modelling efficiency
GAI	Green area index, m^2 m^{-2}
IR/G	Infrared to green ratio
IR/R	Infrared to red ratio
LAI	Leaf area index, m^2 m^{-2}
λ	Wavelength, nm
MR	Multiple regression
N	Nitrogen
n	sample size
NDI	Normalized difference index
NDVI	Normalized difference vegetation index
NIRS	Near infrared spectroscopy
N_{shoot}	Total nitrogen amount in the shoot, kg ha^{-1}
OSR	Winter oilseed rape
r^2	Correlation coefficient
REIP	Red edge inflection point
RMSE	Root mean square error
SAVI	Soil adjusted vegetation index
SR	Simple ratio
VI	Vegetation index

1. Introduction

Spatial knowledge of crop canopy parameters like green area index (GAI), shoot dry matter (DM_{shoot}) and total nitrogen amount in the shoot (N_{shoot}) are an essential prerequisite for many approaches of site-specific crop management (Tarpley et al., 2000; Hansen and Schjoerring, 2003; Johnson et al., 2003; Lukina et al., 2001; Raun et al., 2002). Non-destructive, sensory measurements may be useful measures to assess those parameters in realtime and for large areas (Xue et al., 2004; Boegh et al., 2002). The use of spectral measurements of canopy reflectance is the most common approach for non-destructive measurements of crop canopy parameters (Elvidge and Chen, 1995; Thenkabail et al., 2001; Behrens et al., 2006; Graeff and Claupein, 2003) by correlating discrete spectral bands or combinations of them, so called vegetation indices (VIs) to crop canopy parameters. The mathematical combinations

of VIs can be made of either discrete wavebands from narrowband spectra (5-10 nm intervals) or from broadband spectra (> 50 nm intervals). While broadband spectra can be recorded since about three decades, high resolution spectral reflection measurements became more common just recently (Elvidge and Chen, 1995; Thenkabail et al., 2000) and some authors stated that VIs derived by narrowband spectra are supposed to be more sensitive to chlorophyll and other pigments (Broge and Leblanc, 2000; Blackburn, 1998; Thenkabail et al., 2002). Comparisons between broad- and narrowband based vegetation indices showed that the estimation of crop parameters by broadband measurements of canopy reflectance were less accurate than those by narrowband indices (Elvidge and Chen, 1995; Blackburn, 1998; Carter, 1998). For cereal crops and especially for winter wheat, several investigations on the prediction power of different vegetation indices were conducted (Reusch, 1997; Aparicio et al., 2000; Mistele, 2006). The therefore commonly used indices are derived from discrete spectral bands of the green, red and near infrared areas of the reflection spectrum (Reusch, 1997; Thiessen, 2002). Reusch (1997) as well as Filella et al. (1995) and Aparicio et al. (2000) stated that commonly used indices showed good relations to GAI, DM_{shoot} and N_{shoot} of cereal crops. Though, for winter oilseed rape (OSR) only few studies have been carried out regarding the spectral reflection based estimation of crop parameters. Behrens et al. (2006) applied spectral indices commonly used for cereals to OSR, which, however, resulted in less accurate predictions of crop canopy parameters like shoot fresh mass and shoot nitrogen content as compared to cereal crops. Recent sensors for spectral reflectance measurements allow for the discrimination of a large number of wavelength bands resulting in a high spectral resolution, so that methods have to be developed to systematically derive VIs out of all available spectral bands. VIs, which were newly derived, showed better correlations to different crop parameters of cereal crops than commonly used ones (Reusch, 2003), but those were also not tested for OSR yet. Therefore, there exists the potential to derive new VIs for a more precise prediction of OSR crop canopy parameters as compared to previous approaches.

The aim of our study was the derivation and identification of optimum VIs for the prediction of OSR crop canopy parameters as GAI, DM_{shoot} and N_{shoot} by a systematic comparison of VIs obtained by three different approaches based on narrow-band spectral reflectance measurements.

2. Materials and methods

2.1. Field experiments

Field experiments were carried out in 2005 and 2006 at the Hohenschulen experimental farm, 15 km to the west of Kiel. Winter oilseed rape (*Brassica napus* L.) was grown on an 11 ha field in 2005 and on an 18 ha field in 2006. Information on sowing dates, seeding densities, varieties and nitrogen application are shown in table 1. The fields were fertilized according to usual practice (200 kg N ha^{-1}) except for two unfertilized strips each year. Four blocks on selected positions within a strip contained four plots with different nitrogen treatments: Unfertilized (N0), 80 kg N ha^{-1} (N1), 200 kg N ha^{-1} (N2) and 240 kg N ha^{-1} (N3). The nitrogen was applied as ammonium nitrate/urea solution in two dressings at the beginning of plant growth in spring and the beginning of stem elongation. Otherwise the plants were treated according to best practice German recommendations.

2.2. Plant sampling

Plant sampling was carried out twice before winter and weekly from beginning of the growth period in spring until anthesis, so that an overall sample size of 339 was obtained. At each sampling date an area of 0.88 m^2 was harvested for analysis of green area index (GAI), total dry mass (DM_{shoot}) and total nitrogen content (N_{shoot}). The plants were fractionized into leaf blades and stem, whereas the petioles were counted as stem fraction. After drying and weighing, the fractions were ground for the near infrared spectroscopy (NIRS) analysis of the nitrogen concentration (NIRSystems 5000 scanning monochromator, FOSS GmbH, Rellingen, Germany). NIRS data were analysed using the WINISI software package (Infrasoft International, Port Matilda, PA, USA).

Table 1: Crop management information for the field experiment of spectral analysis on the experimental farm Hohenschulen in the years 2005 and 2006

Vegetation period	Sowing dates	Seeding density (seeds/m^2)	Variety	Date of 1st N-Application	Date of 2nd N-Application
2004/05	4 Sept. 2004	50	Talent	23 March 2005	14 April 2005
2005/06	24 Aug. 2005	45	Talent	22 March 2006	19 April 2006

2.3. Spectral reflectance measurements

Spectral reflectance of winter oilseed rape was determined using a HandySpec® Field spectrometer of tec5 AG (Oberursel, Germany). The measuring head of this device consists of two optical receive channels, of which the upper one quantifies the incoming light as

reference and the lower one records the reflectance by vegetation and ground, if visual. The HandySpec Field spectrometer measures in a spectral range from 400 nm - 1000 nm in 10 nm steps. Both optical channels were calibrated by using a white panel.
Reflectance measurements were carried out in spring 2005, autumn 2005, spring 2006 and autumn 2006. In parallel to intermediate destructive harvests from emergence in autumn to the flowering period, measurements were carried out by holding the measuring head about 1 m above the crop. During flowering the spectral reflectance of OSR changed considerably because of the yellow petals. Furthermore, after flowering the plants were too tall for holding the instrument manually above the crops. In order to obtain comparable reflectance data, the measurements were taken between two hours before and after solar zenith under consistent sky conditions.

2.4. Methods for calculation of vegetations indices and statistical analysis

To investigate correlations between crop parameters like GAI, DM_{shoot}, N_{shoot} and plant reflectance properties three approaches for the derivation of vegetation indices (VI) were used. The first and the second approach consisted of linear regressions between destructively measured crop parameters and all 3660 possible two-band combinations of 61 measured bands in a simple ratio (SR) form λ1/ λ2 and in the normalized difference index (NDI) form (λ1-λ2)/(λ1+λ2). These calculations were done using a self written software implemented in Delphi®, Borland. This tool gives a matrix output with all correlation coefficients (r^2) of the linear regressions (Fig. 1). For the third approach, a stepwise forward multiple regression (MR) was conducted to identify the best linear combination of all available bands for describing the parameters mentioned above. As long as the improvement of the correlation coefficient was better than 5%, more wavebands were added to the MR. Additionally, commonly used VIs were calculated, which are derived from very few discrete red, green and near infrared bands (Table 2). For the commonly used indices NDVI and SAVI, which showed saturation in the curve progression, linear regression was conducted after logarithmical transformation of the measured values. The SAS statistical package (SAS 8.2, SAS Institute Inc.) was used for statistical calculations.

Validation was carried out on an independent data set, containing 89 samples, of the vegetation period 2005/06 from another experiment field at the same site, which varied by two seeding dates, two varieties and four different N treatments, (N0), 80 kg N ha^{-1} (N1), 120 kg N ha^{-1} (N2) and 200 kg N ha^{-1} (N3). To characterize the predictive force of the derived VIs, slope (b) and intercept (a) and coefficient of correlation (r^2) of the linear regression (y=a+bx) between VIs and destructive measurements, root mean square error (RMSE, Eq. 1) of the 1:1 line (y=x), coefficient of determination (CD, Eq. 2) and modelling efficiency (EF, Eq. 3) are given.

$$RMSE = \sqrt{\frac{\sum (x_i - y_i)^2}{n}} \quad (1),$$

the coefficient of determination:

$$CD = \frac{\sum_{i=1}^{n} (x_i - \bar{x})^2}{\sum_{i=1}^{n} (y_i - \bar{x})^2} \quad (2),$$

and the modelling efficiency

$$EF = 1 - \frac{\sum (x_i - y_i)^2}{\sum (x_i - \bar{x})^2} \quad (3),$$

where x_i are the measured values, y_i are the estimated values, n is the number of samples, and $\bar{x}$ is the mean of the measured data.

Slope and intercept were tested on being significantly different to one and zero, respectively. Low RMSE values gave best account for the degree of precision of the estimated values. CD values served as a measure of how much the derived values lie under or over the measured ones. It is scaled from zero with no upper limit, whereas one stands for no differences from measured to estimated values. EF reflects the quality of the prediction curve compared to the data points. The values range from minus infinity to one, with higher values indicating better prediction power.

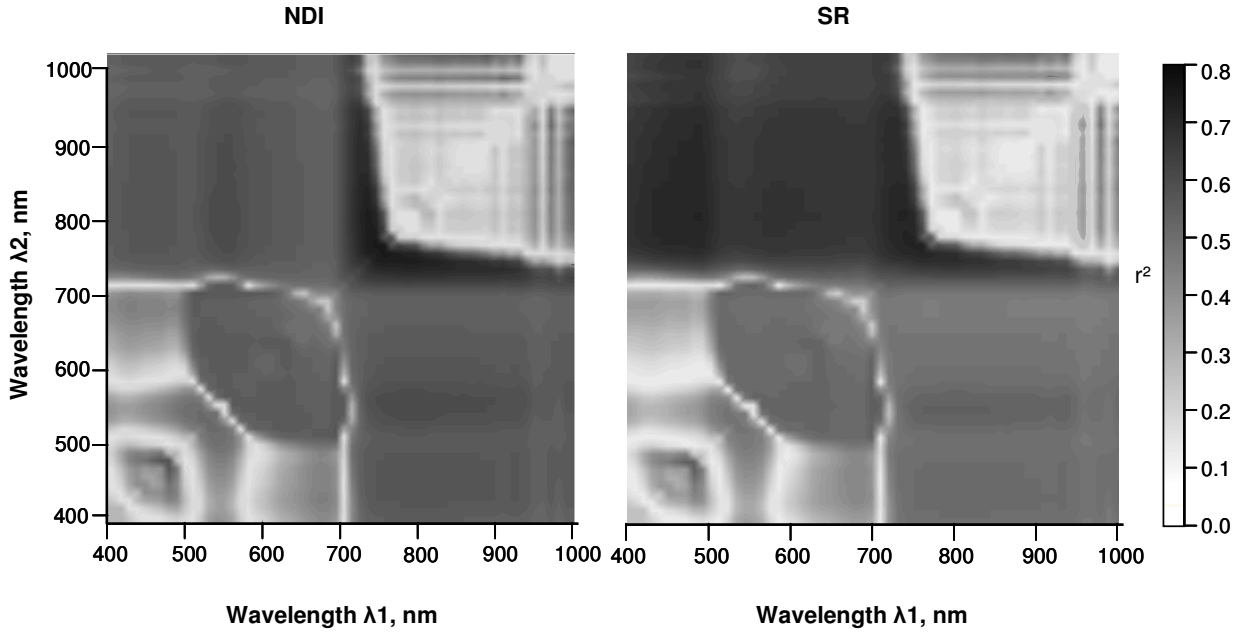

Figure 1: Matrix of the correlation coefficient (r^2) of the normalized difference indices (NDI) on the left and the simple ratio indices (SR) on the right to total nitrogen amount in the shoot, respectively. High r^2 values are indicated by dark coloured areas, lower values by brighter ones.

2.5. Applicability of newly generated VIs to distinguish differences of GAI, DM_{shoot} and N_{shoot}

To analyse the applicability of the newly generated VIs to indicate existent differences in crop canopy parameters like GAI, DM_{shoot} and N_{shoot}, an analysis of variance was calculated using the SAS statistical package. This was done for each intermediate harvest date from the first application in spring to anthesis.

Table 2: Definition of commonly used vegetation indices of visible and near-infrared reflectance for the estimation of crop parameters for winter crops and winter oilseed rape.

Commonly used indices	Equation	Reference
Reflectance at 850 nm	$\mathbf{R_{850nm}}$	Behrens et al. (2006)
SR 810/560	$\mathbf{SR} = \frac{\mathbf{R_{810nm}}}{\mathbf{R_{560nm}}}$	Xue et al. (2004)
Infrared to red ratio	$\mathbf{IR/R} = \frac{\mathbf{R_{780nm}}}{\mathbf{R_{670nm}}}$	Pearson and Miller (1972)
Infrared to green ratio	$\mathbf{IR/G} = \frac{\mathbf{R_{780nm}}}{\mathbf{R_{550nm}}}$	Takebe et al. (1990)
Normalized difference vegetation index	$\mathbf{NDVI} = \frac{\mathbf{R_{780nm}} - \mathbf{R_{670nm}}}{\mathbf{R_{780nm}} + \mathbf{R_{670nm}}}$	Bausch (1993)
Soil adjusted vegetation index	$\mathbf{SAVI} = \frac{1.5(\mathbf{R_{780nm}} - \mathbf{R_{670nm}})}{\mathbf{R_{780nm}} + \mathbf{R_{670nm}} + 0.5}$	Huete (1988)
Red edge inflection point	$\mathbf{REIP} = 700\mathbf{nm} + 40\mathbf{nm}\frac{0.5(\mathbf{R_{670nm}} + \mathbf{R_{780nm}}) - \mathbf{R_{700nm}}}{\mathbf{R_{740nm}} - \mathbf{R_{700nm}}}$	Guyot and Baret (1988)

3. Results

3.1. Correlation between vegetation indices and crop canopy parameters of winter oilseed rape in a calibration data set

For the NDI form VI most relevant bands were identified between 720 nm and 800 nm in the near infrared area of the reflection spectrum (Fig.1, NDI). The SR combinations also showed high correlations in the near infrared area, but there are several combinations of near infrared and visible light reflection areas, which resulted in good correlations (Fig. 1, SR). This applies especially for SR combinations, where the first wavelength is taken from the near infrared and the second from the visible light spectrum.

There were marked differences in the adjusted r^2 and the RMSE values based on linear regressions of crop canopy parameters GAI, DM_{shoot} and N_{shoot} against the five best VIs that were newly derived by approach one and two, the commonly used ones and the best linear waveband combination by the multiple regressions for each crop parameter (Table 3). Since crop parameter values were logarithmically transformed for the commonly used indices NDVI and SAVI, RMSE for these two indices was calculated with retransformed values. New indices achieved higher correlations with all crop canopy parameters from the calibration data set for winter oilseed rape than commonly used indices. Highest r^2 for correlations of GAI (0.81) and DM_{shoot} (0.76) were calculated with wavebands selected by MR. Correlation coefficients for regressions between these crop canopy parameters and the other newly generated indices lay scantily below these results. For correlations to N_{shoot}, there were three new indices, which yielded an r^2 of 0.82.

IR/G and SR 810/560 achieved highest r^2 (0.71) of the commonly used indices to GAI, regarding DM_{shoot} the IR/G ratio yielded the highest value with 0.66 and for N_{shoot} REIP showed the best result with r^2=0.73.

Results for RMSE values were analogue to those of adjusted r^2 for new and commonly used indices. For GAI and DM_{shoot} the MR waveband combinations showed lowest RMSE with 0.43 $m^2\ m^{-2}$ and 58.78 g m^{-2}, respectively. With regard to N_{shoot}, SR 780/740 yielded the lowest value with 2.10 g m^{-2}. SR 810/560 achieved the lowest RMSE value among the commonly used indices regarding GAI with 0.53 $m^2\ m^{-2}$, for DM_{shoot} the lowest value was achieved by IR/G with 69.53 g m^{-2} and for N_{shoot} REIP showed the best result with 2.57 g m^{-2} (Table 3).

Since a large data base, with data from different development phases of winter oilseed rape over different years, was used for the correlations, it is important to assess the accuracy of several indices for the estimation of crop canopy parameters in differing growth periods based on just one regression over all growth phases. Figure 2 shows five plots (a-e) for the linear regressions of measured N_{shoot} to estimated N_{shoot} by five new indices, respectively; function parameters for the regressions were taken from table 4. The data points have different symbols for four different periods: after beginning of spring growth in 2005 and in 2006, before winter 2006 and 2007. The data points for each time period are evenly distributed along the regression line in each figure. No apparent aggregation of data for any specific period could be observed. Between the five VIs, there are marginal differences of distribution.

Table 3: Correlation coefficients of linear regressions and RMSE of different indices and green area index (GAI), shoot dry matter (DM_{shoot}) and total shoot N (N_{shoot}) of winter oilseed rape derived from the calibration data set. Number of n was 339 for each regression.

		Adj. r^2			RMSE		
		GAI [$m^2\ m^{-2}$]	DM_{shoot} [g m^{-2}]	N_{shoot} [g m^{-2}]	GAI [$m^2\ m^{-2}$]	DM_{shoot} [g m^{-2}]	N_{shoot} [g m^{-2}]
New indices	NDI 780,740	0.74***	0.72***	**0.82*****	0.51	63.06	2.13
	NDI 750,740	0.78***	0.74***	**0.82*****	0.46	61.28	2.13
	SR 780/740	0.75***	0.73***	**0.82*****	0.50	62.58	**2.10**
	SR 740/780	0.73***	0.72***	0.81***	0.51	63.62	2.16
	MR	**0.81*****	**0.76*****	0.81***	**0.43**	**58.78**	2.14
Commonly used indices	R850	0.26***	0.15***	0.16***	0.86	110.31	4.55
	SR 810/560	0.71***	0.65***	0.71***	0.53	70.44	2.66
	IR/R	0.70***	0.60***	0.63***	0.55	75.48	3.00
	IR/G	0.71***	0.66***	0.72***	0.54	69.53	2.63
	NDVI	0.71***	0.57***	0.55***	0.65[a]	86.52[a]	3.59[a]
	SAVI	0.65***	0.52***	0.51***	0.72[a]	100.14[a]	4.03[a]
	REIP	0.66***	0.63***	0.73***	0.58	72.39	2.57

Highest r^2 and lowest RMSE are bolded. The limit of significance was ***p<0.001, **p<0.01 and *p<0.05, respectively. [a] presents RMSE for logarithmically retransformed values.

3.2. Validation of newly generated VIs for winter oilseed rape

To validate the applicability of the VIs, the linear regression parameters (Table 4) for each index and all crop canopy parameters were used to estimate all three crop canopy parameters of an independent data set. In order to rank the different VIs in their predictive power we calculated several statistical parameters like the slope (b), intercept (a) and r^2 of the linear regressions (y=a+bx) along with the root mean square error values (RMSE) of the reference 1:1 line (y=x), coefficients of determination (CD) and modelling efficiency (EF) (Table 5). Since the regression is ideally supposed to have a slope of one and an intercept of zero, both functional parameters were tested on being significantly different to these values, respectively.

For GAI, MR was the only index, whose slope and intercept were not significantly different from one and zero, respectively. However, with regard to the other statistical parameter, this index lay above the average for RMSE of 0.81 $m^2\ m^{-2}$ and under the average for EF of 0.585; regarding CD, MR overestimated the predicted values compared to the measured data to a higher degree than the other indices underestimated them. All other new indices yielded slopes significantly different from one, but intercepts, which did not differ from zero. Although NDI 750,740 showed lowest RMSE with 0.77 $m^2\ m^{-2}$ and highest EF with 0.632 among the new indices, it also underestimated GAI to the highest degree a CD value of 1.416. All commonly used indices showed values significantly different from one and zero for slope and intercept, respectively. As a result, SR, IR/R and IR/G yielded lowest RMSE and highest EF values among all indices. With regard to CD, all commonly used indices showed a higher degree of underestimation of measured GAI values than the new ones, except for NDI 750,740.

For DM_{shoot}, again, MR was the only waveband combination with a slope and an intercept, which were not significantly different from one and zero, respectively, whereas RMSE and EF values for this index lay above and under the averaged ones. Also, MR was the only index that overestimated the measured DM_{shoot} among all indices. The rest of the new indices, except NDI 750,740, yielded slopes, which differed significantly from one, but the intercepts were not significantly different from zero. All four remaining indices showed similar results for RMSE of about 56 g m^{-2} and for EF around 0.83. For this crop parameter, commonly used indices showed higher RMSE and lower EF. SAVI was the only index that had a CD value closer to one than the new indices apart from NDI 750,740. Slopes and intercepts of the regression lines of estimated DM_{shoot} by the old indices to measured DM_{shoot} differed significantly from one and zero, respectively.

For N_{shoot}, there were three new indices, which showed either slopes as well as intercepts significantly different from one and zero, respectively. Among the new indices, these three indices yielded CD values, which were closest to one. Additionally, they showed EF results of

about 0.83 and RMSE less than 2.3 g m^{-2}. Slope and intercept for NDI 750,740 were significantly different from one and zero; slope for MR was significantly different from one, but its intercepts differed not significantly from zero. Again, MR reached highest RMSE and lowest EF among the new indices, whereas NDI 750,740 yielded lowest RMSE and highest EF. In contrast to the CD values for DM_{shoot} and GAI, all new indices, except for NDI 750,740, yielded values lower than one, indicating, that they overestimated N_{shoot}. Among the commonly used indices, REIP was the only one that had an intercept, which did not differ from zero significantly. All other slopes and intercepts were significantly different from one and zero, respectively. Among all indices REIP achieved the second highest EF value and the second lowest RMSE. With regard to CD values, all commonly indices, except for R850 and NDVI, yielded values closer to one than the new indices.

Since waveband combinations of 780 and 740 in either the SR or the NDI form showed best results among all statistical measures for estimating GAI, DM_{shoot} and N_{shoot}, 1:1 plots for estimated parameter values to measured ones are shown exemplarily for SR 740/780 in figure 3 (a-c). Regarding the 1:1 lines, highest estimation accuracy was achieved for N_{shoot} (c) and lowest for GAI (a).

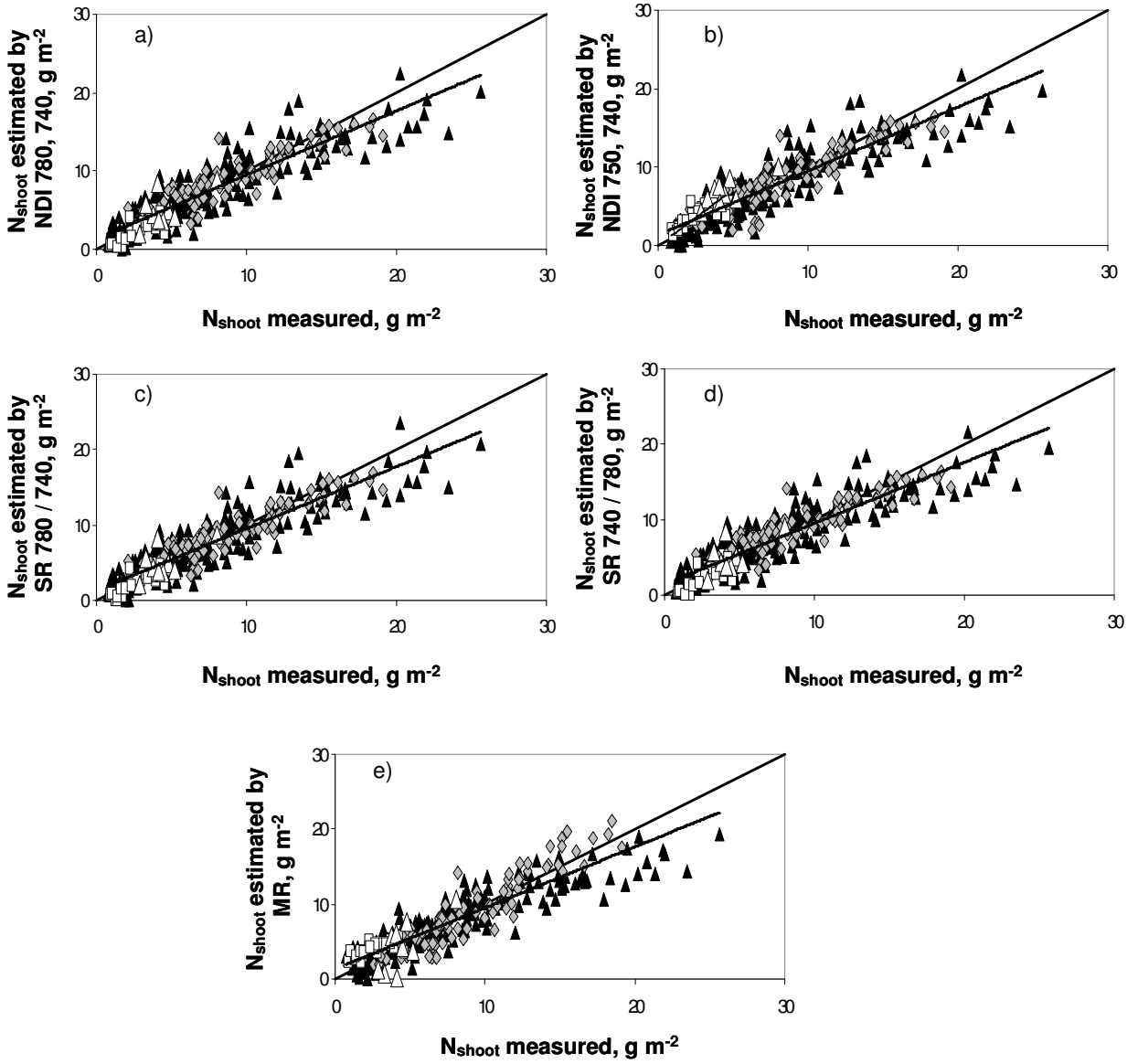

Figure 2: Linear regression of the total amount of N in the shoot (N_{shoot}) estimated by five different new indices to measured N_{shoot} values. All regressions contain data from four different time periods: after beginning of spring growth in 2005 (▲) and in 2006 (◇) and before winter 2006 (△) and 2007 (□). The regression functions and r^2 for all subfigures are as followed: a) NDI 780,740, y=0.82x+1.36, r^2=0.82 b) NDI 750,740, y=0.82x+1.37, r^2=0.82 c) SR 780/740, y=0.82x+1.32, r^2=0.82 d) SR 740/780, y=0.81x+1.41, r^2=0.81 and e) MR, y=0.81x+1.38, $r^2$0.81

Table 4: Functional parameters of several indices for estimating green area index (GAI), shoot dry matter (DM_{shoot}) and total shoot N (N_{shoot}) of winter oilseed rape.

	Estimation of Green-Area-Index by GAI = a +b*Index and for NDVI and SAVI lnGAI = a +b*Index		Estimation of dry matter shoot by DM_{shoot} = a +b*Index and for NDVI and SAVI $lnDM_{shoot}$ = a +b*Index		Estimation of total shoot N by N_{shoot} = a +b*Index and for NDVI and SAVI lnN_{shoot} = a +b*Index	
	b	a	b	a	b	a
NDI 780,740	35.91	-0.71	4243	-92.45	187.3	-4.25
NDI 750,740	56.67	-0.58	6585	-73.04	287.4	-3.27
SR 780/740	15.63	-16.21	1843	-1919	81.36	-84.87
SR 740/780	-20.36	19.51	-2409	2301	-106.3	101.3
R850	2.72	0.27	245.0	58.97	10.52	2.57
SR 810/560	0.42	-0.54	48.03	-63.90	2.08	-2.80
IR/R	0.14	0.27	15.48	32.04	0.66	1.46
IR/G	0.44	-0.61	51.21	-73.99	2.22	-3.23
NDVI	3.02	-1.93	3.05	2.73	2.77	-0.19
SAVI	3.02	-1.41	3.02	3.26	2.77	0.28
REIP	0.35	-247	40.63	-29071	1.81	-1297
Estimations by MR						
GAI = 0.38*λ660 - 24.13*λ730 + 18.30*λ780 + 1.35						
DM_{shoot} = -5565*λ400 + 2225*λ570 - 3226*λ730 + 2220*λ780 + 219.7						
N_{shoot} = -1.09*λ400 – 129.2*λ730 + 93.61*λ780 + 8.65						

3.3. Efficiency of vegetation indices to indicate relative differences of crop canopy parameters of winter oilseed rape

Increasing amounts of nitrogen application to winter oilseed rape led to increasing values for crop canopy parameters GAI, DM_{shoot} and N_{shoot} (Table 6). This relationship is also depicted in figure 4, where increasing amounts of fertilizer N lead to increased reflectance in the near-infrared region, which is caused by increased biomass. Analysis of variance was calculated for each date after the second nitrogen application in springtime for all three crop canopy parameters and four different new indices in 2005, only (Table 6). On the first date, there were significant differences between the N0 treatment and the other N treatments for GAI, N_{shoot} and the indices, whereas the indices values additionally gave significant differences between the N1 and N3 treatments. For DM_{shoot} no differences could be found. GAI and N_{shoot} showed the same response to N application on the second date as compared to the first date. DM_{shoot} was significantly different between N0 and N3 on the second date. For this date, all indices values resulted in significant differences of N0 to the other treatments and between N1 and the two higher fertilized treatments. On the last date, before anthesis, GAI and N_{shoot} showed the same levels of significance as the indices on the second date. The response of DM_{shoot} was the same as for the second date. For all indices there were significant differences between N0 and the other three treatments, and for N1 and N2 in comparison to N3.

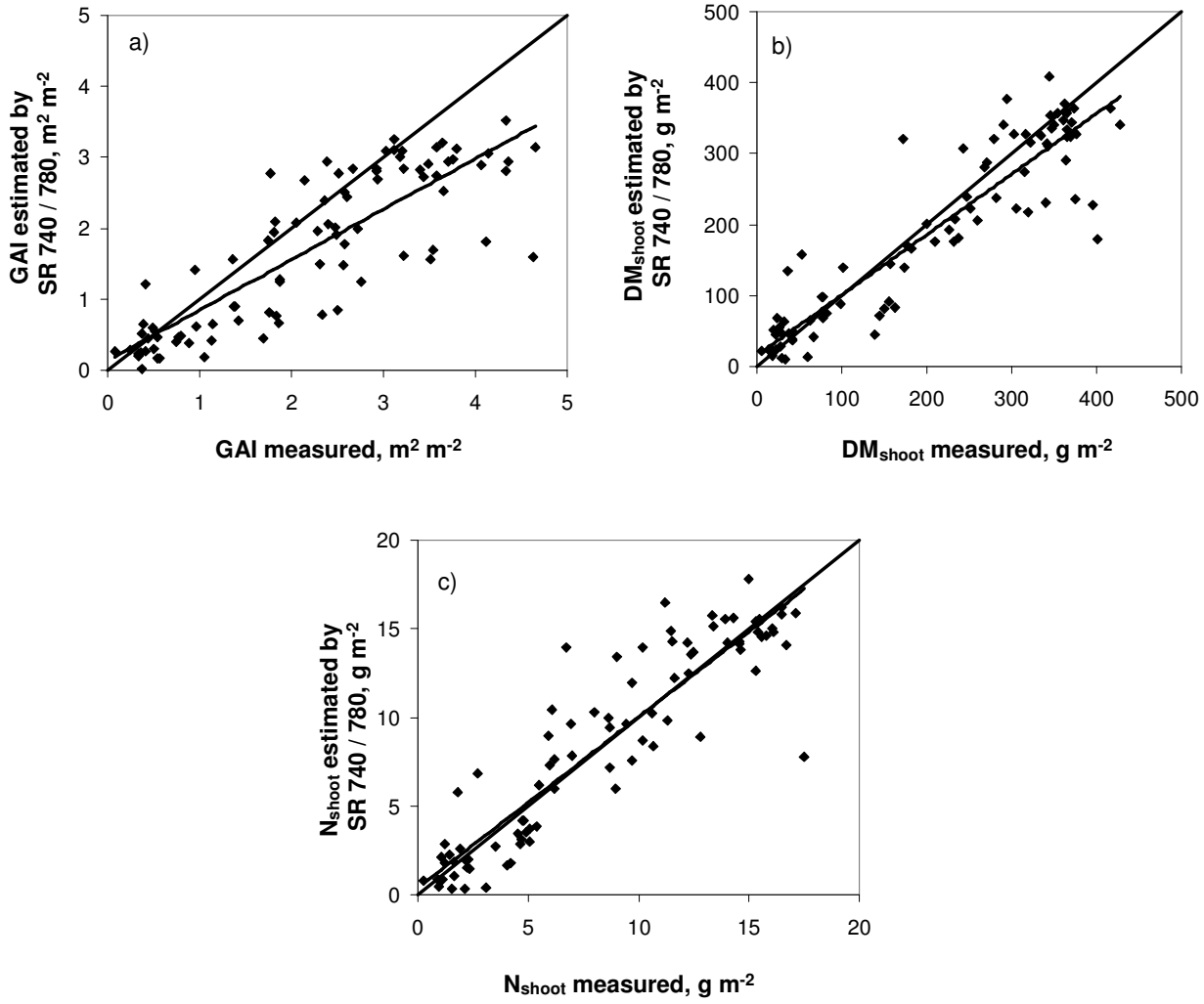

Figure 3: Linear regression of estimated crop canopy parameters green area index (GAI), shoot dry matter (DM_{shoot}) and total shoot N (N_{shoot}) by SR 740/780 to measured parameter values for the validation data set. The regression functions and r^2 for all subfigures are as followed: a) y=0.71x+0.14, r^2=0.71 b) y=0.85x+15.45, r^2=0.85 and c) y=0.96x+0.39, r^2=0.84

Table 5: Slopes (b), intercepts (a) and correlation coefficients (r^2) of linear validation regressions (y=a+bx), root mean square errors (RMSE) of the 1:1 regression line (y=x), coefficients of determination (CD) and modelling efficiency (EF) of estimated values of green area index (GAI), shoot dry matter (DM_{shoot}) and total shoot N (N_{shoot}) by several indices to measured values derived from the validation data set. Additionally, the averaged statistical parameter over all indices is given. Number of n was 89 for each regression.

GAI		b	a	r^2	RMSE [$m^2\ m^{-2}$]	CD	EF
New indices	NDI 780,740	0.712***	0.145	0.71***	0.84	1.162	0.563
	NDI 750,740	0.669***	0.283	0.76***	**0.77**	1.416	**0.632**
	SR 780/740	0.712***	0.157	0.70***	0.84	1.165	0.565
	SR 740/780	0.711***	0.137	0.71***	0.84	**1.161**	0.560
	MR	0.954	0.029	0.68***	0.84	0.744	0.564
Commonly used indices	R850	0.366***	1.317***	0.49***	0.94	3.593	0.454
	SR 810/560	0.689***	0.567***	0.72***	**0.68**	1.501	0.712
	IR/R	0.663***	0.854***	0.73***	**0.68**	1.630	**0.713**
	IR/G	0.687***	0.549***	0.72***	0.69	1.500	0.706
	NDVI	0.355***	1.073***	0.67***	0.94	3.894	0.452
	SAVI	0.673***	0.958***	0.62***	0.82	1.311	0.583
	REIP	0.664***	0.132***	0.75***	0.89	**1.227**	0.513
	Mean	0.655	0.517	0.69	0.81	1.692	0.585
DM_{shoot}		b	a	r^2	RMSE [$g\ m^{-2}$]	CD	EF
New indices	NDI 780,740	0.852***	16.72	0.84***	56.22	1.146	0.831
	NDI 750,740	0.755***	41.54***	0.83***	57.65	1.453	0.822
	SR 780/740	0.850***	18.49	0.84***	56.98	**1.145**	0.827
	SR 740/780	0.852***	15.45	0.85***	**55.74**	1.149	**0.834**
	MR	1.032	8.95	0.78***	76.70	0.725	0.686
Commonly used indices	R850	0.318***	159.6***	0.52***	103.87	4.708	0.423
	SR 810/560	0.783***	72.91***	0.82***	64.40	1.270	0.778
	IR/R	0.697***	114.1***	0.76***	85.65	1.267	0.608
	IR/G	0.790***	69.32***	0.83***	62.76	1.265	0.790
	NDVI	0.360***	125.0***	0.68***	94.05	5.172	0.527
	SAVI	0.694***	118.0***	0.66***	96.79	**1.126**	0.499
	REIP	0.771***	19.55*	0.84***	**62.23**	1.337	**0.793**
	Mean	0.730	64.97	0.77	72.75	1.814	0.702
N_{shoot}		b	a	r^2	RMSE [$g\ m^{-2}$]	CD	EF
New indices	NDI 780,740	0.966	0.424	0.84***	2.29	0.896	0.814
	NDI 750,740	0.855***	1.530***	0.85***	**2.12**	1.150	**0.841**
	SR 780/740	0.966	0.480	0.83***	2.31	0.892	0.811
	SR 740/780	0.963	0.388	0.84***	2.27	**0.901**	0.817
	MR	1.193**	-0.116	0.80***	3.60	0.542	0.540
Commonly used indices	R850	0.353***	1.681***	0.53***	5.29	1.429	0.007
	SR 810/560	0.870**	3.009***	0.81***	3.02	0.940	0.676
	IR/R	0.762***	4.858***	0.75***	3.95	0.928	0.446
	IR/G	0.875**	2.870***	0.82***	2.96	0.944	0.690
	NDVI	0.357***	5.583***	0.63***	3.72	4.865	0.509
	SAVI	0.696***	5.185***	0.66***	4.10	**1.012**	0.404
	REIP	0.881**	0.505	0.83***	**2.24**	1.062	**0.821**
	Mean	0.811	2.200	0.77	3.16	1.297	0.615

Slopes and intercepts were tested on being significantly different to 1 and 0, respectively. Lowest RMSE, higest EF and CD closest to one are bolded for new and commonly used indices. The limit of significance was ***p<0.001, **p<0.01 and *p<0.05, respectively.

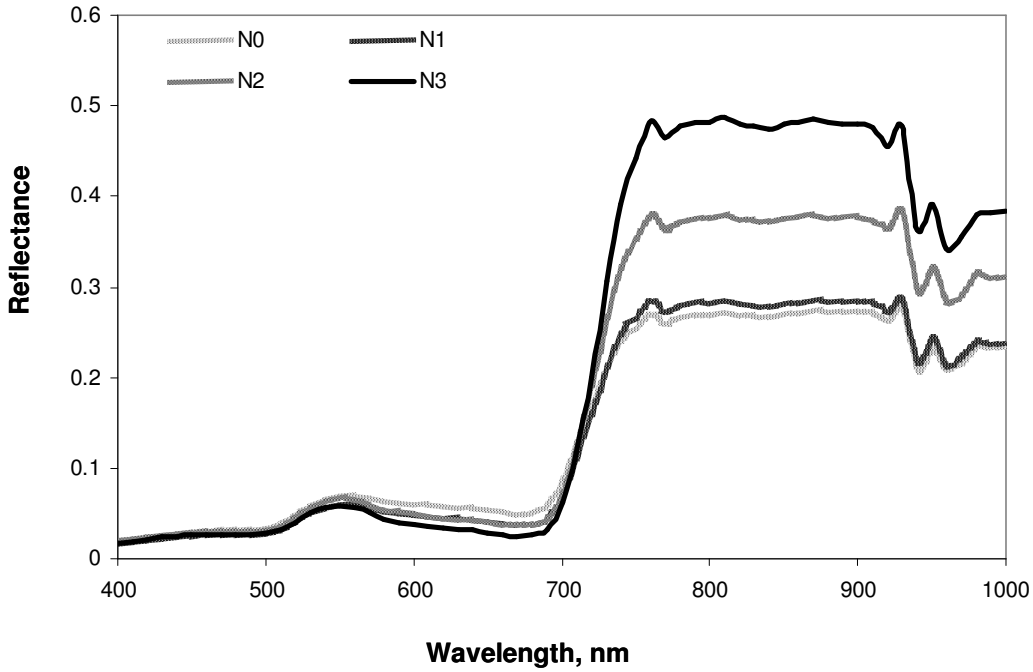

Figure 4: Canopy reflectance spectra of four differently fertilized winter oilseed rape plots of one block on 29 April 2005: 0 kg N ha^{-1} (N0), 80 kg N ha^{-1} (N1), 160 kg N ha^{-1} (N2) and 240 kg N ha^{-1} (N3).

Table 6: Green area index (GAI), shoot dry matter (DM_{shoot}), total shoot N (N_{shoot}), NDI 780/740, NDI 750/740, SR 780/740 and SR 740/780 as affected by four different N treatments on three different measuring dates

		N rate (kg ha^{-1})			
		0	80	160	240
18.04.2005	GAI	1.01 b	1.60 a	1.79 a	1.82 a
	DM_{shoot} [g m^{-2}]	147.78 a	199.96 a	209.83 a	204.46 a
	N_{shoot} [g m^{-2}]	4.67 b	8.33 a	10.37 a	10.80 a
	NDI 780,740	0.044 c	0.062 b	0.072 ab	0.076 a
	NDI 750,740	0.249 c	0.038 b	0.044 ab	0.046 a
	SR 780/740	1.092 c	1.134 b	1.157 ab	1.165 a
	SR 740/780	0.917 a	0.883 b	0.867 bc	0.860 c
26.04.2005	GAI	1.03 b	1.65 a	2.00 a	2.10 a
	DM_{shoot} [g m^{-2}]	187.27 b	271.16 ab	273.01 ab	297.89 a
	N_{shoot} [g m^{-2}]	5.31 b	9.60 a	13.10 a	13.22 a
	NDI 780,740	0.039 c	0.068 b	0.086 a	0.091 a
	NDI 750,740	0.020 c	0.041 b	0.053 a	0.054 a
	SR 780/740	1.083 c	1.146 b	1.188 a	1.200 a
	SR 740/780	0.925 a	0.874 b	0.843 c	0.834 c
03.05.2005	GAI	1.32 c	2.30 b	3.43 a	3.71 a
	DM_{shoot} [g m^{-2}]	241.58 b	319.26 ab	390.20 a	383.80 a
	N_{shoot} [g m^{-2}]	6.39 c	10.81 b	16.84 a	18.12 a
	NDI 780,740	0.051 c	0.091 b	0.097 b	0.119 a
	NDI 750,740	0.032 c	0.057 b	0.060 b	0.073 a
	SR 780/740	1.108 c	1.200 b	1.215 b	1.270 a
	SR 740/780	0.903 a	0.834 b	0.824 b	0.788 c
Values followed by different letters are significantly different with $p<0.05$.					

4. Discussion

In our study, newly generated indices of the SR and NDI form showed improvements in estimating all three crop canopy parameters compared to the commonly used ones, even though some commonly used indices like the IR/G and the REIP showed stable prediction power for individual crop canopy parameters. Among the newly derived VIs, the waveband combinations of two bands from the infrared region particularly showed good correlations. From these waveband combinations especially those derived from λ750 und λ740 in the NDI form and from λ740 und λ780 in the NDI form as well as in the SR form showed stable results for most crop canopy parameters and both calibration and validation. Mainly for N_{shoot}, EF as well as RMSE showed best results for these waveband combinations in the range of 0.82 and 2.1 g m^{-2}, respectively. Correlation coefficients for the multiple regression were highest among all indices for GAI and DM_{shoot} for the calibration, but in the course of validation, this method showed comparable large prediction errors. The reason for this is presumably the higher number of parameters, which can be object to parameter uncertainty and as a result lead to considerably higher prediction error compared to the description error in the parameterisation data set. This explanation is also underlined by the fact, that the commonly used less complex indices with a lower number of parameters in the SR or the NDI form, show stable results for calibration and validation. Least applicability for estimating crop canopy parameters showed the single waveband R850, which had highest RMSE, lowest EF and CD values that were most different from one for all three crop canopy parameters. This may be due to the interference of single wavebands with noise of the measuring instrument, which responds sensitive to changes of radiation intensity and sky condition (Reusch, 1997).

Since reflectance in the visible region of the spectrum approaches saturation with leaf area index (LAI) values of higher than three, VIs derived from those wavelengths are not applicable for the estimation of crop canopy parameters in later stages of plant development (Filella et al., 1995; Aparicio et al., 2000). Near infrared light needs a higher LAI to reach saturation of reflectance, and therefore VIs based on these wavelengths can be used to estimate crop canopy parameters like biomass even in late phases of the vegetation period (Tarpley et al., 2000). However, not only the amount of leaves, but also their thickness and structure influence the near infrared reflectance (Slaton et al., 2001; Read et al., 2002). The higher the fraction of spongy tissue inside the mesophyll and thereby the cell surface area which is exposed to intercellular air spaces, the higher the amount of internal reflection (Terashima and Saeki, 1983; Knapp and Carter, 1998) and hence measurable reflectance above the canopy. Reflectance in the visible light area is also influenced by the leaf structure, but mainly by the consistence, disposal and amount of photosynthetic pigments (Carter,

2001; Gitelson et al., 2003). In contrast to the mesophyll of OSR leaves, which is separated into palisade and spongy tissues (bifacial leaves), leaves of winter wheat have a non-differentiated mesophyll, leading to fewer structural differences among winter wheat leaves (Gausman and Allen, 1973). Among bifacial leaves, there are strong distinctions concerning the ratios of palisade to spongy tissues caused by age and exposure differences (Vogelmann, 1993; Stefanowska et al., 1999). The uniform structure of winter wheat leaves might be the reason, why VIs derived by visible wavebands reached better correlations to crop canopy parameters of winter wheat compared to those of OSR.

Overall, regarding statistical parameters like RMSE, CD and EF, newly derived VIs were firstly well suited to estimate crop canopy parameters (Table 5) and were secondly applicable to detect differences between differently treated OSR crops (Table 6). Their applicability to detect differences between different N treatments thereby was higher than the power of the destructive reference methods we used. This may be attributed to the fact that a larger sampling area is included in each single reflectance measurement and that therefore reflection measurements are less sensitive to local variations in crop canopy parameters caused by plant-to-plant variability. Strongest correlations of VIs were identified with N_{shoot}, but also predictions of GAI and DM_{shoot} with newly derived indices were better than with commonly used ones. In case of N_{shoot} reflectance is not based on one single parameter, but a combination of two different canopy character traits, biomass and amount of chlorophyll in the plant. This combination might stabilize N_{shoot} prediction based on crop reflectance measurements.

Even though the results were calibrated and validated on data from only one location, there is strong evidence, that they are also applicable to other locations due to the fact that reflection depends on physical properties of leaves. Since the reflection in the near-infrared region is determined mainly by vital biomass, estimation of crop canopy parameters by VIs from near-infrared wavebands is likely transferable to other sites.

Because one advantage of this method is the estimation of crop canopy parameters in realtime for a large area with less effort than destructive measurements would take, it can be used in different ranges of application. One the one hand, it can be used for new fertilization techniques, which calculate optimal amounts of nitrogen fertilizer based on different soil and crop canopy parameters, and therefore need information on the current aboveground biomass, which can be derived by vegetation indices. On the other hand, it can be used by plant breeders, who might need to identify crop canopy parameters for many different and differently treated varieties in a time saving way.

To sum up, the outcomes of this study give strong evidence that VIs derived by narrowband reflectance spectra are not only helpful measures for estimating and predicting crop canopy parameters for cereal crops, but could be applied with a similar accuracy also for winter

oilseed rape. By systematically deriving VIs in different approaches from hyperspectral measurements, new VIs were successfully detected and their applicability was successfully assessed for winter oilseed rape. For the estimation of GAI, especially NDI 750,740 showed best prediction power according to calibration and validation. DM_{shoot} and N_{shoot} were best predicted by either NDI 750,740 or SR combinations of 780 nm and 740nm, depending on results of calibration or validation.

5. Conclusions

Systematic analysis of hyperspectral reflectance measurements in the SR and NDI form for winter oilseed rape was a useful approach for deriving new vegetation indices. These indices were successfully used to estimate crop canopy parameters like GAI, DM_{shoot} and N_{shoot} during the vegetation period and their prediction power exceeded commonly used indices. Particularly, NDI 750,740 served best to estimate GAI and DM_{shoot} and N_{shoot} were best predicted by either NDI or SR forms of 740 nm and 780 nm. Using these indices enables to identify small differences between crop canopy parameters in realtime and for large areas. Regarding calibration and validation, the indices showed stable results and there is strong evidence, that they are also applicable to other locations. There are several application potentials to transfer this method into practice. Fertilization techniques may benefit from this method as well as plant breeders, who both need to accurately identify crop canopy parameters.

Acknowledgements

Thanks to Dr. Andreas Pacholski for his constructive comments on the manuscript. Thanks to the DBU, German Federal Environmental Foundation, for kindly supporting my project.

References

Aparicio, N., Villegas, D., Casadesus, J., Araus, J.L., Royo, C. (2000). "Spectral vegetation indices as nondestructive tools for determining durum wheat yield." Agronomy Journal 92: 83-91.

Bausch, W. C. (1993). "Soil background effects on reflectance-based crop coefficients for corn." Remote Sensing of Environment 46:213-222.

Behrens, T., Müller, J., Diepenbrock, W. (2006). "Utilization of canopy reflectance to predict properties of oilseed rape (*Brassica napus* L.) and barley (*Hordeum vulgare* L.) during ontogenesis." European Journal of Agronomy 25: 345-355.

Blackburn, G. A. (1998). "Spectral indices for estimating photosynthetic pigment concentrations: a test using senescent tree leaves." International Journal of Remote Sensing 19: 657-675.

Boegh, E., Soegaard, H., Broge, N., Hasager, C.B., Jensen, N.O., Schelde, K., Thomsen, A. (2002). "Airborne multispectral data for quantifying leaf area index, nitrogen concentration, and photosynthetic efficiency in agriculture." Remote Sensing of Environment 81: 179-193.

Broge, N. H., Leblanc, E. (2000). "Comparing prediction power and stability of broadband and hyperspectral vegetation indices for estimation of green leaf area index and canopy chlorophyll density." Remote Sensing of Environment 76: 156-172.

Carter, G. A. (1998). "Reflectance Wavebands and Indices for Remote Estimation of Photosynthesis and Stomatal Conductance in Pine Canopies - a promising technique to rapidly determine nitrogen and cholophyll content." Remote Sensing of Environment 63: 61-72.

Carter, G. A., Knapp, A. K. (2001). "Leaf optical properties in higher plants: Linking spectral characteristics to stress and chlorophyll concentration." american Journal of Botany 88(4): 677-684.

Elvidge, C. D., Chen, Z. (1995). "Comparison of broad-band and narrow-band red and near-infrared vegetation indices." Remote Sensing of Environment 54: 38-48.

Filella, I., Serrano, L., Serra, J., Penuelas, J. (1995). "Evaluating wheat nitrogen status with canopy reflectance indices and discriminant analysis." Crop Science 35: 1400-1405.

Gausman, H. W., Allen, W. A. (1973). "Optical Parameters of Leaves of 30 Plant Species." Plant Physiology 52: 57-62.

Gitelson, A. A., Gritz, Y., Merzlyak, M. N. (2003). "Relationships between leaf chlorophyll content and spectral reflectance and algorithms for non-destructive chlorophyll assessment in higher plant leaves." Journal of Plant Physiology 160: 271-282.

Graeff, S., Claupein, W. (2003). "Quantifying nitrogen staus of corn (*Zea mays* L.) in the field by reflectance measurements." European Journal of Agronomy 19: 611-618.

Guyot, G., Baret, F., Major, D. J. (1988). "High spectral resolution: Determination of spectral shifts between the red and the near infrared." International Archives of Photogrammetry and Remote Sensing 11: 750-760.

Hansen, P. M., Schjoerring, J.K. (2003). "Reflectance measurement of canopy biomass and nitrogen status in wheat crops using normalized difference vegetation indices and partial least squares regression." Remote Sensing of Environment 86: 542-553.

Huete, A. R. (1988)." A soil adjusted vegetation index (SAVI)." Remote Sens. Envir. 25: 295-309.

Johnson, C. K., Mortensen, D. A., Wienhold, B. J., Shanahan, J. F., Doran, J. W. (2003). "Site-Specific Management Zones Based on Soil Electrical Conductivity in a Semiarid Cropping System." Agronomy Journal 95: 303-315.

Knapp, A. K., Carter, G. A. (1998). "Variability in leaf optical properties among 26 species from a broad range of habitats." American Journal of Botany 85: 940-946.

Lukina, E. V., Freemann, K. W., Wynn, K. J., et al. (2001). "Nitrogen fertilization optimization algorithm based on in-season estimates of yield and plant nitrogen uptake." Journal of Plant Nutrition 24: 885-898.

Mistele, B. (2006). Tractor based spectral reflectance measurements using an oligo view optic to detect biomass, nitrogen content and nitrogen uptake of wheat and maize and the nitrogen nutrition index of wheat. Institute of plant nutrition. Munich, Technische Universität München: 72.

Raun, W. R., Solie, J. B., Johnson, G. V., Stone, M. L., Mullen, R. W., Freemann, K. W., Thomason, W. E., Lukina, E. V. (2002). "Improving Nitrogen Use Efficiency in Cereal Grain Production with Optical Sensing and Variable Rate Application." Agronomy Journal 94: 815-820.

Read, J. J., Tarpley, L., McKinion, J. M., Reddy, K. R. (2002). "Narrow-Waveband reflectance ratios for remote estimation of nitrogen status in Cotton." Journal of Environmental Quality 31: 1442-1452.

Reusch, S. (1997). Entwicklung eines reflexionsoptischen Sensors zur Erfassung der Stickstoffversorgung landwirtschaftlicher Kulturpflanzen. Institut für Landwirtschaftliche Verfahrenstechnik. Kiel, Christian-Albrechts-Universität: 156.

Reusch, S. (2003). N-uptake under changing irradiance conditions. 4th ECPA, Berlin, Wageningen Academic Publishers.

Slaton, M. R., Hunt, E. R., Smith, W. K. (2001). "Estimating near-infrared leaf reflectance from leaf structural characteristics." American Journal of Botany 88: 278-284.

Stefanowska, M., Kuras, M., Kubacka-Zebalska, M., Kacperska, A. (1999). "Low temperature affects pattern of leaf growth and structure of cell walls in Winter Oilseed Rape (*Brassica napus* L., var. *oleifera* L.)." Annals of Botany 84: 313-319.

Takebe, M., Yoneyama, T., Inada, K., Murakami, T. (1990). "Spectral reflectance ratio of rice canopy for estimating crop nitrogen status." Plant and Soil 122: 295-297.

Tarpley, L., Reddy, K. R., Sassenrath-Cole, G. F. (2000). "Reflectance indices with precision and accuracy in predicting cotton leaf nitrogen concentration." Crop Science 40: 1814-1819.

Terashima, I., Saeki, T. (1983). "Light Environment within a leafI. Optical Properties of paradermal Sections of Camellia leaves with special reference to differences in the

optical properties of palisade and spongy tissues." Plant and Cell Physiology 24: 1493-1501.

Thenkabail, P. S., Smith, R. B., De Pauw, E. (2002). "Evaluation of narrowband and broadband vegetation indices for determing optimal hyperspectral wavebands for agricultural crop characterization." Photogrammetric engineering and remote sensing 68: 607-621.

Thenkabail, P. S., Smith, R.B., Pauw, de E. (2001). "Hyperspectral vegetation indices and their relationships with agricultural crop characteristics." Remote Sensing of Environment 71: 158-182.

Thenkabail, P. S., Smith, R.B., Pauw, de E. (2000). Hyperspectral vegetation indices for determining agricultural crop characteristics. New Haven, Yale University.

Thiessen, E. (2002). "Optische Sensortechnik für den teilflächenspezifischen Einsatz von Agrarchemikalien." Institut für Landwirtschaftliche Verfahrenstechnik. Kiel, Christian-Albrechts-Universität: 88.

Vogelmann, T. C. (1993). "Plant tissue optics." Annual Reviews Plant Physiology and Plant Molecular Biology 44: 231-251.

Xue, L., Cao, W., Luo, W., Dai, T., Zhu, Y. (2004). "Monitoring leaf nitrogen status in rice with canopy spectral reflectance." American Society of Agronomy 96: 135-142.

Chapter 3

Revision and Parameterisation of a Phenological Model for Winter Oilseed Rape (*Brassica napus* L.)

Karla Müller, Ulf Böttcher, Henning Kage

Abstract

Phenological models can be useful tools for a more precise production management in agriculture and they are inevitable parts of mechanistic crop growth models. For most major crops a number of phenological models have been developed and evaluated. For winter oilseed rape (*Brassica napus* L.) (OSR) only few studies are available. Particularly, models that give detailed description of distinct development stages according to the most commonly used BBCH scale are missing for winter oilseed rape. To obtain a more detailed description of development according to the BBCH scale, BRASNAP-PH, an existing phenological model for OSR was modified in several ways. Some parameters were deleted or displaced interchanged, an additional developmental rate was integrated, enabling the calculation of leaf development and stem elongation rates separately. Also, equations for the derivation of BBCH stages out of DVS were implemented. During leaf development, BBCH stages were derived from the number of visible leaves, which were estimated using the newly estimated phyllochron. These structural changes of the model enabled an easier parameterization from field observations, because BBCH stage is defined by visible events of plant morphology. The modified model was calibrated and validated on a large data set that contains 114 different year/location combinations for 11 years, 76 locations and 37 varieties throughout Germany. Validation and cross validation let to a root mean square error (RMSE) of 3.11 and 3.25 BBCH stages, respectively for the whole developmental phase. The modified model was able to estimate phenological development of OSR across different sites within Germany. Since all important developmental stages depend on temperature and photoperiod only, the model can be used for other agro-ecological regions after adapting the parameters to the local situation.

Nomenclature

BBA	Federal Biological Research Centre for Agriculture and Forestry
BBCH	Biologische Bundesanstalt and Chemical industry
CD	Coefficient of determination
°C	Degree celcius
°Cd	Degree day
d	Day
DVS	Development stage
E	Emergence
EF	Modelling efficiency
EFl	End of flowering
F_p	Photoperiodical factor
F_v	Vernalization factor
GDD	Growing degree day
M	Maturity
OFl	Onset of flowering
OSR	Winter oilseed rape
r^2	Coefficient of correlation
RMSE	Root mean square error
S	Sowing
SE	Standard error
SS	Sum of squares
Teff	Effective daily temperature
ZEPP	Zentralstelle der Länder für EDV-gestütze Entscheidungshilfen und Programme im Pflanzenschutz

1. Introduction

During the last decades, many models have been developed predicting the phenological development of most major crops. Knowledge on phenology is important to generally understand the development of crops and its prediction can be used as a decision tool for a more precise production management. Phenology models are inevitable parts of mechanistic crop growth models as partitioning processes of carbon and nutrients are strongly influenced by the phenological status of a crop. Many phenological models have been investigated for cereal crops, notably winter wheat, while only few have been developed and tested for winter oilseed rape (OSR). Concerning the modelling of development, photoperiod and

vernalization are the main factors that control the process of transition from the vegetative to the generative phase for winter oilseed rape as well as for other winter annual crops (Hodges et al., 1991). Gabrielle et al. (1998) developed a crop growth model for winter oilseed rape based on CERES-Wheat, thereby containing, among others, components for crop phenology. Farré et al. (2002) applied the APSIM modelling framework to canola, putting emphasis on the prediction of flowering and grain yield. Roßberg et al. (2005) worked on a phenological model, SIMONTO, for cereals and winter oilseed rape, that contained components of ONTO and CERES-Wheat. His model achieved only low prediction power for OSR, although a large data set was used for calibration. Intensive work has been done by Habekotté (1997), who developed BRASNAP-PH that was parameterized for northwest Europe. This model achieved high accuracy for the prediction of five selected developmental stages. A more detailed description of development, according to the BBCH scale for example, however, was not achieved, so that its applicability for practical purposes is still limited.

The object of this study was on the one hand to test and parameterize Habekottés phenological model, using a large data set obtained from different locations in Germany. On the other hand the model structure of BRASNAP-PH should be modified for a higher resolution of developmental stages according to the BBCH scale to improve its options for diverse application in science and practice.

2. Materials and methods

2.1. BRASNAP-PH

The basic structure of the phenological model used in this study is taken from the model of Habekotté (1997), who developed BRASNAP-PH, an empirical model to predict OSR phenological development. According to this model the whole developmental cycle is characterized by five distinctive developmental stages (DVS); sowing (S), emergence (E), onset of flowering (OFl), end of flowering (EFl) and maturity (M). These stages are numbered serially from 0 to 4 DVS. This central state variable of the model is calculated by integrating the rates of change of DVS over time (dDVS/dt) in time steps of one day numerically. The rate of change itself is defined by the parameter aT_x multiplied by an effective daily temperature (Teff), which is derived from the daily average air temperature minus a base temperature parameter Tb_x that differs for all stages. During the time from emergence to the onset of flowering, the developmental rate is influenced by a vernalization factor (F_v) and a photoperiodical factor (F_p). Fv, a state variable that varies between 0 and 1, is calculated by integrating the vernalization rate from emergence to full vernalization (F_v=1), however, no

further increase of Fv is calculated after stem elongation. Fp is calculated each day from the actual daylength using a linear-plateau function, which returns values between 0 and 1. External inputs to the model are temperature, longitude and latitude combined with daylength and sowing date. The descriptions of the developmental equations of Habekotté and the model parameters are given in table 1 and 2, respectively. The model BRASNAP-PH was newly implemented using an object oriented component library (HUME, Kage, 1999), which uses the concept of visible software components of the Delphi®/C++ Builder®, Borland.

Table 1: Differential equations for the calculation of developmental stages (DVS) for different growth stages of the phenological model of Habekotté and the modified model and the derivation equations of BBCH codes (Teff = daily average temperature – base temperature (=3 °C), Fp = factor for photoperiodical effects; Fv = factor for vernalization effects; aT_x = respective growth parameter for the relevant developmental phase, pc = phyllochron)

Principal growth stage	**DVS**	**Rate of change of DVS "Habekotté"**	**Rate of change of DVS "modified model"**	**Rate of Change of BBCH code**	**BBCH code**
Sowing	0				0
		$\frac{dDVS}{dt} = Teff * aT_1$	$\frac{dDVS}{dt} = Teff * aT_1$	$BBCH = DVS * 9$	0 - 9
Emergence	1				9
Leaf development		$\frac{dDVS}{dt} = Teff * aT_2 * F_p{}^{*'}F_v$	$\frac{dDVS}{dt} = Teff * aT_2 * F_p{}^{*'}F_v$	$BBCH = 9 + \frac{(DVS - 1) * 2}{DVS_{13} - 1}$	9 - 11
				$BBCH = 11 + Leafnumber$ $\frac{dLeafnumber}{dt} = \frac{T_{eff}}{pc}$	11 - 19
Stem elongation & Inflorescence emergence			$\frac{dDVS}{dt} = Teff * aT_{2a}$	$BBCH = 30 + \frac{(DVS - DVS_{30}) * 18}{2 - DVS_{30}}$	30 – 39
				if BBCH ≥ 40 then BBCH = BBCH +10	50 - 59
Onset of flowering	2				60
		$\frac{dDVS}{dt} = Teff * aT_3$	$\frac{dDVS}{dt} = Teff * aT_3$	$BBCH = 60 + (DVS - 2) * 9$	60 - 69
End of flowering	3				69
Development of the fruit & Ripening		$\frac{dDVS}{dt} = Teff * aT_4$	$\frac{dDVS}{dt} = Teff * aT_4$	$BBCH = 70 + (DVS - 3) * 19$	70 – 79 80 - 89
Maturity	4				89

Table 2: Description of original and re-calibrated values of parameters for the phenological model of Habekotté as well as description of added and changed parameters for the modified model including their calibrated values

Parameter	Description	Original Value	Calibrated value for Habekotté model	Dimension
Temperature				
aT_1	Growth parameter 0< BBCH ≤ 9	7.72	11.34 ± 0.026	10^{-3} d^{-1} $°C^{-1}$
aT_2	Growth parameter for 9 < BBCH ≤ 60	2.01	1.92 ± 0.001	10^{-3} d^{-1} $°C^{-1}$
aT_3	Growth parameter for 60 < BBCH ≤ 69	5.10	7.46 ± 0.008	10^{-3} d^{-1} $°C^{-1}$
aT_4	Growth parameter for 69 < BBCH ≤ 89	1.47	0.902 ± 0.003	10^{-3} d^{-1} $°C^{-1}$
Tb_1	Base Temperature 0< BBCH ≤ 9	0.30	0.30[1)]	°C
Tb_2	Base Temperature for 9 < BBCH ≤ 60	0.54	0.54[1)]	°C
Tb_3	Base Temperature for 60 < BBCH ≤ 69	4.92	4.92[1)]	°C
Tb_4	Base Temperature for 69 < BBCH ≤ 89	0.69	0.69[1)]	°C
Vernalization				
Tv_{min}	Minimum temperature for vernalization	-3.7	-	°C
Tv_{opt1}	Lowest optimum temperature for vernalization	0.7	-	°C
Tv_{opt2}	Highest optimum temperature for vernalization	5.4	-	°C
Tv_{max}	Maximum temperature for vernalization	17.2	-	°C
Rv_{max}	Maximum rate for vernalization	1.46	2.13 ± 0.03	10^{-2} d^{-1} $°C^{-1}$
Photoperiod				
Dlp_{min}	Basic photoperiod	5.7	-	h
Dlp_{opt}	Saturating photoperiod	14.8	14.3 ± 3.9	h
1) Original values were used, because SE of optimized values ranged from 2 to 36, indicating marginal impact of Tb_x on calculation of DVS.				

2.2. Model modification

Plant phenology is classified according to the BBCH scale (Biologische Bundesanstalt and CHemical industry) suggested by the Federal Biological Research Centre for Agriculture and Forestry, BBA (Table 3) (Lancashire et al., 1991). It is based on the cereal code developed by Zadoks et al. (1974). The BBCH scale is divided into principal and secondary growth stages, which are numbered from 0 to 9 each, leading to a double-digital code.

Compared to the phenological model of Habekotté several main modifications have been introduced.

First of all, changes concerning model parameters were accomplished. Initially, to reduce the amount of parameters, only one base temperature, T_{base} = 3°C according to Marshall and Squire (1996), instead of four different ones, was used for all developmental phases. Thereafter, three additional parameters were introduced to the model: pc, DVS_{13} and DVS_{30} (Table 4). The parameter pc represents the phyllochron, which is by definition the thermal interval for leaf tip appearance in growing degree days, GDD, per leaf (°Cd/leaf). DVS_{13} and DVS_{30} define the values of the state variable DVS representing onset and end of the leaf developmental phase. Secondly, an additional developmental rate was added between emergence and onset of flowering (Table1). The first rate covers the period from emergence to the end of leaf development and the second rate contained the development from stem elongation to onset of flowering. Analogue to the second rate of Habekotté (Equation 1), the developmental rate for the leaf developmental phase is influenced by the effective temperature, vernalization and photoperiod, described by Teff, F_v and F_p, respectively,

$$dDVS/dt = Teff * aT_2 * F_v * F_p \quad \text{(Eq. 1)},$$

with Teff = mean daily temperature - T_{base}.

The differential equations for the remaining developmental rates follow the general form (Equation 2)

$$dDVS/dt = Teff * aT_x \quad \text{(Eq. 2)},$$

with aT_x as a parameter, quantifying the developmental rate of the relevant phase.

As a third step, equations for the derivation of BBCH codes out of DVS were implemented. Six linear equations are described to convert DVS to BBCH codes (Table 1). The last modification has been conducted concerning the period of leaf development, where BBCH is not derived from DVS, but from the number of visible leaves, which can be described by phyllochron. Because BBCH stage is defined by visible events of plant morphology, the model is more easily parameterized and evaluated from field observations. The modified model was implemented as a new module in HUME, as well.

Table 3: Conversion from Schuette scale to the BBCH scale in single code steps

Schuette scale	BBCH scale	Description
Germination and emergence		
01	00	Dry seed
03	02	Imbibition of seed
05	05	Radicle emerged from seed
07	07	Hypocotyl with cotyledons emerged from seed
09	08	Hypocotyl with cotyledons growing towards soil surface
11	09	Cotyledons emerge through soil surface
13	10	Cotyledons completely unfolded
Leaf development		
15	11	First leaf unfolded
17	12	Two leafs unfolded
19	13	Three leaves unfolded
21	14	Four leaves unfolded
22	15	Five leaves unfolded
23	16	Six leaves unfolded
24	17	Seven leaves unfolded
25	18	Eight leaves unfolded
26	19	Nine or more leaves unfolded
27	19	More than twelve leaves unfolded
Stem elongation		
30	30	Beginning of stem elongation: no internodes (“rosette”)
31	31	One visible extended internode
33	33	Three visible extended internodes
35	35	Five visible extended internodes
37	37	Seven visible extended internodes
39	39	Nine or more visible extended internodes
Inflorescence emergence		
51	50	Flower buds present, still enclosed by leaves
53	51	Flower buds visible from above or free, level with the youngest leaf
55	52	Flower buds free, level with the youngest leaves
57	53	Flower buds raised above the youngest leaves
58	55	Individual flower buds (main inflorescence) visible but still closed
59	57	Individual flower buds (sec. Inflorescence) visible but still closed
60	59	First petals visible, flower buds still closed (“yellow bud”)
Flowering		
61	60	First flowers open
62	61.7	20% of flowers on main raceme open
63	63.3	30% of flowers on main raceme open
64	65	Full flowering: 50 % flowers on main raceme open
65	67	Flowering declining: majority of petals fallen
69	69	End of flowering
Development of the fruit		
71	71	10% of pods have reached final size
75	75	50% of pods have reached final size
79	79	Nearly all pods have reached final size
Ripening		
81	80	Beginning of ripening: seed green, filling pod cavity
83	81	10% of pods ripe, seeds dark and hard
85	83	30% of pods ripe, seeds dark and hard
87	85	50% of pods ripe, seed dark and hard
89	89	Fully ripe: nearly all pods ripe, seeds dark and hard

Table 4: Description of added and changed parameters for the modified model including the calibrated values of these parameters

Parameter	Description
Temperature	
aT_2	Growth parameter for 9 < EC ≤ 30
aT_{2a}	Growth parameter for 30 < EC ≤ 60
Tb	Base temperature for winter oilseed rape
Leaf development	
pc	Phyllochron = Growing degree days (GDD) for the emergence of one leaf
DVS_{13}	Lower value of DVS to derive EC from phyllochron
DVS_{30}	Upper value of DVS to derive EC from phyllochron

2.3. Data

Experimental data of phenological development of winter oilseed rape crops were provided by ZEPP (Zentralstelle der Länder für EDV-gestützte Entscheidungshilfen und Programme im Pflanzenschutz, Bad Kreuznach, Germany). The data contained 111 data sets with 811 observations of 11 different years, 37 varieties and 75 locations of four different federal states in Germany (Table 5). The geographical coordinates ranged from 49.5 to 54.4 northern latitude and from 6.5 to 15 eastern longitude. The northern, coastal part of Germany is characterized by a maritime, the southern inland part by a more continental climate. Notations were conducted on behalf of national variety field trials; the observed phenological stages, which were notified according to the BBCH scale (Table 3), represent mean values of three or four replicates.

Three additional data sets with 28 observations were obtained by a field experiment that was carried out from the beginning of the vegetation period in 2004 to harvest in 2006 at the Hohenschulen experimental farm, 15 km west of Kiel. Winter oilseed rape (*Brassica napus* L.) was grown on an 18 ha field in 2004 and 2006 and on an 11 ha field in 2005. The observations are averaged values, resulting out of notation on eight different blocks in the field. Plant phenology was determined twice before winter and weekly from beginning of the growth period in spring until anthesis, according to the phenological scale of Schuette et al. (1982). This scale, which is a pre-stage of the BBCH scale, was used, because it is better adapted to the growth of dicot plants. Since the main data set observations from ZEPP were conducted according to the BBCH scale, notations from the experiment in Hohenschulen were converted to the BBCH scale (Table 3).

Phyllochron, which is the inverse of the slope of the linear regression of number of emerged leaves versus growing degree days (GDD), was determined using 37 data sets from ZEPP,

which had a high resolution of BBCH observations during the phase of leaf development. It is needed for the derivation of BBCH code in the model during this phase. GDD was calculated using the effective day temperature; the accumulation started with the emergence of the first leaf. Number of leaves was counted serially, whereas the first one was counted as zero (Figure 1), so that the intercept of the regression line fit the point of origin, leaving the slope as the only functional parameter for the calculation of phyllochron.

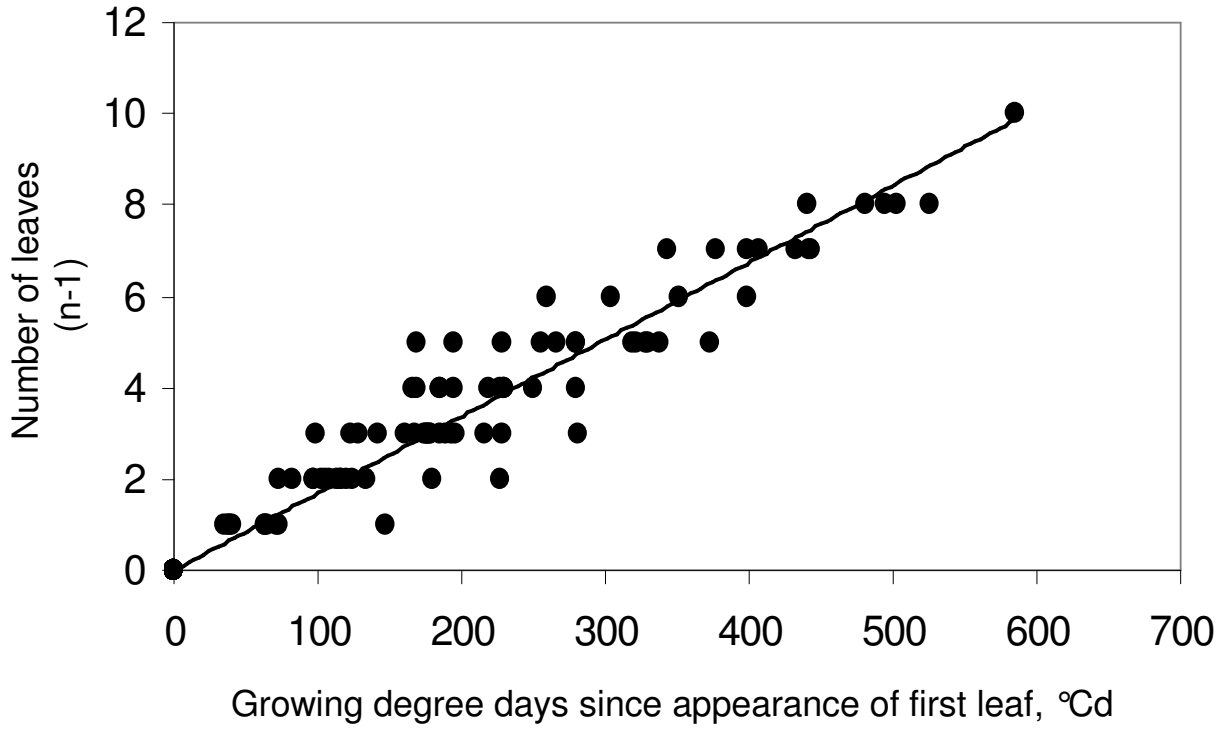

Figure 1: Linear regression between number of leaves and accumulated growing degree days (GDD, °Cd) of winter oilseed rape, based on 37 data sets throughout Germany. Leaf numbers were derived from BBCH codes during leaf development. The regression function, r^2 and RMSE are as followed: $y=0.0169x$, $r^2=0.94$ and RMSE=0.60

Table 5: Distribution of observations, years, varieties and locations of ZEPP data set within four different German federal states.

State	Number of data sets	Number of observations	Number of years	Number of varieties	Number of locations	Range of longitude and latitude
Mecklenburg-Vorpommern	5	22	2	2	5	10.2-12.7 E 53.9-54.4 N
Brandenburg	65	553	4	25	46	11.9-14.6 E 51.7-53.3 N
Sachsen	19	98	5	13	14	12.2-15.0 E 50.6-51.3 N
Rheinland-Pfalz	22	138	4	9	10	6.5-10.1 E 49.5-50.5 N

2.4. Calibration and validation

All parameters were optimized by the Levenberg-Marquard-Algorithm, which is an algorithm for a non-linear parameter estimation that is comparably robust and effective (Kuhlmann, 1980), and allows for the estimation of several parameters at the same time. Only the parameter for the first developmental rate had to be identified manually, using “Chi-Square-Analysis”, because only one observation point, emergence, was available for the relevant data sets, which is not sufficient to run an optimization according to the Levenberg-Marquard-Algorithm. “Chi-Square-Analysis” is based on several model runs with one parameter, which changes in a pre-defined range, delivering, among others, the sum of squares (SS) as a statistical parameter. For this study, the parameter for optimization was changed as long as SS did improve more than 0.5 % compared to the preceding model run. As statistical parameter for the prediction power of the model served on the one hand the functional parameters of the linear regression of predicted BBCH codes versus observed ones and the coefficient of correlation (r^2). On the other hand root mean square error (RMSE, Eq. 3) of the 1:1 line (y=x), coefficient of determination (CD, Eq. 4) and modelling efficiency (EF, Eq. 5) were calculated.

$$RMSE = \sqrt{\frac{\sum (x_i - y_i)^2}{n}} \quad (3),$$

the coefficient of determination:

$$CD = \frac{\sum_{i=1}^{n}(x_i - \bar{x})^2}{\sum_{i=1}^{n}(y_i - \bar{x})^2} \quad (4),$$

and the modelling efficiency:

$$EF = 1 - \frac{\sum(x_i - y_i)^2}{\sum(x_i - \bar{x})^2} \quad (5),$$

where x_i are the measured values; y_i are the estimated values; n is the number of samples; and $\bar{x}$ is the mean of the measured data. Low RMSE values gave best account for the degree of precision of the estimated values. CD values served as a measure of how much the derived values lay under or over the measured ones. It is scaled from zero with no upper limit, whereas one stands for no differences from measured to estimated values. EF reflects the quality of the prediction curve compared to the data points. The values range from minus infinity to one, with higher values indicating better prediction power (Loague and Green, 1991).

2.4.1 BRASNAP-PH

For the calibration of the basic model, data sets that contained at least one BBCH code equivalent to the five DVS of Habekotté (Table 1) had to be extracted. Therefore, only 70 data sets with 103 observations could be considered, which in turn had to be splitted so that one half remained for the validation. The calibration was conducted using a step-by-step procedure, estimating the parameters for the developmental rates, using relevant observations of developmental stages, only. Since the parameters aT_x and Tb_x together define the respective rate, they were optimized at the same time. Because the standard error for Tb_x showed a very high variation, aT_x values were optimized again, while Tb_x values were kept as suggested by Habekotté. The calibration was always conducted using only the BBCH observations up to the developmental stage which could be influenced by the parameter to be estimated. After all aT_x parameters had been optimized, aT_2 were again optimized together with Rv_{max} and Dlp_{opt}. Validation was run with the original and the optimized parameters (Table 6).

2.4.2 Modified model

All added parameters and all parameter concerning temperature and developmental rates were optimized with the modified model. Most parameter values concerning vernalization and photoperiod were taken from BRASNAP-PH, just the maximum rate of vernalization, Rv_{max} and the saturating photoperiod Dlp_{opt} were optimized.

Data sets, which were used for the calibration of the modified model, had to contain at least one observation of the boundary values leading from one developmental phase to the next according to the classification in table 6. A total of 74 out of 114 data sets met this requirement, so that half of these sets (37 sets with 299 observations) were used for the calibration. The remaining 37 data sets were used for cross calibration and together with the remaining 40 data sets for validation, also. Special emphasis was put on an evenly distributed data set for calibration concerning years and locations. The optimization was conducted stepwise, similar to the one of BRASNAP-PH. First, the developmental rate parameters were optimized starting with aT_1. Afterwards, DVS_{13} and DVS_{30} were optimized together with aT_2. All optimizations were conducted with the relevant notations, only. At the end, aT_2, DVS_{13} and DVS_{30} were optimized again, together with Dlp_{opt} and Rv_{max}. Validation was run with the remaining 77 data sets containing 540 observations.

To test the robustness of the calibration and validation, a cross calibration and validation of the parameter was conducted. Therefore the other half of the 74 data sets was used for a stepwise optimization, which otherwise was conducted as described for the calibration (Table 7).

3. Results

3.1. Calibration and validation

3.1.1. BRASNAP-PH

BRASNAP-PH could be optimized and validated using the large data set of ZEPP, compiling 70 location/year combinations from experiments throughout Germany. The optimization has been conducted for all aT_x parameters and for Rv_{max} and Dlp_{opt} (Table 2). The general ranges for the parameters, reported by Habekotté were not exceeded, but the value of aT_1 with 0.0113 d^{-1} $°C^{-1}$ strongly deviated from the original one of 0.00772 d^{-1} $°C^{-1}$. The maximum rate for the vernalization increased from 0.0146 d^{-1} $°C^{-1}$ to 0.0213 d^{-1} $°C^{-1}$, whereas the estimated value for the saturating photoperiod slightly decreased from 14.80 h to 14.36 h with a high standard error. Parameters Tb_x were not calibrated because the interim optimized results had shown high standard error, ranging from 2 to 36, indicating, that the base temperature has

marginal impact on the developmental rate in the basic model. The validation of the model with the optimized compared to the basic parameters showed a huge improvement concerning all chosen statistical parameters (Table 6). Slope and intercept showed a better fit to the 1:1 line, which was also indicated by the improved EF value that increased from 0.72 for the original to 0.98 for the optimized model. RMSE was reduced from 0.64 to 0.098 and the CD value changed from 1.73 to 0.94, therefore approaching 1, which indicated a better fit of predicted to observed values. r^2 was improved as well from 0.88 to 0.99 for the model run with the optimized parameters. The statistical parameters marginally vary concerning the results for calibration and validation of the optimized BRASNAP-PH.

Table 6: Slopes (b), intercepts (a) and correlation coefficients (r^2) of linear regressions (y=a+bx), root mean square errors (RMSE) of the 1:1 line (y=x), modelling efficiency (EF) and coefficient of determination (CD) of estimated developmental stages to observed ones for validation and calibration with original and optimized parameters for the phenological model of Habekotté with data set of ZEPP (Zentralstelle der Länder für EDV-gestützte Entscheidungshilfen und Programme im Pflanzenschutz, Bad Kreuznach, Germany).

	n	b	a	r^2	RMSE	EF	CD
Validation with original parameters	50	0.651***	0.787***	0.88	0.639	0.724	1.73
Calibration with optimized parameters	53	0.948***	0.152***	0.99	0.090	0.993	0.957
Validation with optimized parameters	50	0.953***	0.157***	0.99	0.098	0.990	0.937
Slopes and intercepts were tested on being significantly different to 1 and 0, respectively. The limit of significance was ***p<0.001, **p<0.01 and *p<0.05.							

3.1.2. Modified model

The phyllochron obtained a value of 59.2 °Cd. The linear regression had an r^2 of 0.94 and showed an RMSE of 0.60 leaves (Figure 1).

The results of the stepwise optimization for the parameters with the corresponding standard errors (SE) are shown in table 8. Since, compared to the basic model, the modified model runs with one base temperature only, all parameters for developmental rates highly deviated from the original values. Dlp_{opt} did not change by optimization, whereas Rv_{max} was marginally changed. The newly added parameters DVS_{13} and DVS_{30} showed values of 1.0002 and 1.236 with SE of 0.018 and 0.0228, respectively. Parameters of the cross calibration process slightly differed from the calibrated parameters, having similar SE. Only aT_2 that influences the developmental rate during leaf developmental phase did not change when cross calibrated.

To test the predictive power of the model, validations for the calibrated and cross calibrated parameter values were conducted on independent data sets from ZEPP and the experiment in Hohenschulen (Table 7). This resulted in values for RMSE of 2.97 BBCH stages for the

calibration, therefore outperform the RMSE of cross calibration by 1.57. RMSE for the validation and cross validation was similar with 3.11 and 3.25, respectively. r^2 and EF obtained equal values for all four model runs with 0.97 each. CD values lay slightly above 1, except for the cross calibration, whose CD values met 1. All slopes and intercepts were significantly different from one and zero, respectively, although the linear regressions deviated not substantially from the 1:1 line (Figure 2). Both, calibration and validation showed highest deviation between BBCH codes 30 to 60, whereas the model tended to overestimate BBCH codes between 30 and 39.

Low prediction power for this range is also indicated regarding results of table 9. The r^2 of the linear regression lines for subdivided developmental phases of predicted to observed BBCH codes were lowest for stem elongation (30 - 39) and inflorescence emergence (50 - 59) with 0.28 and 0.35, respectively. Also, RMSE of BBCH codes were highest for these phases with 4.99 and 5.21. Lowest values were obtained for the first two phases, emergence (0 - 9) and leaf development (10 – 19), and for the flowering period (60 – 69) with 0.94, 1.29 and 1.59, respectively. Concerning the deviation in days, leaf development was highest with 33 days; stem elongation has an RMSE of 11 days. Again, lowest estimation error was obtained for emergence with 2 days. According the deviation of GDD, the compounded phase of development of the fruit (71 – 79) and ripening (80 – 89) differed most with 130 GDD. Best results were obtained by emergence and stem elongation, with 33 and 36 GDD, which equals about the half of one phyllochron.

Exemplarily model runs for a northern and a southern location within Germany of one year and two consecutive years of one location are shown in Figure 3a and 4. Similar to the time courses of temperature at these locations (Figure 3b), differentiation started with vegetation period in spring. Time course of vernalization rate (Figure 3c) show differences before winter, because of the different sowing dates. Slopes for both runs lie parallel. Full vernalization was achieved during winter for both locations. Photoperiod marginally differed for northern and southern experimental sites. Figure 4 also shows that the model was well optimized for different years of one location. The model reflects slightly differing developmental changes at the beginning of vegetation period.

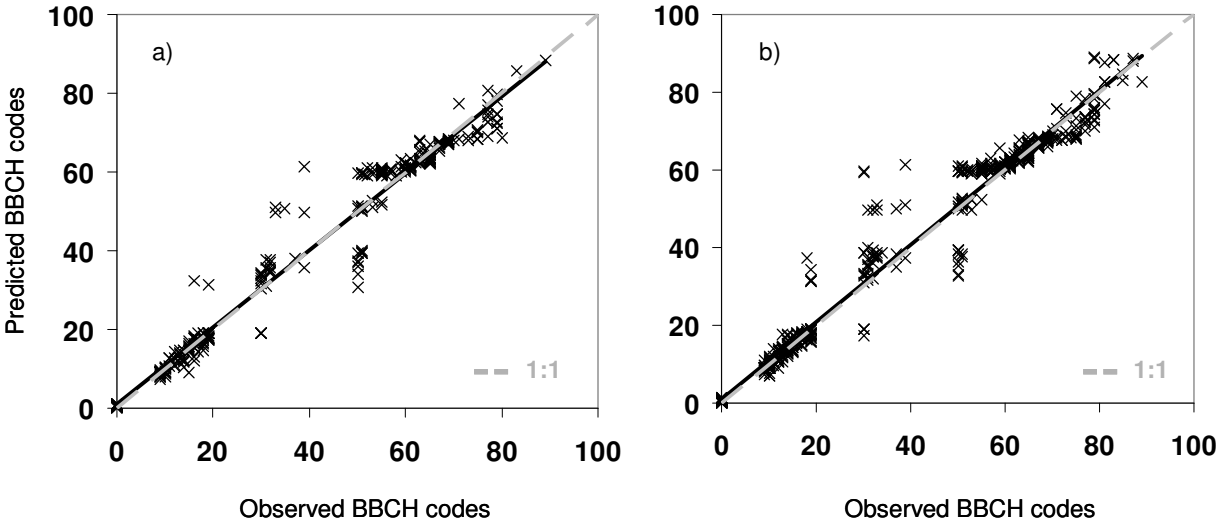

Figure 2: Predicted vs. observed BBCH stages for calibration (a) and validation (b) data sets. Calibration data set contains 299 observations from 37 different year/location/variety combinations; validation data set contains 540 observations from 77 different year/location/variety combinations. Regression function and r^2 for calibration and validation are as followed: a) $y=0.96x+1.63$, $r^2=0.97$ b) $y=0.97x+1.64$, $r^2=0.97$

Table 7: Slopes (b), intercepts (a) and correlation coefficients (r^2) of linear regressions (y=a+bx), root mean square errors (RMSE) of the 1:1 line (y=x), modelling efficiency (EF) and coefficient of determination (CD) of estimated BBCH codes to measured ones for calibration and validation compared to results of cross calibration and cross validation

	n	Slope	Intercept	r^2	RMSE	EF	CD
Calibration	299	0.96***	1.63***	0.97	2.97	0.97	1.06
Validation	540	0.97***	1.64***	0.97	3.11	0.97	1.04
Cross calibration	297	0.98*	0.87*	0.97	4.54	0.97	1.00
Cross validation	542	0.99*	1.19***	0.97	3.25	0.97	1.01
Slopes and intercepts were tested on being significantly different to 1 and 0, respectively. The limit of significance was ***p<0.001, **p<0.01 and *p<0.05.							

Table 8: Comparison of optimized parameter values and corresponding standard error (SE) for calibration and cross calibration

	Calibration		Cross calibration	
Parameter	**Value**	**SE**	**Value**	**SE**
aT_1	1.38×10^{-2}	-	1.002×10^{-2}	-
aT_2	1.96×10^{-3}	6.19×10^{-5}	1.96×10^{-3}	1.03×10^{-4}
aT_{2a}	7.06×10^{-3}	3.85×10^{-4}	7.68×10^{-3}	6.70×10^{-3}
aT_3	2.24×10^{-3}	2.38×10^{-3}	2.07×10^{-3}	2.38×10^{-3}
aT_4	1.71×10^{-3}	1.64×10^{-3}	1.92×10^{-3}	1.77×10^{-3}
DVS_{13}	1.0002	1.80×10^{-2}	1.0004	1.97×10^{-2}
DVS_{30}	1.236	2.28×10^{-2}	1.207	2.99×10^{-2}
Dlp_{opt}	14.80	0.57	14.37	0.53
Rv_{max}	1.58×10^{-2}	8.64×10^{-4}	1.29×10^{-2}	9.64×10^{-3}

Table 9: Slopes (b), intercepts (a) and correlation coefficients (r^2) of linear regressions (y=a+bx) of predicted BBCH codes to observed ones; root mean square errors (RMSE) of BBCH codes, days and growing degree days (GDD) of the validation data set for individual developmental phases for the validation data set.

BBCH range	n	Data sets	$BBCH_{predicted} = a + b*BBCH_{observed}$			RMSE		
			Slope (b)	Intercept (a)	r^2	BBCH	Days	GDD
0 - 9	49	49	0.91***	1.39***	0.98	0.94	2	33
10 - 19	160	52	0.98	0.73	0.87	1.29	33	87
30 - 39	42	21	0.97	3.63	0.28	4.99	11	36
50 - 59	98	35	1.20	-4.38	0.35	5.21	9	50
60 - 69	132	43	0.78***	9.88***	0.68	1.59	7	65
71 - 89	59	21	1.10	-7.57	0.59	4.41	9	130
0 - 89	540	76	0.97***	1.64***	0.97	3.11	19	69
Slopes and intercepts were tested on being significantly different to 1 and 0, respectively. The limit of significance was ***p<0.001, **p<0.01 and *p<0.05.								

4. Discussion

The objective of this study was on the one hand to test and parameterize the phenological model BRASNAP-PH on a large data set that was obtained from different locations with several varieties in Germany and on the other hand to modify the model structure to obtain a higher resolution of developmental stages according to the BBCH scale to improve its options for diverse application in science and practice. Although the total data set provides a large number of notations, it only presents results of five different federal states out of sixteen throughout Germany, with an emphasis on the northeastern part. These five states cover all longitudes and almost all latitudes of Germany, only results from the southernmost part of Germany are missing. The data set includes 37 different varieties, thereby covering a wide range of different OSR cultivars. Since no significant differences concerning the developmental character traits of these varieties were found, analyses were conducted without regarding this matter. Notations were obtained for all developmental phases of winter oilseed rape, most of them were obtained for leaf developmental phase, which in turn enabled for the derivation of phyllochron. Overall, the available data set exceeds concerning the number of observations other data sets, which are obtained during seasonal, project related studies, so that it is well suited for the parameterization of phenological models for Germany.

Even though BRASNAP-PH has been developed and parameterized for northwest European conditions, the parameterization using our larger data set, obtained throughout Germany over different years and varieties, gave considerable different values for some parameters and the newly parameterised model was highly improved in terms of prediction accuracy.

High standard errors for the four optimized base temperatures, $Tb_{1-4,}$ indicated that the model does not react sensitively on these parameters when applied to our data set. The temperature impact expressed by the parameters aT_{1-4} seemed to be more relevant for the control of developmental progress. This is also supported by the fact that the modified model worked well with one base temperature, only. Highest deviations from the original parameter aT_x were obtained for aT_1 and aT_4. The optimization of aT_1 led to a prediction of emergence that occurred almost twice as fast as predicted by BRASNAP-PHs aT_1, whereas the optimized aT_4 value indicated that BRASNAP-PH estimated faster development after flowering. Since Rv_{max} and the Dlp_{opt} were marginally changed by optimization, vernalization and photoperiod and their impact on phenological development in Germany seemed to be negligibly different from the results of BRASNAP-PH. Overall, Habekottés model, BRASNAP-PH, could be optimized for German conditions and afterwards served well to predict the five developmental stages equivalent to respective BBCH stages. However, it cannot be used for prediction of more detailed developmental stages.

The modification of BRASNAP-PH allows for the prediction of development stages throughout the total BBCH scale by implementing conversion functions to derive BBCH stages from DVS.

The modified model as well as BRASNAP-PH uses a simple linear temperature sum approach to estimate emergence of plants. In contrast, Marshall and Squire (1996) and Squire et al. (1997) discussed a non-linear temperature approach of germination for oilseed rape, which should be considered when temperature from sowing to emergence lies below 10°C average daily temperature. Since temperatures across Germany at regular sowing times lie above this value, a simple linear approach proofed to be appropriate. However, the model does not consider germination and emergence under unfavourable conditions like drought. High accuracy of prediction power for emergence in our model runs indicates, however, that drought is not generally limiting emergence of OSR across Germany.

Many studies have been conducted on the sensitivity of the development of winter oilseed rape and related plants to vernalization and photoperiod (Andrew et al., 1991, Mendham et al., 1981, Myers et al., 1982, Robertson et al., 2002, Huang et al., 2001, Yan et al., 1998). Myers et al. (1982) reported that both factors interact in a way that they are interchangeable to some degree, thereby ensuring that flowering occurs in cases vernalization requirements are not completely fulfilled. There exist different opinions concerning the sensitive time interval for vernalization and photoperiod, ranging from emergence to stem elongation or to onset of flowering (Robertson et al., 2002, Habekotté, 1997). According to the modified model calculations, vernalization was achieved during winter and therefore during the leaf developmental phase. Also according to the model calculations, daylength and therefore photoperiodical effectiveness fell below the threshold value during winter period only, so that

vernalization and photoperiod affect calculation of phenological development before winter, only. Further development is mostly influenced by different temperature courses, which can be seen in Figure 3a and b. Since Fv and Fp affect developmental rate of leaf development, an additional rate for the integration of DVS from stem elongation to the onset of flowering and two new parameters to define the new rate had to be implemented. Values for DVS_{13} and DVS_{30} indicated that leaf development in the model takes only about 20% from the inner phase duration from emergence to the onset of flowering. During this phase BBCH stages are defined by phyllochron, which is 59 GDD. Miralles et al. (2001) found an averaged phyllochron of 53 GDD, obtained with a base temperature of 0 °C for spring oilseed rape in Argentinia. However, he distinguished phyllochron for earlier and later emerged leaves, showing that early emerged leaves (1-12) have a higher phyllochron of up to 83 GDD and later ones (13-29), partly growing during stem elongation, a lower one of down to 25 GDD. Since leaf developmental phase describes the early phase of leaf emergence from one to about 15 leaves, the application of a higher phyllochron seems reasonable. In general, the application of a standardized morphological growth trait, like phyllochron, allows for a parameterization and correction of model predictions by field observations, which can be conducted easily.

Regarding the validation, the modified model showed high prediction power for the whole developmental cycle. However, for single BBCH ranges, statistical parameter indicated that the prediction power of the model is highly variable. Regarding r^2 and RMSE of BBCH values, stem elongation and emergence of inflorescence showed highest deviation, which can also be seen regarding the 1:1 plots of predicted versus observed BBCH codes for calibration and validation. Concerning the derivation of days, early stages, besides emergence, show a higher inaccuracy than later developmental phases. Especially leaf development deviates with 33 RMSE days, but 1.29 RMSE of BBCH, only. One reason might be that differences of just one BBCH stage, which last for the whole wintertime are less sensitive for RMSE in BBCH than for RMSE in days. An additional reason might be that early development rates are usually slower than later ones, so that differences in BBCH are low, but high if expressed in days. In the model this fact is taken into account by the depression of development by the photoperiodical and the vernalization factors, which both slow down development, whereas the rest of developmental rates is influenced by temperature, only. Figure 5 also confirms this growth trait, showing that development before winter went on more slowly than after it, although the accumulated effective temperature sum has a higher slope before winter. The high temperature sum before winter might also be a reason for the high RMSE of 87 GDD during leaf development, which occurs before winter for the most part. The high RMSE of GDD for development and maturity of the seeds is likely caused by

higher temperature in these days compared to earlier phases during development; so that the same RMSE in days of late phases compared to early phases leads automatically to a higher error of temperature based deviations.

Generally, reasons for high prediction errors, according to Kirby and Weightman (1997), can be that on the one hand frequency of notations is generally too low and on the other hand accuracy and prediction of notations are poor. Even though incorrect observations cannot be excluded, the whole data set still allowed a robust calibration, which can be seen by the results of cross calibration and validation. Single observation errors were diminished by the total amount of notations, so that a robust parameterization for German conditions could be achieved.

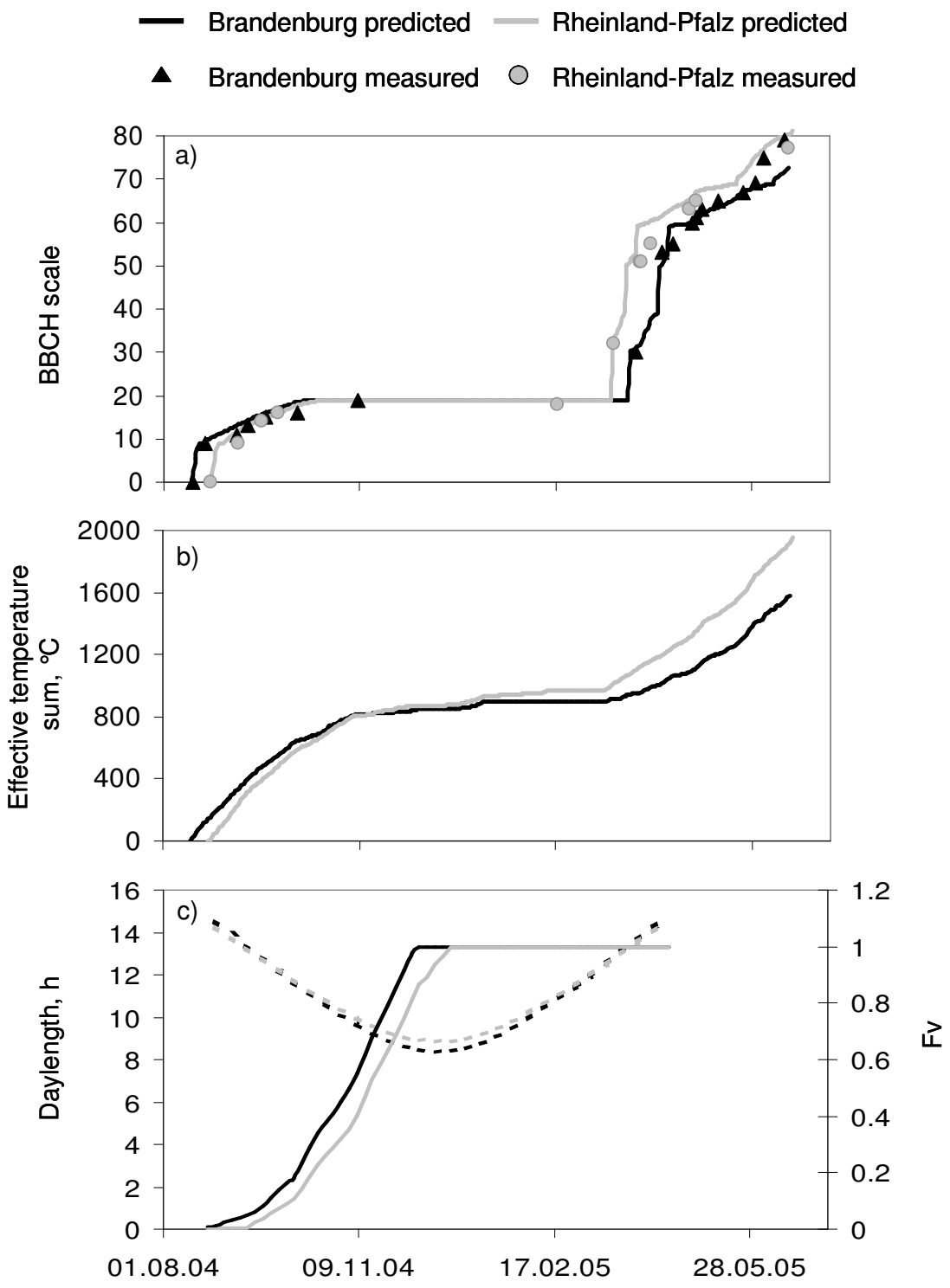

Figure 3: Time course of observed and predicted phenological developments of two different locations (Brandenburg and Rheinland-Pfalz) with contrasting climatic conditions and latitudes in Germany (a), with corresponding accumulated effective temperature sum (b) and daylength and vernalization factor, F_v (c).

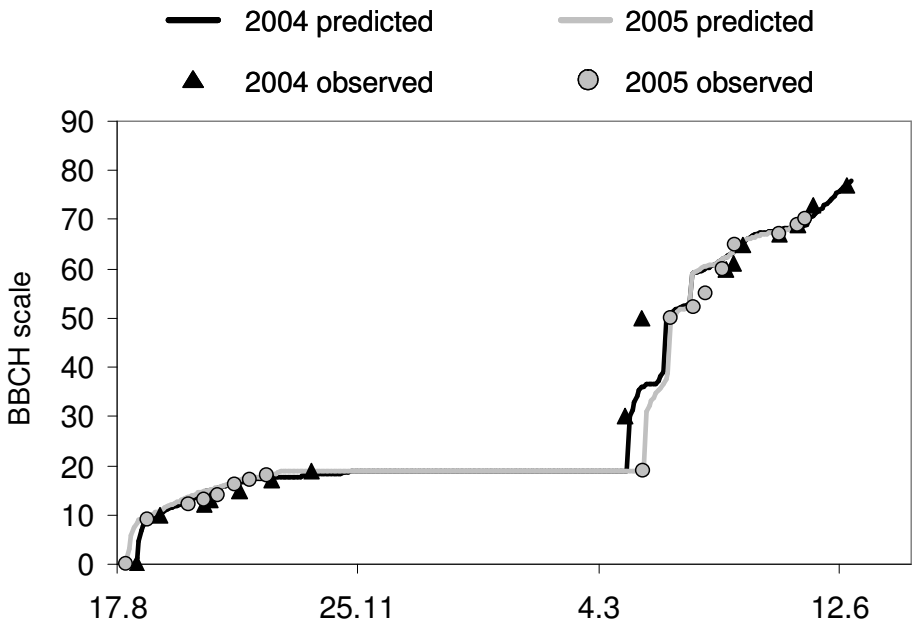

Figure 4: Time course of observed and predicted phenological development of Feldheim, Brandenburg in 2004 (black) and 2005 (grey).

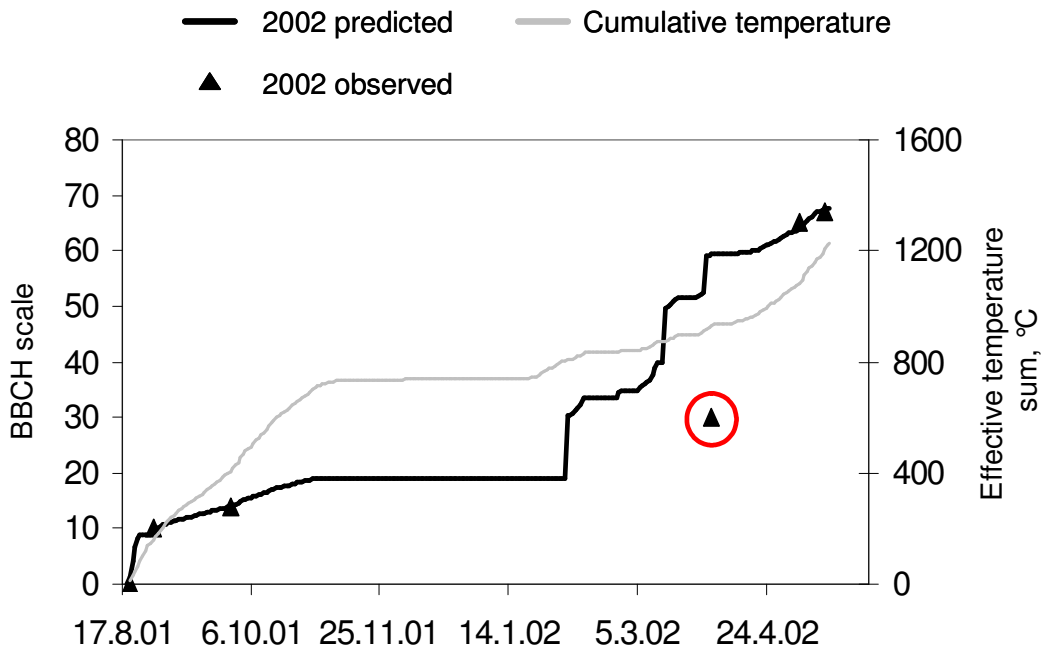

Figure 5: Time course of observed and predicted phenological development of Limbach, Sachsen, together with related accumulated effective temperature sum.

Another reason for prediction errors can occur by defining development according to the BBCH scale. Even though the BBCH scale gives a description of development with high resolution, its standardized classification has been developed with an emphasis on cereal crops, so that its applicability for the description of dicot plants must be seen critically. The scale is discontinuous due to the fact that there are two principal growth stages that do not exist: side shoots formations (20 – 29) and description of harvestable vegetative plant parts (40 – 49). Therefore, the model has to skip these growth stages. Additionally, there are substantial overlappings of morphology between phases of stem elongation and inflorescence emergence, whereby notations highly differ between different observers. Another problem is the inaccurate description of development for dicot plants, caused by the imprinting of the description of morphological growth traits of cereal crops. Concerning the growth stage for stem elongation (30 – 39), development is characterized by length between internodes, whereas dicot plants do not develop straight internodes with defined lengths. Concerning ripening, BBCH scale distinguishes percentages of totally matured pods with completely darkened seeds, whereas winter oilseed shows a gradual change of colour of pods and seeds. An alternative to the BBCH scale is given by using the scale according to Schuette et al. (1982). This scale has been especially developed for rape and related crops, also using a double-digital code. By giving a more precise and better adapted description of development, notations according to Schuette et al. (1982) might serve for a more accurate parameterisation. One example for an obvious observation error during stem elongation is given in figure 5. A BBCH code of 30, indicating that no stem elongation had taken place, seems implausible regarding the related temperature time course. These uncertainties, which result from poorly described morphological development caused by a standardized characterization lead to mistakes while notating. However, also these uncertainties were to a large extent compensated by the huge amount of available data.
Considering all these sources of errors for observations and predictions of phenology of plants, the modified model is well suited to predict phenology of different OSR varieties within Germany.

5. Conclusions

Prediction of phenological development can be used as a decision tool for a more precise production management as well as a support tool to improve crop growth models. BRASNAP-PH, which has been developed by Habekotté (1997) for North-West Europe, showed high accuracy in predicting five developmental stages after calibration on a large data set obtained in different years and with several varieties throughout Germany. Modifications on BRASNAP-PH, led to a more detailed description of development.

Vernalization and photoperiod were the most important factors besides temperature to estimate leaf development, whereas temperature was determinant during all phases of development. The modified model showed high prediction power for developmental stages according to the BBCH scale. Some uncertainties occurred during leaf development and stem elongation, which can be explained to some extend by failure of a systematic description of morphology of the BBCH scale. Another reason might be that the accuracy of notations in the field was partly poor. However, the amount of data for the calibration and validation led to a robust parameterization, which can be seen by the similar parameter values of calibration and cross calibration, so that both parameter sets can be used to predicted phenology. Overall, the modified model was well suited to estimate phenological development across different sites and varieties within Germany. The model is generally valid for the description of OSR phenological development as all important developmental stages only depend on air temperature and photoperiod. Thus, it can be used for other agro-ecological regions after adapting the parameters to the local situation.

Acknowledgements

Many thanks to Dr. Erich Jörg and Kristina Falke from ZEPP, who provided the large data set, which, apart from my own experiments, enabled me to conduct this study. I also thank M. and L. Miller and Andreas Pacholski for their constructive comments on the manuscript and the DBU, German Federal Environmental Foundation, for kindly supporting my project.

References

Andrew, M., Tommey, M., Evans, E.J. (1991). "Temperature and daylength control of flowering initiation in winter oilseed rape (*Brassica napus* L.)." Annals of Applied Biology 118: 201-208.

Farré, I., Robertson, M., Walton, G. H., Asseng, S. (2002). "Simulating phenology and yield response of canola to sowing date in Western Australia using the APSIM model." Australian Journal of Agricultural Research 53: 1155-1164.

Gabrielle, D., P., Gosse, G., Justes, E., Andersen, M. N. (1998). "A model of leaf area development and senescence for winter oilseed rape." Field Crops Research 57: 209-222.

Habekotté, B. (1997). "A model of the phenological development of winter oilseed rape (*Brassica napus* L.)." Field Crops Research 54: 109-126.

Huang, J. Z., Shrestha, A., Tollenaar, M., Deen, W., Rajcan, I., Rahimian, H., Swanton, C. J. (2001). "Effect of temperature and photoperiod on the phenological development of wild mustard (*Sinapis arvensis* L.)." Field Crops Research 70: 75-86.

Kage, H., Stützel, H. (1999). "HUME: An object oriented component library for generic modular modelling of dynamic systems." European Society of Agronomy, Lleida.

Kirby, E. J. M., Weightman, R. M. (1997). "Discrepancies between observed and predicted growth stages in wheat." The Journal of Agricultural Science 129: 379-384.

Kuhlmann, W. (1980). "Parameterschätzung von Eingleichungsmodellen im unbeschränkten Parameterraum." Würzburg, Physica Verlag.

Lancashire, P.D., Bleiholder, H., Langelüddecke, P., Stauss, R., Boom, T.V.D., Weber, E., Witzenberger, A.. 1991. "An uniform decimal code for growth stages of crops and weeds." Annals of Applied Biology 119: 561-601.

Loague, K., and R.E. Green. (1991). "Statistical and graphical methods for evaluating solute transport models: overview and applications." Journal of Contaminant Hydrology 7: 51-73.

Marshall, B., Squire, G. R. (1996). "Non-linearity in rate-temperature relations of germination in oilseed rape." Journal of Experimental Botany 47: 1369-1375.

Mendham, N. J., Shipway, P. A., Scott, R. K. (1981). "The effects of delayed sowing and weather on growth, development and yield of winter oil-seed rape (*Brassica napus* L.)." The Journal of Agricultural Science 96: 389-416.

Miralles, D. J., Ferro, B. C., Slafer, G. A. (2001). "Development responses to sowing date in wheat, barley and rapeseed." Field Crops Research 71: 211-223.

Myers, L. F., Christian, K. R., Kirchner, R. J. (1982). "Flowering Responses of 48 Lines of Oilseed Rape (*Brassica* spp.) to Vernalization and Daylength." Australian Journal of Agricultural Research 33: 927-936.

Robertson, M. J., et al. (2002). "Environmental and genotypic control of time to flowering in canola and Indian mustard." Australian Journal of Agricultural Research 53: 793-809.

Robertson, M. J., Holland, J. F., Bambach, R. (2004). "Response of canola and Indian mustard to sowing date in the grain belt of north-eastern Australia." Australian Journal of Experimental Agriculture 44: 43-52.

Robertson, M. J., Holland, J. F., Kirkegaard, J. A., Smith, C. J. (1999). "Simulating growth and development of canola in australia." 10th International Rapeseed Congress, Canberra, Australia.

Roßberg, D., Jörg, E., Falke, K. (2005). "SIMONTO - ein neues Ontogenesemodell für Wintergetreide und Winterraps." Nachrichtenblatt des Deutschen Pflanzenschutzdienstes 57: 74-80.

Schuette, F., Steinberger, J., Meier, U. (1982). "Entwicklungsstadien des Raps - einschl. Rübsen, Senfarten, und Oelrettich - zum Gebrauch für das Versuchswesen, die Beratung und die Praxis in der Landwirtschaft." Biologische Bundesanstalt für Land- und Forstwirtschaft Merkblatt Nr. 27(7).

Squire, G. R., Marshall, B., Dunlop, G., Wright, G. (1997). "Genetic basis of rate-temperature characteristics for germination in oilseed rape." Journal of Experimental Botany 48: 869-875.

Yan, W., Wallace, D. H. (1998). "Simulation and Prediction of Plant Phenology for Five Crops Based on Photoperiod x Temperature Interaction." Annals of Botany 81: 705-716.

Zadoks, J. C., Chang, T. T., Konzak, C.F. (1974). "A decimal code for the grown stages of cereals." Weed Research 14: 415-421.

Chapter 4

New model approaches for plant area, dry matter production and nitrogen uptake of winter oilseed rape (*Brassica napus* L.) during vegetative growth under German conditions

Karla Müller, Ulf Böttcher, Henning Kage

Abstract

During the last decades, winter oilseed rape (OSR) became more and more important. High nitrogen (N) fertilizer requirements and low N efficiency causes high N surpluses after harvest, which enhance the risk of N losses by leaching during winter. Crop models can be helpful tools for a substantial analysis and thus, for the understanding of nitrogen processes in the crops. This study presents a dynamic, empirical growth model for OSR that predicts dry matter production based on the concept of light use efficiency (LUE) for vegetative growth from emergence to flowering. Since evidence was found that LUE depends on radiation intensity before winter, it is calculated according to a linear regression function for this specific period. Furthermore, the model calculates dry matter partitioning into leaf and stem fraction according to an allometric approach. Leaf and stem area is derived from the respective dry matter and specific area. The N concentration of leaves is assumed to be constant, whereas stem N concentration depends on stem dry matter according to an exponential dilution curve. N uptake for the shoot is obtained by adding leaf and stem N uptake. Additionally, dry matter losses during winter are also calculated, therefore enabling a continuous prediction from emergence to flowering without interruption. After parameterization, model predictions for plant parameters like green area index, shoot dry matter and nitrogen uptake were validated on three independent data sets. The variable LUE approach before winter improved dry matter predictions compared to calculations with an optimized, constant LUE. Prediction for all validation data set highly differed concerning quality, revealing that additional analysis for improving the crop growth model should be conducted.

1. Introduction

Winter oilseed rape (OSR) has become more and more important during the last decades. Its high fertilizer requirements and its low nitrogen (N) efficiency (Lickfett et al., 1993; Lickfett and Przemeck, 1995; Sieling, 1997a) enhance the risk of N losses from the soil-crop system to the environment by leaching during winter rainfall. Several approaches in plant production like an adjusted nitrogen fertilizer application (Sieling et al., 1997; Lickfett and Przemeck, 1995) deal with these problems. For an adjusted fertilizer application, accurate knowledge of crop growth and yield potential are necessary. Especially vegetative growth, which serves as a prerequisite for yield formation processes (Habekotté, 1997), is important.

Several models for OSR growth have already been presented in literature. Gabrielle et al. (1998) developed a CERES-type model that predicts leaf area, dry matter production and N in the plant for vegetative and generative phase using constant LUE for the whole vegetation

period. Focus was laid on the implementation of a leaf developmental model, especially after flowering, when leaf senescence occurs. Habekotté (1997) developed LINTUL-BRASNAP, putting emphasis on simulating yield formation processes from flowering to ripening; therefore neglecting growth in the vegetative phase. Husson et al. (1998) presented CECOL, derived from CERES also, which does not simulate N uptake by OSR. Colnenne et al. (1998) described the relation of nitrogen concentration in the shoot (Nc_{shoot}) to shoot dry matter (DM_{shoot}) for OSR according to a power function based on the concept of Lemaire and Salette (1984). A quantitative model for vegetative growth, which gives detailed information on dry matter production, its partitioning into leaf and stem fraction and that also predictes N uptake is still missing. Additionally, several authors already discussed differing values for LUE during growth (Justes et al., 2000; Mendham et al., 1981; Kiniry et al., 1995; Gosse et al., 1983; Rode et al., 1983; Habekotté, 1997a). This aspect has not been implemented in an OSR model, yet.

The presented crop growth model for OSR dynamically calculates dry matter production with a variable LUE that depends on radiation intensity during fall. It also provides dry matter partitioning into leaf and stem fraction according to an allometric approach and it calculates dry matter losses during winter time, which enables for a continuous estimation of growth between fall and spring without interruption. In agreement to findings by Colnenne et al. (1998), it also derives N concentration according to a dilution curve, but not for DM_{shoot}, but for stem dry matter (DM_{stem}) only, whereas evidence was found that N concentration for the leaf fraction (Nc_{leaf}) is constant.

2. Material and Methods

2.1. Experimental data

Data from two different field experiments, carried out on the Hohenschulen experimental farm, 15 km to the west of Kiel, were used in this study. The first one, lasting from 2005 until 2007, was carried out to investigate differences in growth response of winter oilseed rape (OSR) between four different N treatments: unfertilized (N0), 80 kg N ha^{-1} (N1), 160 kg N ha^{-1} (N2) and 240 kg N ha^{-1} (N3). Treatments were done in 8 replicates established as eight blocks, each containing four differently fertilized plots. Only treatments N2 and N3, which are assumed to have sufficient N supply during the growth period, were used. In the second experiment, in year 2006, the influence of two different seeding dates and five different N treatments on growth and yield of OSR was investigated, each treatment with four replicates. For model calibration, only the highest fertilizer treatment (240 kg N ha^{-1}) of both seeding dates was used.

In both experiments N was applied as ammonium nitrate/urea solution in two dressings at the beginning of plant growth in spring and the beginning of stem elongation. Otherwise, plants were treated according to German best practice recommendations.

At each sampling date an area of 0.88 m² was harvested for analysis of leaf area index and stem area index (LAI and SAI), total dry matter of leaves and stems (DM_{leaf} and DM_{stem}) and N concentration of leaves and stems (Nc_{leaf} and Nc_{stem}). Green area index (GAI), dry matter of the aboveground shoot (DM_{shoot}) and the N content of the fractions and the shoot were derived from the measured plant data. Only leaf blades were attributed to the leaf fraction, whereas the petioles were counted as stem fraction. After drying and weighting, N concentrations in the fractions were determined by near infrared spectroscopy (NIRS) (NIRSystems 5000 scanning monochromator, FOSS GmbH, Rellingen, Germany). NIRS data were analysed using the WINISI software package (Infrasoft International, Port Matilda, PA, USA).

Three additional data sets were used for model validation. Two were obtained in 2003 and 2004 at the experimental farm of Hohenschulen; a third independent data set was collected in 1995 in Chalon, France (Gosse et al., 1999). For validation, only the variables GAI, DM_{shoot} and N_{shoot} were used, because other variables were not available. Site and crop management information as well as number and distribution of sampling dates of all data sets are given in table 1.

Table 1: Description of all data sets regarding specific crop management information.

Code	Vegetation period	Location	Number of plots	Sowing dates	Total amount fertilizer kg N/ha	Number of sampling dates		Used for	
						before winter	after winter	Cali-bration	Vali-dation
1	2004/2005	Hohenschulen, Germany	8	04.09.2004	160 240	2	6	**X**	
2	2005/2006	Hohenschulen, Germany	8	24.08 2005	160 240	2	6	**X**	
3	2005/2006	Ufop, Hohenschulen, Germany	4	19.08.2005 01.09.2005	240	2	2	**X**	
4	2006/2007	DBU, Hohenschulen, Germany	8	02.09.2006	200	5	2	**X**	
5	1994/1995	Chalon, France	9	08.09.1994	273	5	7	**X** (LUE)	**X**
6	2002/2003	Hohenschulen, Germany	4	21.08.2002	206	1	3		**X**
7	2003/2004	Hohenschulen, Germany	8	22.08.2003	160	1	5		**X**

2.2. Model

Analogous to the empirical model for cauliflower of Kage (1999), the growth model for OSR calculates plant dry matter production (DM_{plant}), describes partitioning into leaf and stem dry matter (DM_{leaf} and DM_{stem}), the development of leaf and stem area (LAI and SAI), the N concentration of the stem fraction (Nc_{stem}) and the amount of N in leaf and stem as well as in the aboveground dry matter of the shoot (N_{leaf}, N_{stem}, N_{shoot}). The model runs on a daily time step with daily input and output values. External data inputs required for running the model are daily mean temperature and incoming global radiation. However model calculations are based on effective daily mean temperature (T_{eff}) with a base temperature of 3°C (Marshall and Squire, 1996) and photosynthetic active radiation (PAR) derived from the global radiation using a factor of 0.5 (Szeicz, 1974).

Additional inputs to the model are developmental stages according to BBCH codes, which are calculated by a phenological sub model that is linked to the growth model.

The growth model for winter oilseed rape was implemented using an object oriented component library (HUME, Kage, 1999a), which uses the concept of visible software components of the Delphi®/C++ Builder®, Borland.

2.2.1. Phenology model

According to the phenological model (Müller et al., unpublished), emergence of OSR occurs after 72 growing degree days (GDD) with a base temperature of 3°C. Temperature, vernalization and photoperiod are the main factors that determine development. Output values are developmental stages according to the BBCH scale, which offer a highly resoluted description of phenological development (Lancashire et al., 1991).

2.2.2. Dry matter production

Dry matter production is a function of absorbed photosynthetic active radiation (Q), light use efficiency (LUE) and a temperature dependent factor for photosynthetic activity (fT).

$$\frac{dDM_{plant}}{dt} = Q * LUE * fT \qquad \text{(Eq. 1)}$$

Q is calculated by

$$Q = PAR * (1 - e^{-k*GAI}) \qquad \text{(Eq. 2),}$$

and

$$GAI = LAI + SAI \qquad \text{(Eq. 3).}$$

k is the light extinction coefficient, which is assumed to be 0.85 (Dreccer et al., 2000) for winter oilseed rape and GAI, LAI and SAI are green area index, leaf area index and stem area index, respectively.
fT is calculated by an optimum function with four cardinal temperatures, $T_1 - T_4$, as followed.

$$fT = \begin{cases} 0 & T_{mean} < T_1 \\ \frac{T_{mean} - T1}{T2 - T1} & T_1 \le T_{mean} \le T_2 \\ 1 & T_2 < T_{mean} \le T_3 \\ \frac{T4 - T_{mean}}{T4 - T3} & T_3 < T_{mean} \le T_4 \\ 0 & T_{mean} > T_4 \end{cases} \qquad \text{(Eq. 4)}$$

T_{mean} is the daily mean air temperature. The cardinal temperatures, T_1 to T_4, for the calculation of fT were set to 3°C, 10°C, 20°C and 35°C, respectively.
From DM_{plant}, dry matter of the root fraction (DM_{root}) is calculated by the factor f_{Root},

$$\frac{dDM_{root}}{dt} = f_{Root} * \frac{dDM_{plant}}{dt} \quad \text{(Eq. 5)}$$

which in turn is a linear function of the temperature sum after emergence (TS_{em}) characterized by the two parameters for slope (f_R) and intercept ($Root_0$) (Kage et al., 2000).

$$f_{Root} = f_R * TS_{em} + Root_0 \quad \text{(Eq. 6)}$$

Subsequently, aboveground dry matter, DM_{shoot} is equal to the difference of DM_{plant} and DM_{root}.

$$\frac{dDM_{shoot}}{dt} = (1 - f_{Root}) * \frac{dDM_{plant}}{dt} \quad \text{(Eq. 7)}$$

Because dry matter production is derived from GAI, which in turn results from dry matter, the initial dry matter production has to be calculated independent of GAI until a critical dry matter (DM_{crit}) is reached. Therefore early growth of dry matter from emergence until DM_{crit} has been obtained is described by an exponential function of the temperature sum.

$$\frac{dDM_{plant}}{dt} = k1 * T_{eff} * DM_{plant} \quad \text{(Eq. 8),}$$

where k1 is the relative growth rate.

2.2.2.1. LUE

Initial analysis of our data gave evidence that LUE was not constant, especially under the conditions of rapidly declining radiation intensity in fall. Therefore, calculation of the LUE differs between fall growth and spring growth. After winter, with beginning of spring growth, LUE is set to be constant (LUE_{sp}). Before winter, data gave evidence that LUE depended on the mean daily radiation. LUE is therefore a function of PAR characterized by the two parameters, LUE_0 and f_{LUE}.

$$LUE = f_{LUE} * PAR + LUE_0 \quad \text{(Eq. 9)}$$

2.2.3. Dry matter partitioning of DMshoot

During vegetative growth, DM_{shoot} consists of leaf dry matter (DM_{leaf}) and stem dry matter (DM_{stem}).

$$DM_{shoot} = DM_{leaf} + DM_{stem} \quad \text{(Eq. 10)}$$

Therefore, the growth rate of DM_{shoot} is the sum of the growth rates of DM_{leaf} and DM_{stem}.

$$\frac{dDM_{shoot}}{dt} = \frac{dDM_{leaf}}{dt} + \frac{dDM_{stem}}{dt} \quad \text{(Eq. 11)}$$

For the partitioning of DM_{shoot} an allometric approach is used (Kage, 1999). This assumes that the ratio of the relative growth rates of both fractions is constant, resulting in a linear relation between the natural logarithms of DM_{leaf} and DM_{stem}.

$$\ln DM_{stem} = g * \ln DM_{leaf} + h \quad \text{(Eq. 12)}$$

After transformation and differentiation of equation 12, the above term can be inserted into equation 11, resulting in a term that expresses the leaf growth rate as a function of the growth rate for DM_{shoot} and DM_{leaf} (Kage,1999).

$$\frac{dDM_{leaf}}{dt} = \frac{dDM_{shoot}}{dt} * \frac{1}{(1 + e^{h} * g * DM_{leaf}^{\,g-1})} \quad \text{(Eq. 13)}$$

As for LUE, two different parameter values are applied for both, g and h, during fall and spring growth.
By transformation of equation 11, the rate of change for DM_{stem} can be calculated.

$$\frac{dDM_{stem}}{dt} = \frac{dDM_{shoot}}{dt} - \frac{dDM_{leaf}}{dt} \quad \text{(Eq. 14)}$$

2.2.4. Leaf and stem area

Growth rates for leaf area index (LAI) and stem area index (SAI) were calculated from DM_{leaf} and specific leaf area (SLA) and DM_{stem} and specific stem area (SSA), respectively.

$$\frac{dLAI}{dt} = \frac{dDM_{leaf}}{dt} * SLA \qquad \text{(Eq. 15)}$$

$$\frac{dSAI}{dt} = \frac{dDM_{stem}}{dt} * SSA \qquad \text{(Eq. 16)}$$

SLA after winter and SSA for the whole time period were assumed to be constant. We found evidence that SLA before winter decreased with increasing temperature sum from emergence, so that it was treated as a variable, depending on TS_{em} and two parameters SLA_0 and f_{SLA}.

$$SLA = SLA_0 + f_{SLA} * TS_{em} \qquad \text{(Eq. 17)}$$

An upper limit of 350 cm²/g and a lower limit of 100 cm²/g were set for the calculation of SLA according to equation 17.
The green area index, GAI, which defines the area for the total aboveground biomass, is a simple addition of LAI and SAI (Eq. 3).

2.2.5. Calculation of nitrogen concentration and nitrogen uptake

N concentration for the leaf fraction (Nc_{leaf}) is assumed to be constant from emergence to the beginning of flowering. For the calculation of the amount of N in the leaf fraction (N_{leaf}), Nc_{leaf} was multiplied by the rate of growth of DM_{leaf}.

$$\frac{dN_{leaf}}{dt} = \frac{dDM_{leaf}}{dt} * Nc_{leaf} \qquad \text{(Eq. 18)}$$

In agreement of findings by Colnenne et al. (1998) who determined a nitrogen dilution curve for winter oilseed rape, stem N concentration (Nc_{stem}) decreased with increasing DM_{stem} according to an empirical exponential function. For an upper and lower limit, bounds were set to 5.5 % and 1 %, respectively.

$$Nc_{stem} = pCn_{stem1} * e^{DMstem*pCnstem2} \quad \text{(Eq. 19)}$$

The amount of N in the stem fraction (N_{stem}) can be calculated by multiplying Nc_{stem} and DM_{stem} according to equation 20.

$$\frac{dN_{stem}}{dt} = \frac{dDM_{stem}}{dt} * (Nc_{stem} + DM_{stem} * \frac{dNc_{stem}}{dDM_{stem}}) \quad \text{(Eq. 20)}$$

The rate of increase of N in the aboveground biomass (N_{shoot}) is the sum of the uptake rates of leaf and stem.

$$\frac{dN_{shoot}}{dt} = \frac{dN_{leaf}}{dt} + \frac{dN_{stem}}{dt} \quad \text{(Eq. 21)}$$

To distinguish between this approach and the alternative approach of Colnenne, which will be introduced next, it will be named as N_{shoot}-sum approach. Additionally, the approach by Colnenne et al. (1998) for the calculation of shoot N concentration (Nc_{shoot}) was integrated into the model. The decrease of Nc_{shoot} as a function of DM_{shoot} increase is described by a power equation.

$$Nc_{shoot} = pCn_1 * DM_{shoot}^{pCn_2} \quad \text{(Eq. 22)}$$

An upper and lower limit for Nc_{shoot} was set to 6.5 % and 1 %, respectively.
For Colnennes approach, N in the aboveground biomass (N_{shoot}), is calculated from Nc_{shoot} and DM_{shoot} according to equation 23.

$$\frac{dN_{shoot}}{dt} = \frac{dDM_{shoot}}{dt} * (Nc_{shoot} + DM_{shoot} * \frac{dNc_{shoot}}{dDM_{shoot}}) \quad \text{(Eq. 23)}$$

2.2.6. Losses of DMshoot during winter

During winter, dry matter is lost caused by negative temperatures. Negative daily mean temperatures are added until the negative temperature sum (TS_{minus}) reaches a threshold level (fTS_{minus}). After reaching the threshold the rate of dead dry matter, L_{Shoot}, is a function of DM_{shoot}, the added daily temperatures below 0 °C and a factor for dry matter decrease, f_{WL}.

$$\frac{dL_{Shoot}}{dt} = DM_{shoot} * \frac{dTS_{minus}}{dt} * f_{WL} \qquad \text{(Eq. 24)}$$

L_{Shoot} can never exceed total dry matter, so that DM_{shoot} never becomes negative. L_{Shoot} is then subtracted from DM_{shoot}, so that the rate of change for the wintertime results from the following equation

$$\frac{dDM_{shoot}}{dt} = 1 - \left(1 - f_{Root}\right) * \frac{dDM_{plant}}{dt} - \frac{dL_{Shoot}}{dt} \qquad \text{(Eq. 25)}$$

2.3. Parameterization

Parameters that were taken from literature are described in tables 2. For parameter optimization the Levenberg-Marquard-Algorithm was applied, which is comparably robust and effective for non-linear parameter estimation (Kuhlmann, 1980), and allows for a simultaneous estimation of several parameters. Data sets used in the optimization are specified in table 1 and 3.

For the parameterization of LUE, we fitted exponential curves to the LAI data of every experiment before winter and expolinear curves to the data after winter. Thus, good fits for plant parameters GAI and DM_{shoot} were achieved. Values of DM_{shoot} from the first measurement date after winter were used as initial values, so that fitting after winter started from the second measurement date on. Therefore, only experiments that included at least three measurement dates after winter could be considered. As only two data sets met these requirements, we also used the Chalon data set for a robust optimization of LUE as the most important factor for the calculation of biomass development. The parameters were optimized on data of relevant time spans, only. SLA and allometric parameters were also optimized using the fitted curves for each experiment.

The parameters were optimized following the order in which the model was described (Table 3).

Table 2: Model parameters taken from literature or derived from external data.

Parameter	Description	Value	Dimension	Source
T_1	CT_x = cardinal temperature of the optimum function for the factor of plant physiological acitivity (fT) (Eq. 4)	3	°C	Marshall & Squire 1996
T_2		10	°C	
T_3		20	°C	Porter & Gawith 1999
T_4		35	°C	
DM_{crit}	Upper threshold for the first, linear growing rate	5	g m^{-2}	-
k	Light extinction coefficient (Eq. 2)	0.85		Dreccer 2000
fTS_{minus}	Threshold for decrease of dry matter due to temperatures below 0°C	-20	°Cd	-
f_R	Partitioning factor for the root fraction (Eq. 6)	-2.9 x 10^{-4}	C^{-1} d^{-1}	Gosse 1999
$Root_0$		0.12	-	
SLA_{max}	Maximum and minimum value for specific leaf area	350	cm^2 g^{-1}	Figure 3
SLA_{min}		100	cm^2 g^{-1}	
T_{base}	Base temperature for winter oilseed rape	3	°C	Marshall & Squire 1996

2.4. Validation

Two data sets from Hohenschulen in 2003 and 2004 and one data set from Chalon in 1995 were used for validation. To characterize the predictive force of the model for plant parameters GAI, DM_{shoot} and N_{shoot}, coefficient of correlation (r^2) of the linear regression ($y = a + bx$) between the measured and simulated results were calculated. Additionally, root mean square error (RMSE, Eq. 26), coefficient of determination (CD) and modelling efficiency (EF) are given (Loague and Green, 1991).

$$RMSE = \sqrt{\frac{\sum (x_i - y_i)^2}{n}} \qquad \text{(Eq. 26)},$$

where x_i are the measured values; y_i are the estimated values; n is the number of samples. Low RMSE values indicate high absolute degree of precision of the estimated values. CD values served as a measure of how much the derived values lie under or over the measured ones. They are scaled from zero with no upper limit, whereas 1 means no differences from measured to estimated values. EF reflects the quality of the prediction curve compared to the

data points. The values range from -∞ to 1, higher values indicating better prediction power (Loague and Green, 1991).
To compare the goodness of model prediction among different plant parameters, the relative root mean square error (rRMSE) for GAI, DM_{shoot} and N_{shoot} was calculated

$$rRMSE = \frac{RMSE}{\bar{x}} \quad \text{(Eq. 27)},$$

where $\bar{x}$ is the mean of the measured data.

To analyze the quality of the regressions concerning LUE, allometry, SLA and nitrogen concentration for shoot, leaf and stem, the SAS statistical package was used.

3. Results

3.1. Parameterization

Parameters taken from literature or derived from external data are presented in table 2. Threshold values for the turnover of plant dry matter calculation, DM_{crit}, and for the beginning of necrosis of shoot dry matter, fTS_{minus}, were defined to be 5 g m^{-2} and -20 °C, respectively. Because both parameters connect different rates of change, which are supposed to show fluent transitions within wide boundaries, they responded insensitive to optimization. Parameters that were derived from own data were optimized by using the Levenberg-Marquard-Algorithm implemented in the HUME environment (Table 3). As the first parameterization step, k1, was estimated resulting in 1.63 for the relative growth rate from emergence to the achievement of DM_{crit}. In a second step, all parameters necessary for the calculation of LUE were optimized using DM_{shoot} data. Constant values for LUE in fall and spring were determined as 2.06 g MJ^{-1} d^{-1} and 3.34 g MJ^{-1} d^{-1}, respectively. Since data before winter gave evidence that LUE is a dependent on mean daily radiation, LUE in fall was calculated according to a linear regression (Equation 9) as shown in Figure 1. The optimized functional parameters were -0.504 for f_{LUE} and 3.78 for LUE_0. To test the different LUE approaches in fall, constant and variable LUE, for their suitability for the prediction of DM_{shoot}, the model was run with the calibration and validation data sets (Table 4). All four statistical parameters showed better results with a variable LUE for the calibration as well as for the validation.

Table 3: Optimized parameter values with standard errors obtained by calibration.

Parameter	Description	Value	SE	Data sets (Table 1) used for calibration
k1	Relative growth rate from emergence to DMcrit	1.63×10^{-2}	3.94×10^{-3}	1,2,3,4
f_{LUE}	Functional parameter for the calculation of the	-0.504	1.23	1,2,4,5
LUE_0	variable light use efficiency before winter (Eq. 9)	3.78	4.24	
LUE_{fa}	Constant light use efficiency before winter, g MJ^{-1}	2.06	0.56	1,2,4,5
LUE_{sp}	Constant light use efficiency after winter, g MJ^{-1}	3.34	0.84	1,2,4,5
h_{fa}	Functional parameters for the allometric equation of	-3.01	7.19	1,2,3,4
g_{fa}	leaf and stem dry matter during fall growth (Eq. 14)	1.62	1.82	
h_{sp}	Functional parameters for the allometric equation of	-5.60	28.46	1,2,3,4
g_{sp}	leaf and stem dry matter during spring growth (Eq.14)	2.22	6.09	
f_{SLA}	Functional parameter for the calculation of the	-2.29	12.15	1,2,3,4
SLA_0	variable specific leaf are before winter (Eq. 18)	1368	6071	
SLA_{sp}	Constant specific leaf area after winter, $cm^2\ g^{-1}$	151	60	1,2,3,4
SSA	Constant specific stem area, $cm^2\ g^{-1}$	29	0.58	1,2,3,4
f_{WL}	Factor for dry matter winter losses due to negative temperature sum below 0°C (Eq. 10)	1.06×10^{-2}	4.63×10^{-3}	1,2,3,4
pcn_{leaf}	Leaf nitrogen concentration	6.15	1.08	1,2,3,4
pcn_{stem1}	Functional parameter for the calculation of stem	3.90×10^{-2}	1.85×10^{-2}	1,2,3,4
pcn_{stem2}	nitrogen concentration according to a dilution curve (Eq. 20)	-3.55×10^{-3}	4.81×10^{-3}	
pcn_1	Functional parameter for the calculation of shoot	5.51	1.34	1,2,3,4
pcn_2	nitrogen concentration according to a dilution curve by Colnenne (Eq. 22)	-0.49	0.17	

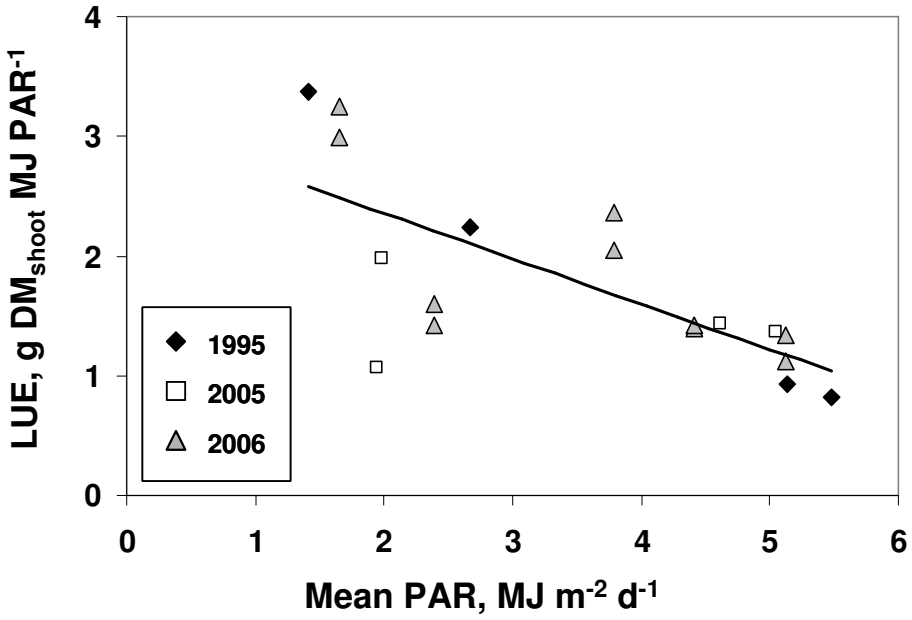

Figure 1: Light use efficiency (LUE) estimated for winter oilseed rape, as a function of the average daily radiation sum before winter, y=-0.38 (±0.09)x + 3.11(±0.35), r^2=0.51***. Different symbols represent different data sets.

Table 4: Adjusted r^2 for optimization and RMSE, CD and EF values for the model runs of calibration and validation data sets for DM_{shoot} calculated with a constant light use efficiency (LUE) during fall growth and with a variable LUE that depends on the radiation intensity in fall.

Statistical parameter	constant LUE		variable LUE	
	Calibration	Validation	Calibration	Validation
Adj. r^2	0.88		0.90	
RMSE	46.32	116.48	39.91	92.86
CD	0.71	0.88	0.77	0.83
EF	0.46	0.61	0.60	0.75

As the next step of parameterization the allometry parameters were optimized, which determine the partitioning of DM_{shoot} into leaf and stem fraction by a linear regression between the natural logarithms of both plant fractions. The parameters g and h were optimized together using DM_{leaf} and DM_{stem} data resulting in 1.62 and -3.01 for fall growth, respectively, and 2.22 and -5.60 for spring growth (Figure 2). Higher inaccuracy of the model calculations for spring growth is indicated by higher SE values (Table 3), and can also be noted in figure 2, where measured values in fall lie closer to the respective regression line than those in spring.

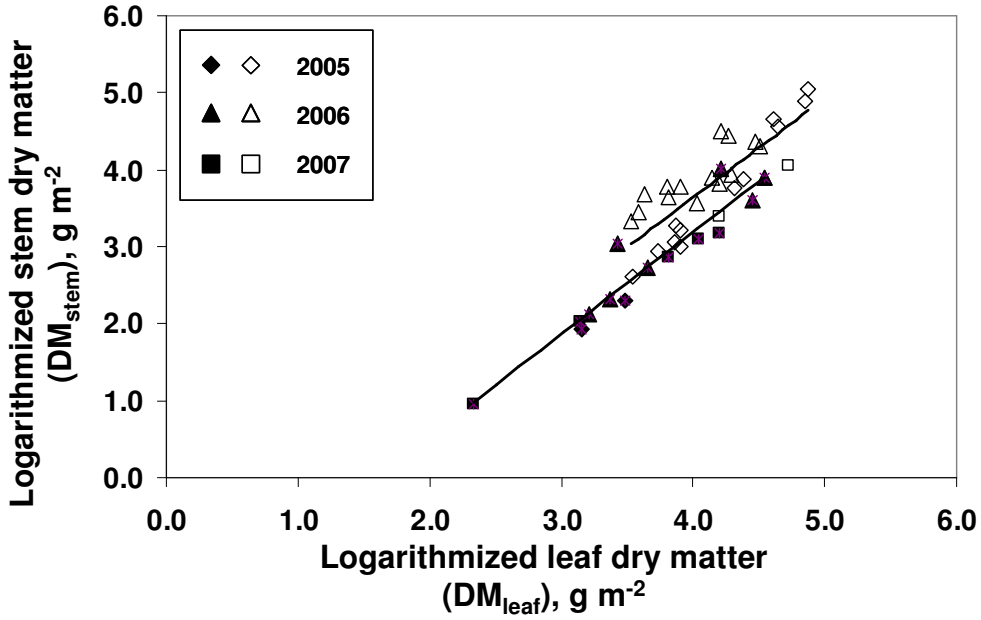

Figure 2: Allometric relation between logarithmized dry matter of stem (DM_{stem}) and leaf (DM_{leaf}) of winter oilseed rape before winter (closed symbols), y= 1.32(±0.12)x - 2.10(±0.45), r^2= 0.91*** and after winter until flowering (open symbols), y= 1.29(±0.17)x - 1.52(±0.69), r^2= 0.70***.

Similar to the decrease of LUE with increasing radiation intensity, SLA showed a decrease with increasing temperature sum during fall (Figure 3). The optimization with an upper and lower limit of SLA of 350 cm g^{-1} and 100 cm g^{-1}, resulted in -2.29 and 1368 for f_{SLA} and SLA_0, respectively. During spring growth no significant evidence could be found for a variable SLA. Optimization yielded a constant SLA of 151 cm^2 g^{-1} with a standard error of 60. SSA for the whole time period was determined as 29 cm^2 g^{-1} with an SE of 0.58.

Table 5: r^2, RMSE, CD and EF values of N_{shoot} for the calibration and the validation data sets. N_{shoot} was calculated (A) by Colnennes approach (see Eq. 22 and 23), and (B) according to the N_{shoot}-sum approach (see Eq. 18-21).

Statistical parameter	A		B	
	Calibration	Validation	Calibration	Validation
r^2	0.61	0.71	0.60	0.75
RMSE	1.89	4.73	2.12	4.37
CD	1.24	2.05	0.95	1.64
EF	0.59	0.55	0.48	0.62

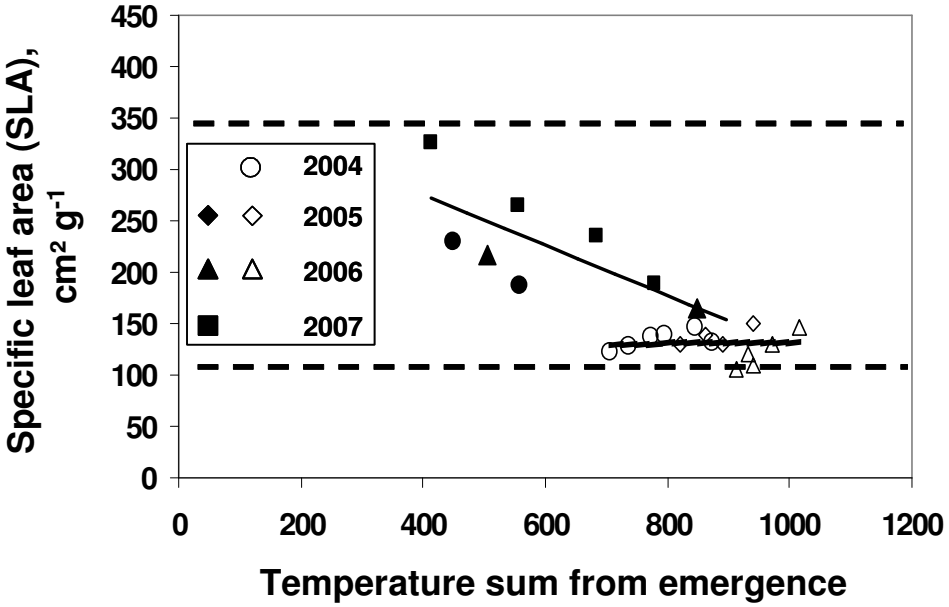

Figure 3: Specific leaf area (SLA) of winter oilseed rape as a function of temperature sum from emergence for the experimental years 2005–2007 before winter (closed symbols), $y = -0.28(\pm0.07)x+397(\pm47)$, $r^2 = 0.67$* and after winter until flowering (open symbols), $y = 0.0035(\pm0.04)x+128(\pm35)$, $r^2=0.0006$. Upper and lower limits for SLA in fall are indicated by dashed lines.

Dry matter losses during winter were assumed to correlate linearly with negative temperatures. The respective optimized value for f_{WL} is1.06×10^{-2}. The whole calibration data set was included in the optimization, but severe losses of DM_{shoot} occurred in 2006, only.

Nc_{stem} was calculated from DM_{stem} using an empirically determined exponential equation, where $Nc_{stem} = 4.47e^{-0.0024x}$ with an r^2 of 0.91 (Figure 4b). Upper and lower limits for Nc_{stem} in the model were set to 5.5 % and 1 %, respectively. N concentration of leaves was assumed to be constant with a mean value of 6.15 % and a SE of 1.08 (Figure 4c). According to the empirical approach by Colnenne et al. (1998), the N concentration of the aboveground dry matter can be calculated by the following parameterization of the power equation $Nc_{shoot} = 4.48x^{-0.25}$. This relation yielded an r^2 of 0.54. The optimized exponential curve showed an r^2 of 0.87 (Figure 4a). The comparison for the results of the statistical analysis for the estimation of N_{shoot} by Colnennes approach and the N_{shoot}-sum approach is shown in table 5. With respect to the results of calibration, Colnennes approach achieved better RMSE and EF values. The N_{shoot}-sum approach obtained a CD value of 0.95, which is closer to one than Colnennes approach with a CD value of 1.24. Concerning the validation, all parameters for quality of fit were better for the N_{shoot}-sum approach compared to the approach of Colnenne (Table 5).

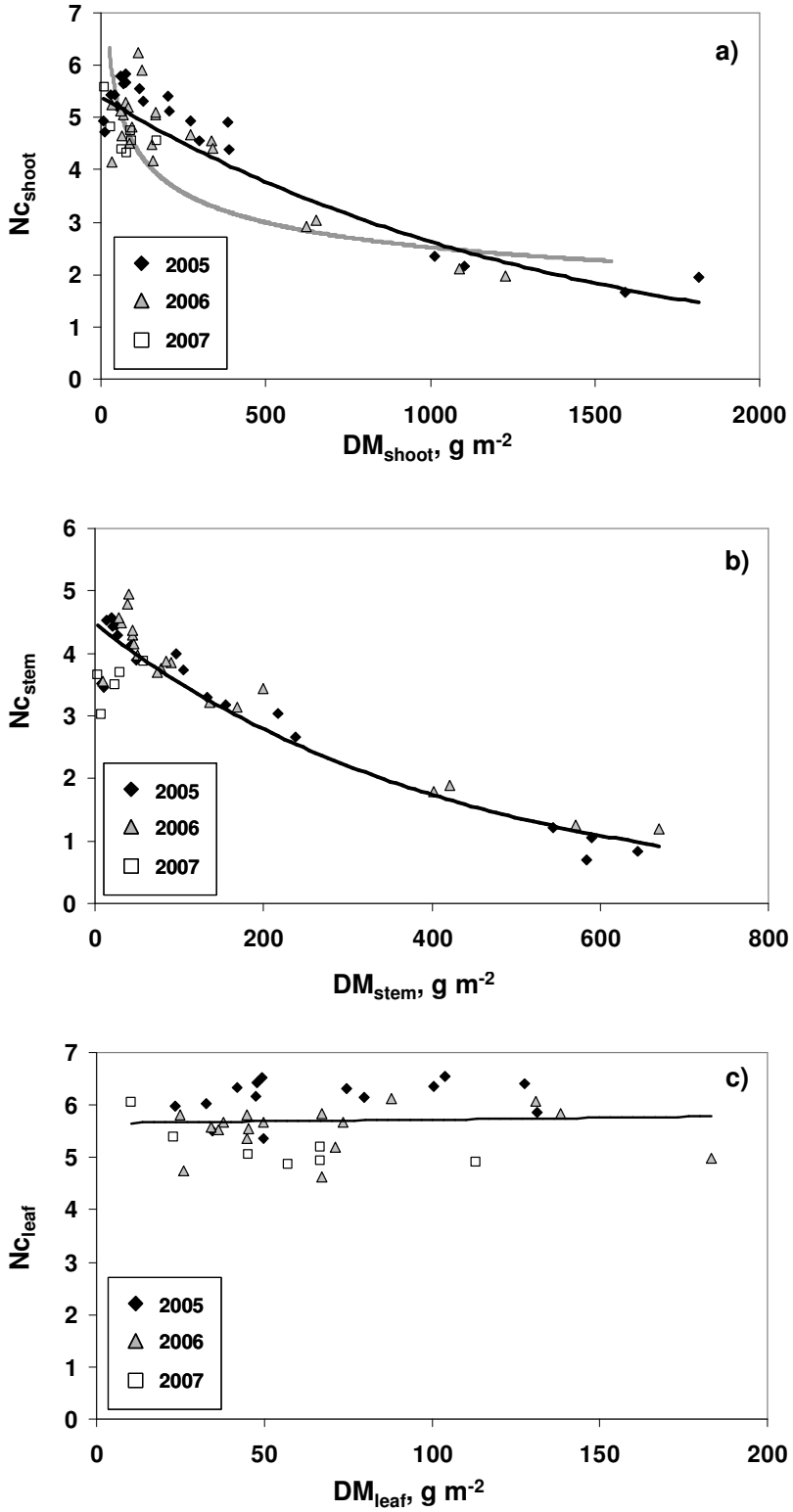

Figure 4: Relation of nitrogen concentration (Nc) to dry matter (DM) for the total aboveground dry matter (a) the stem fraction (b) and the leaf fraction (c) for the experimental years 2005 - 2007. a) Ncshoot to DMshoot according to a power function by Colnenne (grey), y=4.48x-0.25, r^2=0.54 and an exponential function y=5.40(±0.01)e-0.0007x, r^2=0.87***. b) Ncstem to DMstem according to an exponential function y=4.47(±0.09)e-0.0024x, r^2=0.91***. c) Ncleaf to DMleaf according to a linear regression y=0.0007(±0.002)x + 5.65(±0.17), r^2=0.0028.

3.2. Model calibration and validation

Results for the estimation of GAI, DM_{shoot} and N_{shoot} for the calibration and the validation data sets are shown in table 6. For the calculation of LUE in fall, the variable LUE approach and for the calculation of N_{shoot}, the N_{shoot}-sum approach was used. For a better comparison and interpretation, also all results for each year/location combination are given. The corresponding plots of measured vs. simulated values for all plant state variables of the calibration data set are shown in figure 5a/b/c.

The prediction of GAI results in a RMSE of 0.37 m^2 m^{-2} for calibration and a considerably higher value of 1.15 m^2 m^{-2} for validation. Similarly the rRMSE values are 0.37 for calibration and 0.75 for validation. Hohenschulen 2005 and 2006 achieved best results among the calibration data sets concerning r^2, RMSE and CD values. Among the validation data sets, Chalon achieved highest r^2 of 0.98 and Hohenschulen 2004 obtained the lowest RMSE of 1.09 m^2 m^{-2} and the best CD value with 0.75.

Concerning the validation data set, prediction of DM_{shoot} achieved better results than for prediction of GAI. Among the calibration data sets, Hohenschulen 2005 shows best results with r^2 = 0.96 and CD = 0.85. Lowest RMSE and rRMSE values were achieved for Hohenschulen 2006 with 26.8 g m^{-2} and 0.27, respectively. The validation data achieved a higher r^2 with 0.80 than the calibration data set with 0.70. Also, the CD value for validation was closer to 1 with 0.83 than for the calibration data set with 0.77. Although, RMSE of 92.9 g m^{-2} for validation exceeded calibration with 32.9 g m^{-2}, rRMSE indicates that the relative estimation error was almost the same with 0.40 for calibration and 0.45 for validation. Analysis of the model performance on the validation data set in detail reveals that for data sets 5 and 6 (Hohenschulen 2003 and 2004) the model showed poor accuracy. In particular the calculations for 2003 obtained lowest prediction power with an rRMSE higher than 1. The model validation had the best prediction power for data set 5 (Chalon, France 1995) with respect to all statistical parameter.

Almost the same relations could be found for the prediction of N_{shoot}. Among the calibration data sets, Hohenschulen 2005 and 2006 achieved best results with a RMSE and rRMSE of 1.35 g m^{-2} and 0.29 for 2006, and an r^2 and CD value of 0.96 and 0.99 for 2005. Overall, calibration yielded an RMSE of 2.12 g m^{-2} for N_{shoot}, whereas validation obtained 4.37 g m^{-2}. Again, highest r^2 of 0.94 was achieved by the Chalon data set, however, Hohenschulen 2003 yielded lowest RMSE of 2.30 g m^{-2} and Hohenschulen 2004 showed a CD value of 0.92.

To sum up, with respect to the rRMSE values, values for the whole calibration data set are similar for all parameters, ranging from 0.37 for GAI, 0.40 for DM_{shoot} to 0.45 for N_{shoot}. The results for the validation data set showed a higher range with 0.75 for GAI, 0.45 for DM_{shoot}

and 0.52 for N_{shoot}. rRMSE for N_{shoot} for the model calculations using the individual validation data sets were very similar for all three data sets, whereas for DM_{shoot} and GAI rRMSE values strongly differed, with the Hohenschulen data set in 2003 having values higher than one. Among the calibration data sets, rRMSE values showed little variability concerning all three plant parameters, with highest values for the UFOP 2006 data set. For the Hohenschulen data set in 2006, best results among the calibration data sets for all three plant parameters were obtained.

Table 6: r^2, RMSE, rRMSE and CD values of GAI, DM_{shoot} and N_{shoot} for the calibration and validation data sets and each year/location combination separately.

	Data set (Table 1)	r^2	RMSE	rRMSE	CD	n
GAI m^2 m^{-2}						
Calibration	1,2,3,4	0.70***	0.37 m^2 m^{-2}	0.37	0.68	48
	1	0.93***	0.39 m^2 m^{-2}	0.41	0.63	16
	2	0.72***	0.27 m^2 m^{-2}	0.28	0.96	16
	3	0.47**	0.49 m^2 m^{-2}	0.44	0.44	9
	4	0.82***	0.30 m^2 m^{-2}	0.30	0.59	7
Validation	5,6,7	0.19*	1.15 m^2 m^{-2}	0.75	0.76	30
	5	0.98***	1.12 m^2 m^{-2}	0.46	1.81	11
	6	0.55**	1.24 m^2 m^{-2}	1.17	0.13	7
	7	0.88***	1.09 m^2 m^{-2}	0.59	0.75	12
DM_{shoot} g m^{-2}						
Calibration	1,2,3,4	0.70***	39.9 g m^{-2}	0.40	0.77	48
	1	0.96***	34.3 g m^{-2}	0.32	0.85	16
	2	0.84***	26.8 g m^{-2}	0.27	0.45	16
	3	0.26*	61.0 g m^{-2}	0.56	0.84	9
	4	0.96***	42.4 g m^{-2}	0.55	0.40	7
Validation	5,6,7	0.80***	92.9 g m^{-2}	0.45	0.83	30
	5	0.99***	27.8 g m^{-2}	0.11	1.01	11
	6	0.91***	141.0 g m^{-2}	1.04	0.13	7
	7	0.93***	94.7 g m^{-2}	0.48	0.82	12
N_{shoot} g m^{-2}						
Calibration	1,2,3,4	0.60***	2.12 g m^{-2}	0.45	0.95	48
	1	0.96***	2.08 g m^{-2}	0.38	0.99	16
	2	0.67***	1.35 g m^{-2}	0.29	0.62	16
	3	0.06	3.11 g m^{-2}	0.66	0.77	9
	4	0.90***	2.05 g m^{-2}	0.58	0.42	7
Validation	5,6,7	0.75***	4.37 g m^{-2}	0.52	1.64	30
	5	0.94***	4.48 g m^{-2}	0.46	2.13	11
	6	0.89***	2.30 g m^{-2}	0.46	0.41	7
	7	0.90***	5.24 g m^{-2}	0.56	0.92	12

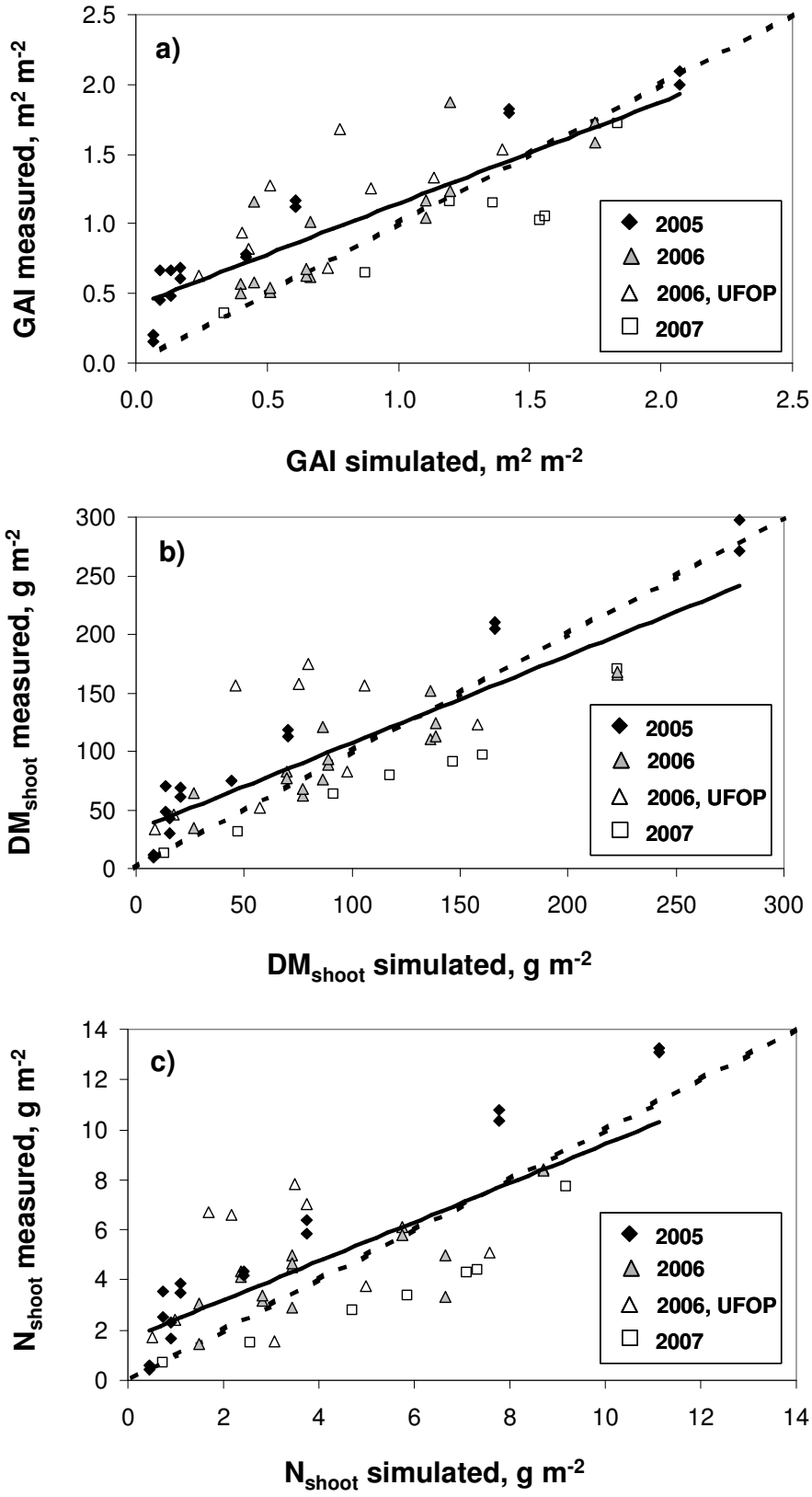

Figure 5: Linear regressions of simulated and measured values for the plant parameters GAI, DM_{shoot} and N_{shoot}. The regression functions and r^2 for all subfigures are as followed: (a) $y = 0.73x + 0.41$, $r^2 = 0.70$; (b) $y = 0.75x + 32.71$, $r^2 = 0.70$; (c) $y = 0.78x + 1.64$, $r^2 = 0.60$.

4. Discussion

The aim of this study is to present a dynamic growth model for winter oilseed rape, which calculates plant area, dry matter production and N uptake from emergence to the onset of flowering including the winter season with a break of vegetative growth and DM loss. It is designed to be applied for unstressed conditions. Additionally, two approaches for light use efficiency (LUE), that mainly determines dry matter production, were tested on being either constant or variable, depending on radiation intensity during fall. Furthermore, two model concepts for the calculation of N uptake in the shoot were compared. The first approach, N_{shoot}-sum, first calculated N uptake for the leaf and the stem fraction, before adding both for the total N uptake for the shoot. The second approach, Colnennes approach, first derived N concentration for the shoot as dependent on shoot dry matter, before multiplying DM_{shoot} and Nc_{shoot}.

Varying LUE during growth of OSR has been the object of many studies (Justes et al., 2000; Mendham et al., 1981; Kiniry et al., 1995; Gosse et al., 1983; Rode et al., 1983; Habekotté, 1997). Justes et al. (2000) discussed seasonal variation of LUE due to changes in temperature, developmental stages and crop N nutrition status. Habekotté (1997a) investigated the effects of different LUE from flowering to ripening on yield formation processes. We also found evidence that LUE for winter oilseed rape shows a decrease with increasing radiation intensity (Figure 1). In early fall, when radiation intensity is high and the canopy is not yet closed, LUE is low because the photosynthetic capacity of single leaves gets saturated. Short time before winter, photosynthetic reaction is exposed to less radiation intensity, so that LUE rises. Dry matter predictions achieved better results with a variable LUE than with a constant one (Table 4) even though standard errors for the parameter optimization were high. The optimized LUE_0 of 3.78, representing highest LUE in fall, is in agreements with results found for planophil plants like OSR by several authors (Rao and Mendham, 1991; Leach et al., 1989). In spring, we achieved best results with a constant LUE, which is higher than the optimized constant LUE in fall. The high difference must be interpreted carefully, because OSR can support early growth with reserves from the taproot. The reason for a constant saturated LUE in spring can be attributed to the fact that the canopy closes fast after beginning of growth in spring. As LUE is determined on a crop scale from stem elongation on, it has to be taken into account that leaves with evitable higher LUE on the top are commonly analyzed with leaves of lower LUE closer to the bottom of the plants.

For the partitioning of shoot dry matter a simple allometric approach was used (Figure 2). Even though the relation of logarithmized stem dry matter to logarithmized leaf dry matter shows the same slope for data in fall and spring, we observed a drift towards DM_{stem} after

winter. This may be explained by the dry matter losses during winter, which mainly affect the leaf fraction. Taking a closer look at data for 2006 (open and closed triangles), which is the only year with severe losses during winter, underlines this hypothesis. Since losses during winter for OSR occur regularly, a separate parameterization for fall and spring is reasonable. In general, we observed that the prediction power for DM_{stem} is lower than for DM_{leaf} (data not shown), but since DM_{stem} is less than DM_{leaf} until flowering, a higher deviation is not critical. Marcelis (1993) states that a descriptive allometric approach for partitioning can be easily parameterized, but its limited explanatory value has to be seen critically. As soon as the model is applied for the calculation of dry matter production and partitioning under unfavourable, stressed conditions it has to be questioned whether the allometric approach still holds valid for the calculation of leaf and stem fraction.

Leaf and stem area are derived by their dry matter fractions and by specific leaf and stem area. Similar to results for LUE in fall, we found evidence that SLA decreases with increasing temperature sum (Figure 3). According to the morphological maturation process, young leaves as well as shadow leaves, with an undeveloped or small mesophyll layer, have a higher SLA than matured leaves with a completely developed mesophyll (Gammelvind et al., 1996). As soon as leaves are completely developed or young and old leaves are considered together on a crop scale like in spring, SLA becomes constant. Relation of stem area and weight does not change during vegetative growth, which is indicated by the optimized SSA and its low standard error.

Regarding the N concentrations in leaf and stem fraction, which are needed to derive N uptake, we found evidence that leaves have a constant N concentration for the whole vegetative growth phase until flowering. This is underlined by the slope of the regression line of Nc_{leaf} to DM_{leaf}, which is not significantly different from zero (Figure 6). Nc_{stem} decreases with increasing DM_{stem}, following an exponential curve, which achieved an r^2 of 0.91 (Figure 5). Colnenne described this inverse relation with his dilution curve for OSR for the total shoot. He used a power function, which achieved an r^2 of 0.54 on our data sets (Figure 4a). The exponential function we used showed an r^2 of 0.87. A comparison of prediction power for the shoot N uptake of the validation revealed that the N_{shoot}-sum approach with separate calculation of N_{stem} an N_{leaf} achieved better results than Colnennes approach. According to the calibration results, Colnennes approach obtained a lower deviation of predicted to measured values. This can be explained by the fact that the N_{shoot}-sum approach consist of two calculations, N_{leaf} and N_{stem}, so that deviations for both prediction are summed up.

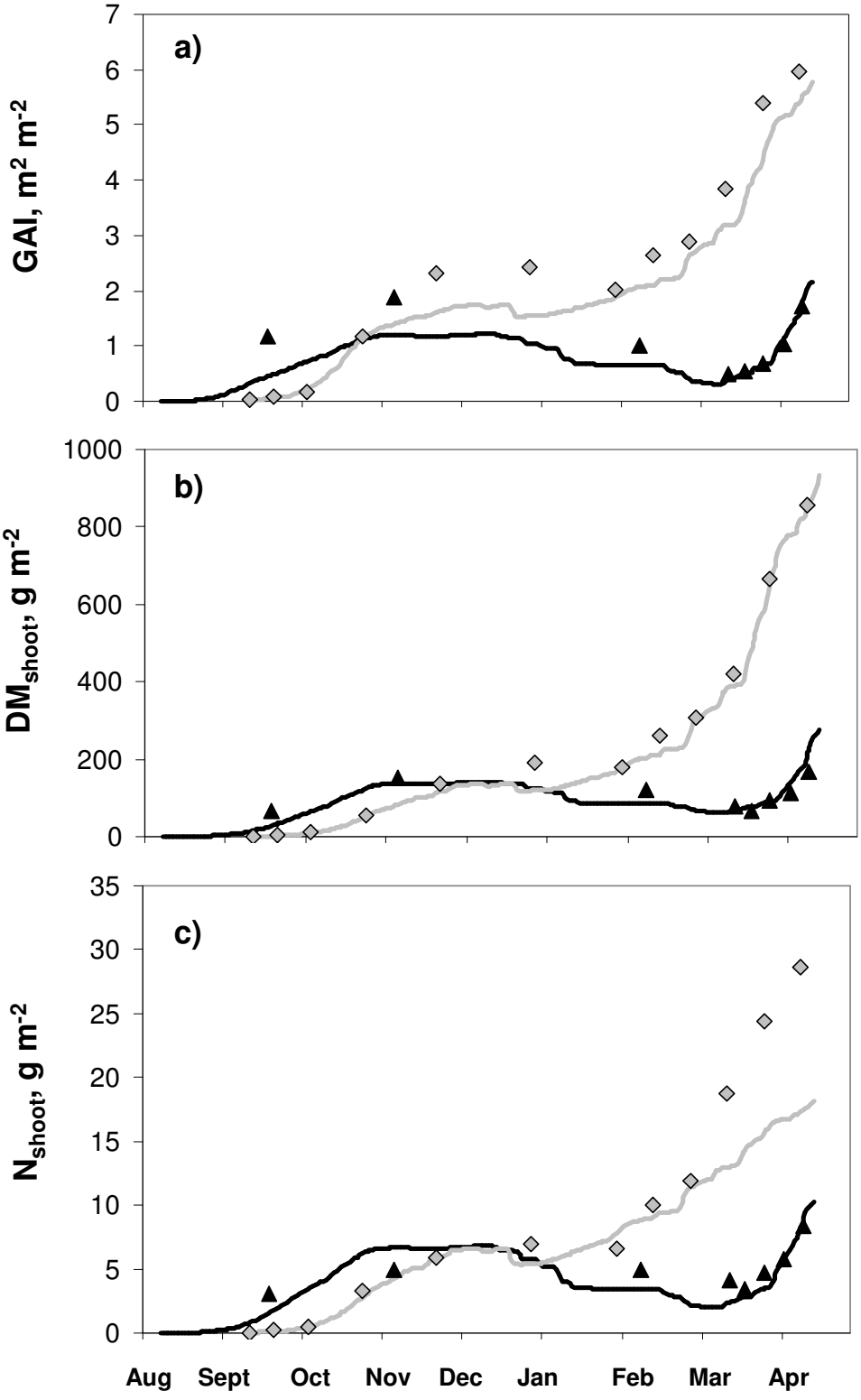

Figure 6: Time course of observed and predicted data of a) GAI, b) DM_{shoot} and c) N_{shoot} for Hohenschulen 2006 (black) and Chalon 1995 (grey).

The presented model differs from other models for winter oilseed rape (Habekotté, 1997a; Husson et al., 1998; Gabrielle et al., 1998) concerning two main aspects. The first one applies for the LUE, which in contrast to other models, is variable in fall, depending on the radiation intensity. The second aspect is the calculation of dry matter losses during winter according to negative temperatures, which enables to calculate dry matter production between fall and spring without interception.

A problem was the availability and amount of suitable data for calibration and validation, which limited model optimization and evaluation. Especially the number of measurement dates in fall, when we found variable parameters for LUE and SLA, was small. Severe winter losses occurred in 2006, only (Figure 6). Additional data sets for a more robust parameterization would be desirable. Against this background optimization must be seen critically.

The model is defined by simple empirical relations. Root growth has only been considered rudimentarily by a simple linear function. Especially under drought conditions, this approach will probably not be sufficient to give valid results on crop growth parameters. Therefore, further model development including more mechanistically based approaches, which might be appropriate to describe growth traits under unfavourable conditions, should be done in the future.

5. Conclusions

The presented crop growth model for OSR was able to predict GAI, DM_{shoot} and N_{shoot} from emergence to flowering. The approach for dry matter production in fall according to a variable LUE proved to be better suited for prediction of dry matter concerning all presented statistical parameters compared to the constant LUE approach. The N_{shoot}-sum approach, which was compared to Colnennes approach, for the calculation of nitrogen uptake, improved the prediction accuracy. The dynamics of dry matter losses during winter could be reproduced by the model, although one year with sever losses was available, only.

Acknowledgements

Thanks to Dr. K. Sieling for his great support concerning statistical matters. Thanks to Dr. A. Pacholski for his constructive comments on this manuscript and to A.-J. Kuhlmann, for her kindly support on this manuscript. Also thanks to the DBU, German Federal Environmental Foundation, for kindly supporting my project.

References

Colnenne, C., Meynard, J. M., Reau, R., Justes, E. & Merrien, A. (1998). "Determination of a critical nitrogen dilution curve for oilseed rape." Annals of Botany 81: 311-317.

Dreccer, M. F., Schapendonk, A. H. C. M., Slafer, G. A., Rabbinge, R. (2000). "Comparative response of wheat and oilseed rape to nitrogen supply: absorption and utilisation efficiency of radiation and nitrogen during the reproductive stages determining yield." Plant and Soil 220: 189-205.

Gabrielle, B., Denoroy, P., Gosse, G., Justes, E., Andersen, M. N. (1998). "Development and evaluation of a CERES-type model for winter oilseed rape." Field Crops Research 57: 95-111.

Gabrielle, D., P., Gosse, G., Justes, E., Andersen, M. N. (1998a). "A model of leaf area development and senescence for winter oilseed rape." Field Crops Research 57: 209-222.

Gammelvind, L. H., Schjoerring, J. K., Mogensen, V. O., Jensen, C. R., Bock, J. G. H. (1996). "Photosynthesis in leaves and siliques of winter oilseed rape (*Brassica napus* L.)." Plant and Soil 186: 227-236.

Gosse, G., Cellier, P., Denoroy, P., Gabrielle, B., Laville, P., Leviel, B., Justes, E., Nicolardot, B., Mary, B., Recous, S., Germon, J.-C., Hénault, C., Leech, P.K. (1999). "Water, carbon and nitrogen cycling in a rendzina soil cropped with winter oilseed rape: the Châlons Oilseed Rape Database. " Agronomie 19: 119-124.

Habekotté, B. (1997a). "Evaluation of seed yield determing factors of winter oilseed rape (*Brassica napus* L.) by means of crop growth modelling." Field Crops Research 54: 137-151.

Habekotté, B. (1997). "A model of the phenological development of winter oilseed rape (*Brassica napus* L.)." Field Crops Research 54: 127-136.

Husson, F., Wallach, D., Vandeputte, B. (1998). "Evaluation of CECOL, a model of winter rape (*Brassica napus* L.)." European Journal of Agronomy 8: 205-214.

Justes, E., Denoroy, P., Gabrielle, B., Gosse, G. (2000). "Effect of crop nitrogen status and temperature on the radiation use efficiency of winter oilseed rape." European Journal of Agronomy 13: 165-177.

Kage, H., Kochler, M., Stützel, H. (2000). "Root growth of cauliflower (*Brassica oleracea* L. botrytis) under unstressed conditions: Measurements and modelling." Plant and Soil 223: 131-145.

Kage, H., Stützel, H. (1999 a). "HUME: An object oriented component library for generic modular modelling of dynamic systems." European Society of Agronomy, Lleida.

Kage, H. S., H. (1999). "A simple empirical model for predicting development and dry matter partitioning in cauliflower." Scientia Horticulturae 80: 19-38.

Kiniry, J. R., Major, D. J., Izaurralde, R. C., Williams, J. R., Gasman, P. W., Morrison, M. (1995). "EPIC model parameters for cereal, oilseed rape and forage crops in the northern Great Plains region." Canadian Journal of Plant Science 75: 679-688.

Kuhlmann, W. (1980). "Parameterschätzung von Eingleichungsmodellen im unbeschränkten Parameterraum." Würzburg, Physica Verlag.

Lancashire, P.D., Bleiholder, H., Langelüddecke, P., Stauss, R., Boom, T.V.D., Weber, E., and Witzenberger, A. (1991). "An uniform decimal code for growth stages of crops and weeds." Annals of Applied Biology 119: 561-601.

Leach, J. E., Milford, G. F. J., Mullen, L. A., Scott, T., Stevenson, H. J. (1989). "Accumulation of dry matter in oilseed rape crops in relation to the reflection and absorption of solar radiation by different canopy structures." Aspects of Applied Biology 23: 117-123.

Lemaire, G., Salette, J. (1984). " Relation entre dynamique de croissance et dynamique de prélèvement d'azote pour un peuplement de graminées fourragères I. Etude de l'effet du milieu." Agronomie 4: 423-430.

Lickfett, T., Kreikenbohm, G., Goebel, C., Przemeck, E. (1993). "Über den Anstieg des Rest-Nmin nach Winterraps und Maßnahmen zur seiner Vermeidung." VDLUFA-Schriftenreihe 36: 91-94.

Lickfett, T., Przemeck, E. (1995). "Ausnutzungsgrad von Mineraldünger-Stickstoff in Rapsfruchtfolgen unterschiedlicher Produktionsintensität." VDLUFA-Schriftenreihe 40: 833-836.

Loague, K., Green, R. E. (1991). "Statistical and graphical methods for evaluating solute transport models: Overview and application." Journal of Contaminant Hydrology 7: 51-73.

Marcelis, L. F. M. (1993). "Simulation of biomass allocation in greenhouse crops - a review." Acta Horticulturae 328: 49-67.

Marshall, B., Squire, G. R. (1996). "Non-linearity in rate-temperature relations of germination in oilseed rape." Journal of Experimental Botany 47: 1369-1375.

Mendham, N. J., Shipway, P. A., Scott, R. K. (1981). "The effects of delayed sowing and weather on growth, development and yield of winter oil-seed rape (*Brassica napus* L.)." Journal of Agricultural Science 96: 389-416.

Porter, J. R., Gawith, M. (1999). "Temperatures and the growth and development of wheat - a review." European Journal of Agronomy 10: 23-36.

Rao, M.S.S., Mendham, N.J. (1991). "Soil-plant water relations of oilseed rape (*Brassica napus* L. and *Brassica campestris* L.)." Journal of Agricultural Science Cambridge 117: 197-205.

Rode, J. C., Gosse, G., Chartier, M. (1983). "Vers une modelisation de la production de graines de colza de printemps." Informations Techniques CETIOM 82: 10-20.

Sieling, K., Günther-Borstel, O. & Hanus, H. (1997). "Effect of slurry application and mineral nitrogen fertilization on N leaching in different crop combinations." The Journal of Agricultural Science 128: 79-86.

Sieling, K. C., O. (1997a). "Effect of preceding crop combination and N fertilization on yield of six oil-seed rape cultivars (*Brassica napus* L.)." European Journal of Agronomy 7: 301-306.

Szeicz, G. (1974). “Solar radiation for plant growth.” Journal of Applied Ecology 11: 617-636.

Chapter 5

General discussion

1. Introduction

Winter oilseed rape (OSR) has become more and more important in Germany in the last decades, which caused a rising acreage. The reasons are its profitability, the potential to grow OSR as a renewable resource for biofuel production and its beneficial value as preceding crop. At the same time, OSR is one of the most inefficient crops concerning nitrogen (N) (Lickfett et al., 1993; Lickfett and Przemeck, 1995; Sieling, 1997). The reasons are early leaf fall during the vegetation period, early harvest causing long time for mineralization, low N-harvest indices and the following crop, wheat, which takes up low amounts of nitrogen before winter. As a consequence, Lickfett (1993) found that soil mineral N (SMN) content regularly increases during autumn, which again can lead to losses of nitrate by leaching into the groundwater (Sieling et al., 1999, Chalmers and Darby, 1992).
For cereal crops, N efficiency was increased due to a site specific N application (Blackmer et al., 1998, Raun et al., 2002; Ebertseder et al., 2003, Delin, 2005). Yield varies within fields because of different soil properties and therefore different water and nitrogen availability. In advance of the presented study, infield variability of the experimental site has been tested 2004 for OSR concerning yield, soil mineral N content (SMN), net mineralization (Table 1) and water availability (Figure 1) in eight blocks at three different positions (hilltops, slopes and dips), each combined with two different fertilizer treatments (unfertilized (N0) and 240 kg N ha^{-1} (N3)). The volumetric water content was determined for the fertilized plots by TDR (Time Domain Reflectometry) from April to harvest at the end of July. Net mineralization was derived from SMN at the beginning of growth in spring and at harvest, shoot dry matter (DM_{shoot}) at the beginning of growth in spring and seed and straw yield and the corresponding nitrogen concentrations.

Table 1: Net mineralization, soil mineral nitrogen and yield of unfertilized (N0) and fertilized (N3 – 240 kg N ha^{-1}) winter oilseed rape crops for different in-field positions in 2004.

In-field position	Slope 1	Dip 1	Hill top 1	Dip 2	Dip 3	Hill top 2	Slope 2	Dip 4	Ø
Yield N0 [dt ha^{-1}]	24.6	38.0	34.4	39.2	39.1	28.9	43.4	29.5	34
SMN N0 at harvest [kg ha^{-1}]	25	42	41	99	49	34	43	57	49
Yield N3 [dt ha^{-1}]	48.2	62.2	72.0	57.5	–	61.0	56.1	60.0	59
SMN N3 at harvest [kg ha^{-1}]	29	101	55	175	89	74	56	70	81
Net minerali-zation [kg ha^{-1}]	43	59	61	73	72	65	100	78	74

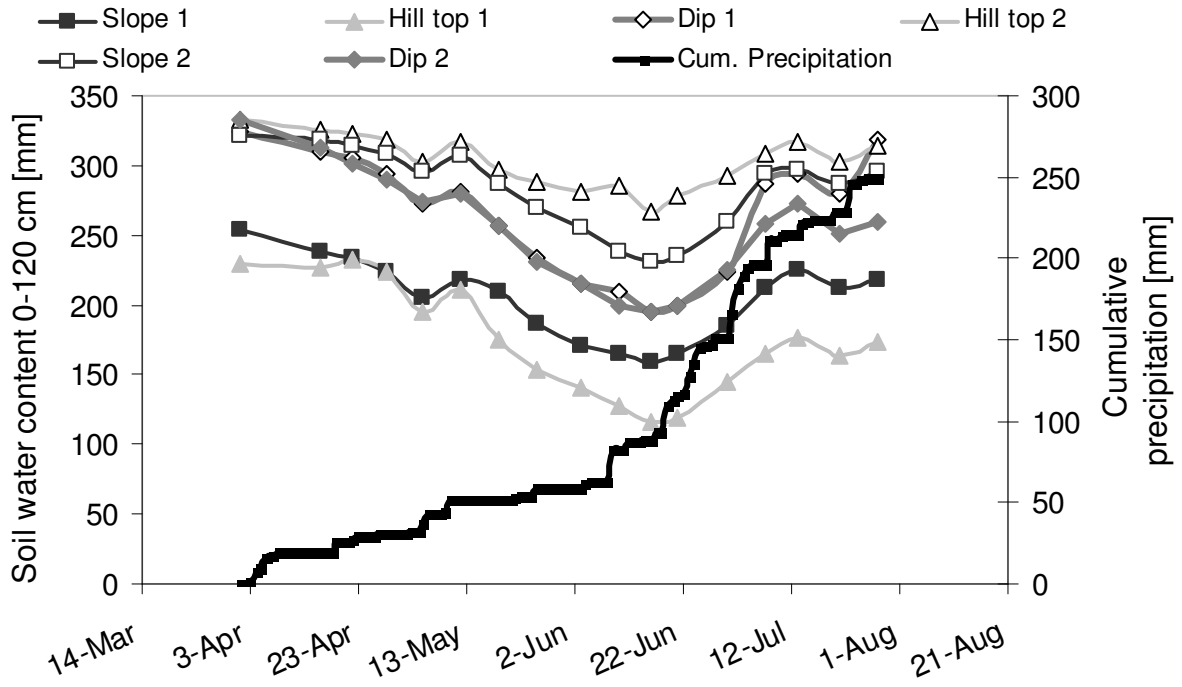

Figure 1: Cumulative precipitation and soil water of fertilized winter oilseed crops from 0-120 cm for different in-field positions in 2004.

Seed yields of the fertilized treatments varied between 48 dt ha^{-1} and 72 dt ha^{-1} with a coefficient of variation (CV) of 11.2 %. Unfertilized treatments even showed a higher CV of 17.4 % with seed yields varying between 25 dt ha^{-1} and 43 dt ha^{-1}. Highest and lowest yields were found between same in-field positions. SMN and net mineralization also showed high variability; especially concerning the dip positions, where high SMN values were found despite average net mineralization and above-average values for both parameters achieved a yield below average. Concerning the volumetric water content, high differences were observed, even among same positions, but caused by the high amount of precipitation in 2004, no drought stress could be found.

These results show that the differences of nitrogen and water availability cannot be seen as the only reasons for yield differences. Other aspects like emergence and establishment in autumn or position depending inclination, which can cause different radiation intensities should be considered also. A plant growth model for OSR might be a useful tool for the analysis of growth and yield determining parameters. For initialization and parameterization of site and year specific depending factors, information of specific growth measures like biomass and N uptake can be used. Since destructive measurements in realtime and for large areas are too labour intensive, sensory measurements may be useful to assess those parameters (Xue et al., 2004, Boegh et al., 2002). Additionally, because phenological

development affects growth and yield formation (Mendham et al., 1981; Leterme, 1985; Habekotté, 1997), knowledge on phenology may be useful to control plant growth simulations.

2. Summarized discussion for all results

Against the above mentioned background, three main objectives were attended. The first one was the establishment of a sensory, non-destructive method to achieve information on site specific variability of the OSR canopy. This was obtained by measuring canopy reflectance and detecting best waveband combinations, so called vegetation indices (VI), for the derivation of plant parameters. Second, a phenological model was developed and parameterized for german conditions to predict developmental stages with a high resolution. Third, a crop growth model for OSR was developed, to predict plant parameters like biomass and nitrogen supply of the crops in the time course, so that fertilizer demand and yield prediction can be derived.

Newly generated VIs proved to be suited for deriving crop canopy parameters like green area index (GAI), shoot dry matter (DM_{shoot}) and nitrogen uptake by the plants (N_{shoot}) for the time course of emergence to flowering. Especially waveband combinations of the near infrared reflectance, 740 nm and 780 nm, achieved best results concerning r^2 and RMSE, presumably because reflectance in the visible region of the spectrum approaches saturation with leaf area index (LAI) values of higher than three. Therefore, VIs derived from those wavelengths are not applicable for the estimation of crop canopy parameters in later stages of plant development (Filella 1995; Aparicio 2000). Near infrared light needs a higher LAI to reach saturation of reflectance, and therefore VIs based on these wavelengths can be used to estimate crop canopy parameters like biomass even in late phases of the growth period (Tarpley 2000). However, algorithms are needed, which convert this information to fertilizer recommendations.

Henke (2008) investigated the correlation of N_{shoot} and soil mineral N (SMN) before and after winter to the optimal N fertilizer amount in spring (Nopt). He found that Nopt correlates with N_{shoot} in late fall, so that N_{shoot} seems to be a suitable indicator for the correction of fertilization rates in spring. Since remote sensing serves site specifically crop information on a field scale, field maps for N_{shoot} in fall may be derived (Figure 2a) by converting appropriate VIs (Müller et al., 2008). These maps in turn can be used as the base for the derivation of fertilizer recommendations (Figure 2b) by using an algorithm (Equation 1) according to Henke (2008), who considered canopy N in fall for optimal N fertilization in spring. The implementation of his approach is based on an average OSR canopy of 50 kg N ha^{-1} in fall, which will be fertilized in spring according to official recommendation (195 kg N ha^{-1}). Each kg N ha^{-1} exceeding the threshold of 50 kg N ha^{-1} reduces the N fertilization in spring by a

correction factor of 0.7 kg N ha^{-1} (Equation 1). If canopy N values in fall are below 50 kg N ha^{-1}, fertilization will be conducted according to official recommendations(195 kg N ha^{-1}). This concept has not yet thoroughly been tested, but is subject of an ongoing project.

N demand kg N ha^{-1}= 195 – 0.7 * (N_{shoot} kg N ha^{-1} – 50) (Eq. 1)

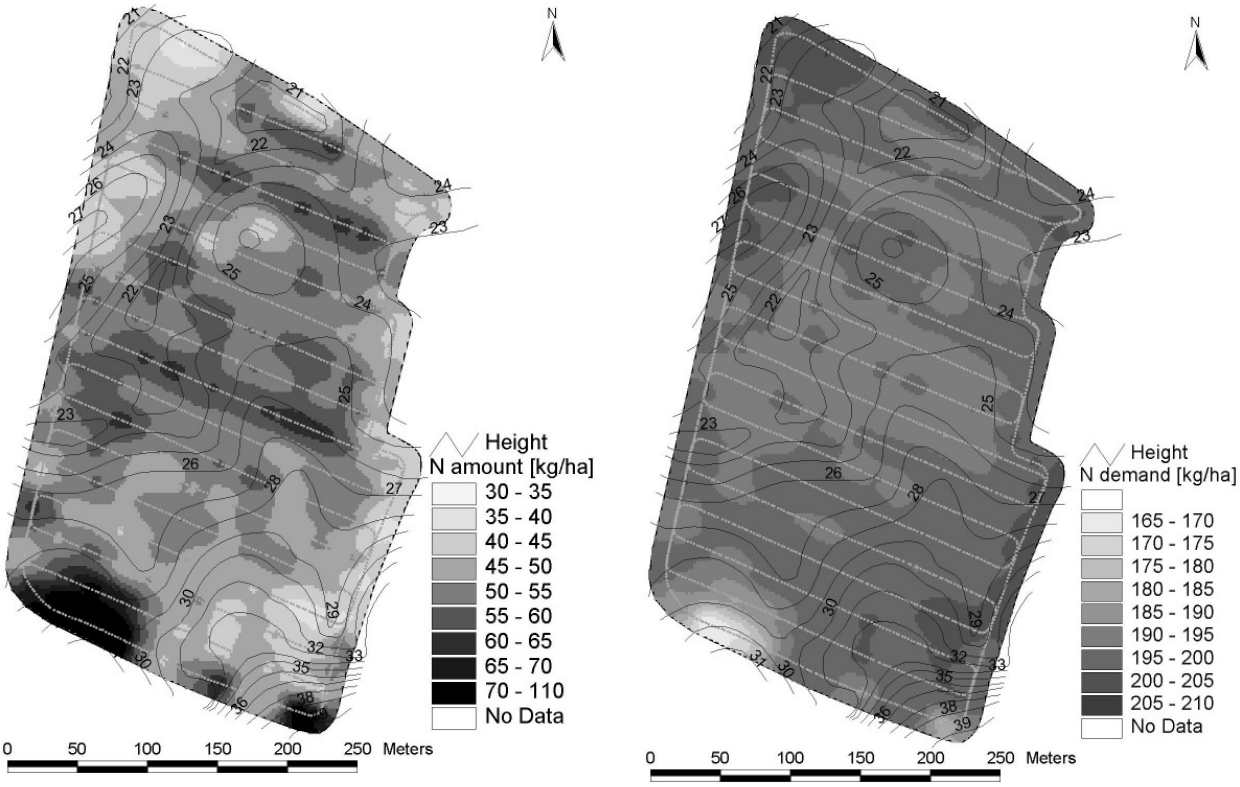

Figure 2: Field maps for (a) N_{shoot} derived from remote sensing measurements in fall 2006 and for (b) derived N demand in spring, obtained by using fertilizer algorithms, which include N_{shoot} in fall (Eq.1).

Recent studies on the suitability (unpublished) of reflection measurements during fall on the field scale revealed problems concerning several aspects. The angle of incoming radiation should be as vertical as possible during the whole measurement time, because changes in inclination can cause high variations for reflectance spectra (Reusch, 1997; Thiessen, 2002). The diagonal angle of the sun for the northern hemisphere during fall and winter causes a short time period around noon for measurements in late fall. Also, measurements of reflection must be conducted with dry crops, because wet canopies distort results. Caused by short days and wet weather conditions, canopies in late fall are often watery, so that proper measurements cannot often be carried out. To obtain information on crop parameter in time course, crop growth models can be used also. Reflectance measurements could be used for initialization or parameterization. The presented model for OSR predicts dry matter

production, green are index and nitrogen uptake in the time course from emergence to flowering, including losses of dry matter during winter. Alternatively to reflectance measurements, predictions for N_{shoot} by the model in late fall could be used to derive fertilizer recommendations. Model predictions can also be used to estimate yield potential, which in turn enables for the derivation of optimized N fertilization rates (Nopt). Maidl (pers. comm.) tries to define Nopt values for differently developed crops, whereas results of other projects (Kage, pers. comm.) revealed only low correlations between Nopt and potential yield level. Since the calculation of a Nopt for winter oilseed rape holds some problems, other approaches for improving N fertilization should be considered. Several authors discussed a growth stage specific application of fertilizers (Sieling, 2004; Barlog, 2004; Ghersa, 1995). Therefore, predicting developmental stages according to a phenological model might be a useful tool. The presented model can predict developmental stages according to the BBCH scale (Lancashire et al. 1991). It is based on BRASNAP-PH (Habekotté, 1997), which was developed for northwest Europe. According to many studies that have been conducted on the sensitivity of the development of winter oilseed rape and related plants to vernalization and photoperiod (Andrew, 1991, Mendham, 1981, Myers, 1982, Robertson, 2002, Huang, 2001, Yan, 1998), the phenological development is mainly based on vernalization, photoperiod and temperature. Parameter optimization on a large data set throughout Germany, lead to robust calibration and cross calibration. Phenological stages can be predicted with a root mean square error (RMSE) of 3.11 for the whole developmental phase. Therefore, it can be used to support growth specific production management strategies for OSR.

3. Analysis of additional strategies for the improvement of nitrogen efficiency and for minimization of leaching of soil mineral nitrogen after winter oilseed rape

Besides site specific fertilization, other strategies were investigated and discussed by several authors to improve nitrogen efficiency for OSR.

Starting point for plant breeders is the enhancement of harvest index (HI) and nitrogen harvest index (NHI) (Möllers et al, 2000; Friedt et al., 2003). This should be accomplished by hybridize conventional winter oilseed rape varieties with dwarf genotypes to achieve semi-dwarf types, which show a reduced growth form. Sieling and Kage (2007) investigated conventional and semi-dwarf varieties concerning their HI and NHI. Although plant height was reduced for the semi-dwarf types, above ground biomass was the same as for the conventional varieties, so that no improved HI or NHI could be found. Habekotté (1997) suggested a genotype that combines early flowering with late ripening so that the source-sink-capacity during seed filling is optimized and higher yields with high HI can be realized.

Möllers (2000) and Friedt (2003) observed higher nitrogen efficiency for hybrid varieties compared to conventional ones, because higher yields were achieved with the same amount of nitrogen fertilizer. In general, breeders did not put much emphasis on improving nitrogen efficiency for winter oilseed rape. Several authors (Schjoerring et al, 1995; Rathke et al., 2006; Allirand et al., 2007) stated that improved nitrogen efficiency must be obtained by different factors like a synchronization of leaf senescence and translocation of nitrogen into the seeds resulting in a reduced amount of fertilized nitrogen.

Besides low nitrogen efficiency, Sieling (2000) and Rathke et al. (2006) observed high losses of nitrogen by leaching after winter oilseed rape. Long time for mineralization, caused by an early harvest of OSR, leads to high amounts of soil mineral nitrogen before winter. Henke (2008) observed that the typical following crop, winter wheat, can take up only 20-25 kg N ha^{-1} before winter. The prevention of soil mineral nitrogen accumulation in the soil after OSR harvest is according to Di and Cameron (2002) the key to reduce leaching. Two different approaches were discussed to avoid accumulation after OSR.

The first one deals with a change of the crop rotation and the integration of catch crops. Catch crops have a higher potential for nitrogen uptake before winter compared to winter wheat (Lickfett, 1993; Beaudoin et al., 2005). Additionally, the consequential higher water use leads to a delayed initiation of leaching during winter. The economical aspect of catch crops is usually negative, because they cause additional costs and the following spring crops are less competitive than winter crops. Another alternative is the growth of volunteer OSR, which can take up and save nitrogen until spring (Lickfett, 1993). However, this approach is limited by phytosanitary aspects and plant diseases like clubroot (*Plasmodiophora brassicae*).

Goss et al. (1993) discussed a second approach to avoid nitrogen leaching by a reduced tillage depth and a delayed tillage after harvest. This could be confirmed by Henke et al. (2008). Reduced tillage causes a reduced soil aeration, which in turn reduces mineralization of soil organic nitrogen (Lickfett, 1993; Catt et al., 2000). In contrast, an intensive tillage would support mineralization of immobilized soil nitrogen (Kristensen et al., 2000). Lickfett (1993) investigated the reducing effect of a delayed tillage on mineralization of soil nitrogen. This also causes a delayed sowing of the subsequent crop, which in turn may cause problems in plant establishment and therefore in nitrogen uptake. Concerning an intensive tillage, C/N ratio of the residues has to be taken into account, also. Sieling (2000) stated that nitrogen can not be mineralized with C/N ratios of residues, exceeding a threshold value of 21 to 30. Henke et al. (2008) found a C/N ratio for OSR residues of 50 and 60, therefore exceeding this threshold. Several authors found a nitrogen immobilization after OSR residue incorporation (Justes et al., 1999, Mary et al., 1999, Nicolardot et al., 2001). Still, Henke (2008) detected rising soil mineral nitrogen values after incorporation of OSR residues in fall,

which can be explained by the long time for mineralization processes because of the early harvest date. Nevertheless, Henke (2008) concluded that minimum or zero tillage and growing winter wheat as following crop after OSR should become the standard practice.

4. Conclusion

The presented results can contribute to the application of a site specific fertilization by providing information on site specific variability of crop parameters on the one hand and by analyzing crop growth in the time course from emergence to flowering with a crop growth model. Prediction of phenological development can support growth-specific production management and serve as control entity for manage different crop growth traits inside crop growth models. To analyze the impact of site specific fertilization on improving N efficiency for winter oilseed rape, this concept has to be tested on the field scale. In general, site specific application cannot be seen as the only factor for improving N efficiency for OSR. Further investigations for the understanding of seed yield forming processes, which has hardly been conducted in the past, should be carried out. This may give insights to possible effects of altered N applications for the improvement of N fluxes to and inside the crop during seed formation. Also, other aspects concerning production management based aspects, like a change in crop rotation and a reduced tillage, or concerning breeding programmes should be considered. A combination of all factors seems to be the most promising approach for improving N efficiency for OSR.

References

Allirand, J. M., Jullien, A., Savin, A. Ney, B. (2007). „Oilseed rape leaves falling off depends on both leaf nitrogen content and transmitted radiation." Proceedings of the 12th International Rapeseed Congress, Wuhan, China: 307-310.

Andrew, M., Tommey, M., Evans, E.J. (1991). "Temperature and daylength control of flowering initiation in winter oilseed rape (*Brassica napus* L.)." Annals of Applied Biology 118: 201-208.

Aparicio, N., Villegas, D., Casadesus, J., Araus, J.L., Royo, C. (2000). "Spectral vegetation indices as nondestructive tools for determining durum wheat yield." Agronomy Journal 92: 83-91.

Barlóg, P. G., W. (2004). "Effect on timing and nitrogen fertilizer application on winter oilseed rape (*Brassica napus* L.) I. Growth Dynamics and seed yield." Journal of Agronomy and Crop Science 190: 305-131.

Beaudoin, N., Saad, J. K., van Laethem, C., Machet, J. M., Maucorps, J. & Mary, B. (2005). "Nitrate leaching in intensive agriculture in Northern France: Effect of farming practices, soils and crop rotations." Agriculture, Ecosystems & Environment 111: 292-310.

Blackmer, A. M., White, S. E. (1998). "Using precision farming technologies to improve management of soil and fertilizer nitrogen." Australian Journal of Agricultural Research 49: 555-564.

Boegh, E., Soegaard, H., Broge, N., Hasager, C.B., Jensen, N.O., Schelde, K., Thomsen, A. (2002). "Airborne multispectral data for quantifying leaf area index, nitrogen concentration, and photosynthetic efficiency in agriculture." Remote Sensing of Environment 81: 179-193.

Catt, J. A., Howse, K. R. Christian, D. G., Lane, P. W., Harris, G. L. & Goss, M. J. (2000). "Assesment of tillage strategies to decrease nitrate leaching in the Brimstone Farm Experiment, Oxfordshire, UK." Soil & Tillage Research 53: 185-200.

Chalmer, A. G., Darby, R. J. (1992)."Nitrogen application to oilseed rape and implications for potential leaching loss." Aspects of Applied Biology 30: 425-430.

Delin, Sofia (2005). "Site-specific nitrogen fertilization demand in relation to plant available soil nitrogen and water." PhD Thesis, Dept. of Soil Sciences, Acta Universitatis agriculturae Sueciae vol.6.

Di, H. J. C., K. C. (2002). "Nitrate leaching in temperate agroecosystems: sources, factors and mitigating strategies." Nutrient Cycling in Agroecosystems 46: 237-256.

Ebertseder, T., Gutser, R., Hege U., Brandhuber, R., Schmidhalter, U. (2003). "Strategies for site-specific nitrogen fertilization with respect to long-term environmental demands." Paper presented at the 4th ECPA, Berlin.

Filella, I., Serrano, L., Serra, J., Penuelas, J. (1995). "Evaluating wheat nitrogen status with canopy reflectance indices and discriminant analysis." Crop Science 35: 1400-1405.

Friedt, W., Lührs, W., Müller, M., Ordon, F. (2003). " Utility of Winter Oilseed Rape (*Brassica napus* L.) Cultivars and New Breeding Lines for Low-input Cropping Systems." Pflanzenbauwissenschaften 7: 49-55.

Ghersa, C. M., Holt, J. S. (1995). "Using phenology prediction in weed management: a review." Weed Research 35: 461-470.

Goss, M. J., Howse, K. R., Lane, P. W., Christian, D. G., Harris, G. L. (1993). "Losses of nitrate-nitrogen in water draining from under autumn-sown crops established by direct drilling of mouldboard ploughing." Journal of Soil Science 1993: 35-48.

Habekotté, B. (1997). "A model of the phenological development of winter oilseed rape (*Brassica napus* L.)." Field Crops Research 54: 127-136.

Henke, J. (2008). "Entwicklung und Bewertung von Strategien zur Verbesserung der Stickstoffeffizienz im Winterrapsanbau." Dissertation, Christian-Albrechts-Universität zu Kiel, Schriftenreihe 54.

Huang, J. Z., Shrestha, A., Tollenaar, M., Deen, W., Rajcan, I., Rahimian, H., Swanton, C. J. (2001). "Effect of temperature and photoperiod on the phenological development of wild mustard (*Sinapis arvensis* L.)." Field Crops Research 70: 75-86.

Justes, E., Mary, B. & Nicolardot, B. (1999). "Comparing the effectiveness of radish cover crops, oilseed rape volunteers and oilseed rape residues incorporation for reducing nitrate leaching." Nutrient Cycling in Agroecosystems 55: 207-220.

Kristensen, H. L., McCarty, G. W. & Meisinger, J. J. (2000). "Effects of soil structure disturbance on mineralization of organic soil nitrogen." Soil Science Society of America Journal 64: 371-378.

Lancashire, P.D., Bleiholder, H., Langelüddecke, P., Stauss, R., Boom, T.V.D., Weber, E., and Witzenberger, A. (1991). "An uniformdecimal code for growth stages of crops and weeds." Ann. appl. Biol. 119: 561-601.

Lickfett, T., Kreikenbohm, G., Goebel, C., Przemeck, E. (1993). "Über den Anstieg des Rest-Nmin nach Winterraps und Maßnahmen zur seiner Vermeidung." VDLUFA-Schriftenreihe 36: 91-94.

Lickfett, T., Przemeck, E. (1995). "Ausnutzungsgrad von Mineraldünger-Stickstoff in Rapsfruchtfolgen unterschiedlicher Produktionsintensität." VDLUFA-Schriftenreihe 40: 833-836.

Mary, B., Beaudoin, N., Justes, E., Machet, J. M. (1999). "Calculation of nitrogen mineralization and leaching in fallow soil using a simple dynamic model." European Journal of Agronomy 50: 549-566.

Mendham, N. J., Shipway, P. A., Scott, R. K. (1981). "The effects of delayed sowing and weather on growth, development and yield of winter oil-seed rape (*Brassica napus* L.)." The Journal of Agricultural Science 96: 389-416.

Möllers, C., Kessel, B., Kahlmeyer, M., Ossenkop, A., Becker, H. C. (2000). "Untersuchungen zur genotypischen Variabilität der Stickstoff-Effizienz bei Winterraps." Stickstoffeffizienz landwirtschaftlicher Kulturpflanzen, Erich Schmidt Verlag: 30-47.

Müller, K., Böttcher, U., Meyer-Schatz, F., Kage, H. (2008). "Analysis of vegetation indices derived from hyperspectral reflection measurements for estimating crop canopy parameters of oilseed rape (*Brassica napus* L.)." Biosystems engineering 101: 172-182.

Myers, L. F., Christian, K. R., Kirchner, R. J. (1982). "Flowering Responses of 48 Lines of Oilseed Rape (*Brassica* spp.) to Vernalization and Daylength." Australian Journal of Agricultural Research 33: 927-936.

Nicolardot, B., Recous, S., Mary, B. (2001). "Simulation of C and N mineralisation during crop residue decomposition: A simple dynamic model based on the C:N ratio of the residues." Plant and Soil 228: 83-103.

Rathke, G.-W., Behrens, T., Diepenbrock, W. (2006). "Integrated nitrogen management strategies to improve seed yield, oil content and nitrogen efficiency of winter oilseed rape (*Brassica napus* L.): A review." Agriculture, Ecosystems & Environment 117: 80-108.

Raun, W. R., Solie, J. B., Johnson, G. V., Stone,M. L., Mullen, R. W., Freemann, K. W., Thomason, W. E.,Lukina, E. V. (2002). "Improving Nitrogen Use Efficiency in Cereal Grain Production with Optical Sensing and Variable Rate Application." Agronomy Journal 94: 815-820.

Reusch, S. (1997). "Entwicklung eines reflexionsoptischen Sensors zur Erfassung der Stickstoffversorgung landwirtschaftlicher Kulturpflanzen." Institut für Landwirtschaftliche Verfahrenstechnik. Kiel, Christian-Albrechts-Universität: 156.

Robertson, M. J., et al (2002). "Environmental and genotypic control of time to flowering in canola and Indian mustard." Australian Journal of Agricultural Research 53: 793-809.

Schjoerring, J. K., Bock, J. G. H., Gammelvind, C. R., Jensen, C. R. & Mogensen, V. O. (1995). "Nitrogen incorporation and remobilization in different shoot components of field grown winter oilseed rape (*Brassica napus* L.) as affected by rate of nitrogen application and irrigation." Plant and Soil 177: 255-264.

Sieling, K., Günther-Borstel, O. & Hanus, H. (1997). "Effect of slurry application and mineral nitrogen fertilization on N leaching in different crop combinations." The Journal of Agricultural Science 128: 79-86.

Sieling, K. C., O. (1997). "Effect of preceding crop combination and N fertilization on yield of six oil-seed rape cultivars (*Brassica napus* L.)." European Journal of Agronomy 7: 301-306.

Sieling, K., Günther-Borstel, O., Teebken, T. & Hanus, H. (1999). "Soil mineral N and N net mineralization during autumn and winter under an oilseed rape-winter wheat-winter barley rotation in different crop management systems." The Journal of Agricultural Science 132: 127-137.

Sieling, K. (2000). " Untersuchungen zu den Auswirkungen unterschiedlicher Produktionssysteme auf einige Parameter des N-Haushaltes von Boden und Pflanze." Habilitationsschrift, Christian-Albrechts-Universität zu Kiel, Schriftenreihe des Instituts für Pflanzenbau und Pflanzenzüchtung: 16.

Sieling, K. (2004). "Growth stage-specific application of slurry and mineral N to oilseed rape, wheat and barley." The Journal of Agricultural Science 142: 1-8.

Sieling, K., Kage, H. (2006). "N balance as an indicator of N leaching in an oilseed rape - winter wheat - winter barley rotation." Agriculture, Ecosystems & Environment 115: 261-269.

Tarpley, L., Reddy, K. R., Sassenrath-Cole, G. F. (2000). "Reflectance indices with precision and accuracy in predicting cotton leaf nitrogen concentration." Crop Science 40: 1814-1819.

Thiessen, E. (2002). Optische Sensortechnik für den teilflächenspezifischen Einsatz von Agrarchemikalien. Institut für Landwirtschaftliche Verfahrenstechnik. Kiel, Christian-Albrechts-Universität: 88.

Yan, W., Wallace, D. H. (1998). "Simulation and Prediction of Plant Phenology for Five Crops Based on Photoperiod x Temperature Interaction." Annals of Botany 81: 705-716.

Xue, Q., Weiss, A., Baenziger, P. S. (2004). "Predicting phenological development in winter wheat." Climate Research 25: 243-252.

Chapter 6

Summary

Zusammenfassung

Summary

Winter oilseed rape (OSR) became more and more important during the last decades due to its profitability, the potential to grow OSR as a renewable resource for biofuel production and its beneficial value as preceding crop. Its high fertilizer requirements and its low nitrogen efficiency enhance the risk of N losses from soil-crop system to the environment by leaching during winter rainfall. Site specific fertilization is one approach to improve N efficiency for OSR. Therefore, high resoluted spatial and time concerning information about current crop parameters like biomass and N uptake as well as information about yield potential is necessary. Two approaches were developed to realize these requirements. First, site specific differences of crop development should become measurable in realtime and for a large scale. Second, time courses of biomass production and N uptake should be comprehended by model simulation. Subsequently, appropriate fertilizer algorithms should be implemented for the derivation of fertilizer recommendations. Furthermore, the applicability of these approaches on field scale must be investigated in the course of additional studies.

The first objective of this thesis was the establishment of a non-destructive, remote sensing based method to achieve information on site specific variability of above ground biomass and crop uptake of OSR during the growth period by measuring canopy reflectance in order to save intensive destructive measurements in the fields. A systematic analysis of hyperspectral reflectance measurements by testing all possible waveband combinations enabled to derive new vegetation indices. These indices were successfully used to estimate crop canopy parameters like the green area index (GAI), shoot dry matter (DM_{shoot}) and nitrogen in the shoot (N_{shoot}) during the vegetation period and their prediction power exceeded commonly used indices in terms of r^2 and RMSE. Particularly, combinations of near-infrared wavebands 740 nm and 780 nm served best to estimate GAI and DM_{shoot} and N_{shoot}. Regarding calibration and validation, the indices showed stable results. Using these indices enables to identify small differences between crop canopy parameters in realtime and for large areas. These information can be used to initialize and parameterize a crop growth model for OSR.
A further objective of this thesis was the development of a growth model to predict plant parameters like biomass and canopy N in the time course, to derive the amount of fertilizer demand. The presented crop growth model follows a dynamic, empirical approach for predicting dry matter production based on the concept of light use efficiency (LUE) for vegetative growth from emergence to flowering. Data gave evidence that LUE before winter was not constant but depended on radiation intensity. Therefore, it was calculated according to a linear regression function for this specific period. Furthermore, the model calculates dry matter partitioning into leaf and stem fraction according to an allometric approach. For the

calculation of nitrogen uptake, nitrogen concentration had to be determined. For leaves, it was set to be constant, whereas stem nitrogen concentration depended on stem dry matter according to an exponential dilution curve. Nitrogen uptake for the shoot was obtained by adding leaf and stem nitrogen uptake. Additionally, the model calculated dry matter losses during winter, which were calculated according to temperatures below 0 °C. Taking these losses into account, enabled for a continuously prediction of dry matter from emergence to flowering without interruption. The variable LUE approach before winter improved dry matter predictions compared to calculations with an optimized, constant LUE. The model could reproduce the dynamic of dry matter losses during winter. Only few data sets were available for calibration and validation, so that parameterization was not robust regarding standard errors for optimized parameters. Prediction for validation data set revealed high differences concerning quality, indicating that additional data set are needed for improving parameterization and prediction of the crop growth model.

Because crop growth differs for different developmental stages, another object of this study was the development of a phenological model. Knowledge about time and duration of growth stages can also be used for a growth specific crop management like N fertilization. The presented phenological model based on BRASNAP-PH, which was developed for north-west Europe. Because BRASNAP-PH predicts only four main developmental stages, modifications were conducted, to predict highly resoluted developmental stages according to BBCH. Vernalization and photoperiod were the most important factors besides temperature to estimate leaf development, whereas temperature was determinant during all phases of development. The modified model was calibrated and validated on a large data set throughout Germany. Optimized parameter values and corresponding standard errors for calibration and cross calibration gave advice for a robust parameterization. Validation and cross validation let to a root mean square error (RMSE) of 3.11 and 3.25 BBCH stages, respectively, for the whole developmental phase.

The presented results of this thesis can contribute to improve N efficiency for OSR in terms of a site specific fertilization implementing fertilizer algorithms to the growth model. Therefore, an accurate, adjusted, site specific N fertilization recommendation should be derived from information of current crop status and of yield potential. Since the site specific fertilization deals only with one aspect for improving N efficiency for OSR, other approaches must be developed and investigated. Especially approaches concerning production management and crop rotations reveal promising for improvement.

Zusammenfassung

Die Anbaubedeutung von Winterraps (*Brassica napus* L.) hat in den letzten Jahren zugenommen. Gründe hierfür sind sowohl seine Verwendungsmöglichkeit als erneuerbare Energie für die Biokraftstoffgewinnung, als auch seine positive Vorfruchtwirkung. Der hohe N-Düngebedarf und die gleichzeitig geringe N-Effizienz bedingen hohe N-Bilanzüberschüsse, die das Risiko von N-Auswaschungsverlusten über Winter erhöhen. Ein möglicher Ansatz zur Verbesserung der N-Effizienz im Winterraps stellt die teilflächenspezifische Düngung dar. Hierfür werden räumlich und zeitlich hoch aufgelöste Informationen über den aktuellen Pflanzenbestand benötigt, aus denen sowohl Schätzungen der Biomasse und der N-Aufnahme als auch Ertragspotenziale abgeleitet werden können. Zwei Ansätze wurden für eine erste Umsetzung der Fragestellung entwickelt. Zum einen sollen teilflächenspezifische Unterschiede im Bestand erfasst werden und zum anderen, sollen die zeitlichen Verläufe der Biomasseentwicklung und der N-Aufnahme des Bestandes mittels einer Modellsimulation abgebildet werden können. Anschließend soll durch den Einbau geeigneter Düngealgorithmen eine entsprechende Düngeempfehlung abgeleitet werden. Allerdings muss die Übertragbarkeit dieser Ansätze auf Schlagebene durch nachfolgende Projekte untersucht werden.

Das Ziel dieser Arbeit war zunächst die Etablierung einer sensorbasierten, nicht-destruktiven Messmethode zu Erfassung teilflächenspezifischer Variabilität. Hyperspektrale Reflexionsspektren von Rapsbeständen, die zeitaufwändige, destruktive Probenahmen ersetzen sollen, wurden im Hinblick auf ihre Eignung zur Ableitung von Pflanzenparametern untersucht. Vegetationsindizes konnten durch die systematische Analyse, bei der alle möglichen Wellenlängenkombinationen getestet wurden, identifiziert und abgeleitet werden. Die neu gebildeten Indizes eigneten sich zur Schätzung von Bestandesparametern wie den Bestandesflächenindex (GAI=green area index), Sprosstrockenmasse (DM_{shoot}) und N-Menge im Spross (N_{shoot}) und erzielten bessere Ergebnisse hinsichtlich r^2 und RMSE Werten als herkömmlich gebräuchliche Indizes. Die Kombinationen der nah-infraroten Wellenlängen 740 nm und 780 nm eigneten sich am besten für die Schätzung der Parameter. Durch die Indizes konnten geringe Unterschiede bezüglich der Bestandesparameter zeitnah und für eine große Fläche identifiziert werden. Die hieraus gewonnenen Informationen können anschließend für die Initiierung und Parametrisierung eines Pflanzenwachstumsmodells für Winterraps verwendet werden.

Ein weiteres Ziel der Arbeit war somit die Entwicklung eines dynamischen Pflanzenwachstumsmodells, das Bestandesparameter im zeitlichen Verlauf schätzen kann, aus denen anschließend der Düngebedarf ermittelt werden kann. Die Berechnung der Biomasseproduktion des präsentierten dynamischen Modells für Winterraps basiert auf dem

Konzept der Lichtnutzungseffizienz (LUE). Das Modell berechnet das Wachstum für den Zeitraum von Auflauf bis zur Blüte, also das vegetative Wachstum. Die Daten der LUE vor Winter ließen vermuten, dass diese von der Einstrahlungsintensität abhängt. Deshalb wird die LUE als Abhängige für diesen Zeitraum durch eine lineare Regression von der Einstrahlungsintensität bestimmt. Des Weiteren berechnet das Modell die Allokation der gebildeten Trockenmasse in einen Blatt- und einen Stängelanteil mittels eines allometrischen Ansatzes. Für die Berechnung der aufgenommenen N-Menge im Bestand muss zunächst die N-Konzentration der jeweiligen Fraktionen bestimmt werden. Während die N-Konzentration der Blätter als konstant angenommen wurde, konnte die der Stängel durch eine Verdünnungsfunktion von Stängel-N-Konzentration zur Stängeltrockenmasse gemäß einem exponentiellen Kurvenverlauf abgeleitet werden. Die Aufsummierung der jeweiligen Fraktions-N-Mengen ergibt die Spross N-Menge. Das Modell berechnet auch die Trockenmasseverluste über Winter in Abhängigkeit der aufsummierten Temperaturen unter 0 °C, wodurch die kontinuierliche Berechnung der Sprosstrockenmasse von Auflauf über den Winter bis zur Blüte ermöglicht wird. Durch die Berechnung einer strahlungsabhängigen LUE konnten im Vergleich zu den Berechnungen mit einer konstant bestimmten LUE Verbesserungen bezüglich der Trockenmasseschätzung erzielt werden. Die Dynamik der Abnahme von Biomasse über Winter konnte dargestellt werden. Da nur wenige geeignete Datensätze zur Kalibrierung und Validierung zur Verfügung standen, konnte keine robuste Parameterschätzung (hohe Standardfehler) erzielt werden. Hinsichtlich der Abbildungsgüte der Validations-Datensätze sind große Unterschiede aufgezeigt worden, so dass zusätzliche Untersuchungen und Parametrisierungsschritte benötigt werden.

Da das Wachstumsverhalten während verschiedener Entwicklungsabschnitte variieren kann, ist die Kenntnis über den Ablauf der phänologischen Entwicklung von Vorteil. Dieses Wissen kann auch für Stadien abhängige produktionstechnische Maßnahmen verwendet werden. Ein weiteres Ziel dieser Arbeit war somit die Entwicklung eines Phänologie-Modells. Das vorgestellte Modell basiert auf BRASNAP-PH, das für die Vorhersage von vier Entwicklungsstadien im Winterraps für Nordwesteuropa entwickelt wurde. Um eine höher aufgelöste Beschreibung der Entwicklung gemäß der BBCH-Skala zu erreichen, wurden diverse Modifikationen vorgenommen. Für die Zeitdauer der Blattentwicklung sind Vernalisation, Photoperiode und Temperatur die Haupteinflussfaktoren. Alle anderen Entwicklungsphasen werden durch Temperatur beeinflusst. Das Modell wurde an einem umfangreichen, deutschlandweiten Datensatz kalibriert und validiert. Kalibrierung und Cross-Kalibrierung führten zu einer robusten Parameterschätzung. Für den gesamten Entwicklungszeitraum von Auflauf bis zur Abreife konnten gemäß der Validierungs- und Cross-Validierungsschritte RMSE Werte von 3,11 und 3,25 BBCH-Stadien erzielt werden.

In Kombination mit geeigneten Düngealgorithmen, leisten die vorgestellten Ergebnisse einen Beitrag zur teilflächenspezifischen N-Düngung von Winterraps und können somit zur Verbesserung der N-Effizienz für Winterraps beitragen. Als nächster Schritt sollte die Anwendung der Ableitung angepasster, teilflächenspezifischer Düngeempfehlungen aus den Informationen zur Biomasse und N-Aufnahme im Bestand für große Flächen getestet werden. Da die teilflächenspezifische Düngung nur einen möglichen Ansatz zur Verbesserung der N-Effizienz von Winterraps darstellt, sollten andere Ansätze weiter verfolgt und untersucht werden. Sowohl die produktionstechnischen Maßnahmen als auch die Änderung der Winterraps enthaltenen Fruchtfolgen scheinen Verbesserungsmöglichkeiten zu beinhalten.

Bedanken möchte ich mich

zuallererst bei Herrn Prof. Dr. H. Kage. Zum einen für die Überlassung des Themas und zum anderen für all die vielen kleinen oder großen Anregungen, die letzten Endes zum großen Ganzen geführt haben.

bei Herrn Prof. Dr. F. Taube, für die unkomplizierte Übernahme des Koreferats.

bei Dr. Ulf Böttcher, für seine unbeschreibliche Geduld und seine recht einzigartige Fähigkeit Sachverhalte auf zahlreiche Arten erklären zu können;
bei PD Dr. Klaus Sieling für seine inhaltlichen und fachlichen Hilfestellungen, aber vor allem für seine unermüdliche Motivation zum Abschluss zu kommen;
bei Dr. Andreas Pacholski für den (gnadenlos) guten, spitzen, roten Stift beim Korrekturlesen;
bei PD Dr. Antje Herrmann für die permanente Präsenz als Ansprechperson bei Schwierigkeiten und Fragen aller Art.

bei Herrn Lambros Rizos für die Tatsache, dass mein PC und alle damit zusammenhängende Funktionen eine solche Selbstverständlichkeit dargestellt haben.

bei allen Doktorandenkollegen für die vielen schönen Stunden des Lachens, des Meckerns, der investigativen Tätigkeiten und vor allem natürlich auch für das produktive Arbeitsklima. Also danke an: Franziska Meyer-Schatz, Babette Wienforth, Michael Kohl, Dorothee Neukam, Dirk Gericke, Tobias Johnen, Ingo Pahlmann und Johannes Henke.

bei dem Gewächshaus-Team, Kirsten Schulz, Gunda Schnack und Doris Ziermann, für den stets reibungslosen Verlauf aller Probenahme bezogenen Arbeitsvorgänge, aber vor allem für die besondere Atmosphäre, die mir die Stunden der Datenerhebung geradezu versüßt hat. Ganz besonders bedanken möchte ich mich allerdings bei Cordula Weise, die mit mir sooo viele Kilometer auf dem Acker zurückgelegt hat und mich trotzdem noch mag!

bei dem gesamten Team von Hohenschulen (die Herren: Rüdiger Ströh, Sepp Nagel, Klaus Horn, Manfred Kunde, Wille Stallmann, Emil Struwe und zahlreiche Azubis) für den reibungslosen Verlauf meines Versuches, aber vor allem für das sehr familiäre Wohnklima! Es war gut zu wissen, dass man nach mir sehen würde, wenn es mir mal nicht gut ging!

bei meiner gesamten, im Laufe der Zeit gewachsenen Familie, die mir den Rückhalt in ausnahmslos allen Lagen gegeben hat, ohne den ich diese Arbeit nicht hätte schreiben können! Lieben Dank an meine Eltern, Martin & Chrissi und Ann-Jorina, Rasmus & Yvonne und Merle & Lilith, Unkas & Janus und vor allem an meine verstorbene Großmutter Marie Heidemann, die so stolz auf mich ist!

bei meinen Patenkindern, Louisa und Jonas, die in der gesamten Zeit sehr stark auf mich verzichten mussten und mich trotzdem so gerne besuchen kommen.

bei all Freunden, die ebenfalls ein wenig zu kurz gekommen sind und doch immer sehr viel Anteilnahme und Interesse an mir und meiner Arbeit hatten.

vor allem bei meinem Freund Oliver! Nur weil sich seine Geduld, Ausdauer und Toleranz mit meiner teilweisen Ungeduld und Gereiztheit so gut ergänzen, aber auch weil er mich in allem sowohl hinterfragt als auch unterstützt hat, konnte ich diese Arbeit zum Abschluss bringen!

bei allen die ich jetzt vergessen habe, die aber trotzdem auf die eine oder andere Art und Weise ihren Anteil an der Arbeit hatten.

Lebenslauf

Name	Müller
Vorname	Karla
Geburtsdatum	06.12.1976
Geburtsort	Bielefeld
Familienstand	ledig
Staatsangehörigkeit	deutsch
Schulausbildung	
1983 - 1987	Grundschule Schweicheln
1987 - 1996	Friedrichs-Gymnasium Herford
Hochschulstudium	
10/1996 – 06/1998	Grundstudium der Biologie, Universität Bielefeld, Abschluss: Vordiplom
08/1998 – 05/ 1999	Auslandsstudium an der Harding University in Searcy, Arkansas, USA
10/1999 – 08/2003	Hauptstudium der Biologie, Universität Bielefeld, Fachrichtung: Ökologie, Botanik, Verhaltensforschung, Abschluss: Diplom-Biologin
Berufstätigkeit	
07/2008 – 03/2009	Mitarbeiterin in der Abteilung Pflanzenbau der Landwirtschaftskammer Schleswig-Holstein
03/2007 – 01/2008	Assistentin der Geschäftsleitung im Tierpark Arche Warder
04/2005 – 03/2008	Stipendiatin der Deutschen Bundesstiftung Umwelt
03/2004 – 03/2005	wissenschaftliche Mitarbeiterin am Institut für Pflanzenbau und Pflanzenzüchtung - Abteilung Acker- und Pflanzenbau - der Christian-Albrechts-Universität zu Kiel
02/2003 – 02/2004	Assistentin der Geschäftsleitung des Tierschutzvereins Boxer Nothilfe Deutschland e. V.